NUMERICAL MODELING OF SHORELINE CHANGES
AROUND MANAVGAT RIVER MOUTH

A THESIS SUBMITTED TO
THE GRADUATE SCHOOL OF NATURAL AND APPLIED SCIENCES
OF
MIDDLE EAST TECHNICAL UNIVERSITY

BY
FATIMA AL SALEH

IN PARTIAL FULFILLMENT OF THE REQUIREMENTS
FOR
THE DEGREE OF DOCTOR PHILOSOPHY
IN
CIVIL ENGINEERING

DECEMBER 2004

Approval of the Graduate School of Natural and Applied Sciences

_____

Prof. Dr. Canan Özgen
Director

I certify that this thesis satisfies all the requirements as a thesis for the degree of Philosophy of Doctorate.

_____

Prof. Dr. Erdal Çokça
Head of Department

This is to certify that we have read this thesis and that in our opinion it is fully adequate, in scope and quality, as a thesis for the degree of Philosophy of Doctorate.

_____

Prof. Dr. Erdal Özhan
Supervisor

Examining Committee Members

Prof. Dr. Vedat Doyuran   _____

Prof. Dr. Erdal Özhan   _____

Prof. Dr. Ayşen Ergın   _____

Assoc. Prof. Dr. Lale Balas   _____

Assist. Prof. Dr. Mehmet Lütfi Süzen   _____

I hereby declare that all information in this document has been obtained and presented in accordance with academic rules and ethical conduct. I also declare that, as required by these rules and conduct, I have fully cited and referenced all material and results that are not original to this work.

Name, Last name : Fatima AL SALEH

Signature :

ABSTRACT

NUMERICAL MODELING OF SHORELINE CHANGES AROUND
MANAVGAT RIVER MOUTH

AL SALEH, Fatima

Ph.D., Departement of Civil Engineering

Supervisopr: Prof. Dr. Erdal OZHAN

December 2004, 172 pages

River mouths are very active coastal regions. Continuous sediment supply by the river and the movement by wave action cause the shoreline to change in time and space. Modeling of shoreline changes is an essential step before the design of any coastal engineering project. This research aimed to develop a system of numerical models to present the shoreline changes around a river mouth. The system of numerical models has three components: 1) modeling of nearshore wave characteristics, 2) modeling of longshore sand transport rates using the results of the first component, 3) modeling of shoreline changes using the estimated sand transport rates. Thus, firstly, deep water

wave characteristics including the annual wave rose affecting Manavgat River mouth have been obtained from the database of NATO TU-WAVES Project. Then REF/DIF1 and SWAN nearshore wave models have been used to find out nearshore wave conditions. Since the results obtained from REF/DIF1 wave model have been found to be more reasonable compared to SWAN's output, REF/DIF1 wave model has been used in preparing a time series nearshore reference wave file with three hours time interval. This reference file has been used to run GENESIS. Last step of the numerical shoreline change modelling of Manavgat River mouth was the calibration procedure in which the "transport parameters" k1 and k2 have been determined. As there is lack of measurements of shoreline positions that can be used in calibrating shoreline change model, k1 and k2 has been approximately found to be k1=0.516 and k2=0.9 by using an empirical sediment transport formula. As a future study, it is recommended that when the protection structure controlling the river mouth is finished, the measurements of shoreline position behind the structure should be used in verification of shoreline change model in order to get more accurate results.

Keywords: Nearshore Modelling, Logshore Sand Transport Modelling, Shoreline Changes Modelling , Manavgat, REF/DIF 1, SWAN, GENESIS.

ÖZ

MANAVGAT IRMAK AĞZINDA KIYI ÇIZGISININ DİĞİŞİMİNİN SAYISAL MODELI

AL SALEH, Fatima

Doktora, İnşaat Mühendisliği Bölümü

Tez Yöneticisi : Prof. Dr. Erdal ÖZHAN

Nehir ağızları çok hareketli kıyı alanlarıdır. Nehirler tarafından sürekli madde taşınması ve dalga etkisiyle oluşan hareketler kıyı çizgisinin zamansal ve alansal değişimine neden olmaktadır. Bu nedenle kıyı çizgisinin değişiminin modellenmesi, her hangi bir kıyı mühendisliği çalışmasının tasarımı öncesinde gerçekleştirilmesi gereken önemli bir adımdır. Bu araştırma, bir nehir ağzı etrafındaki kıyı çizgisi değişimini gösterebilecek bir sayısal modeller sistemi geliştirmeyi amaçlamaktadır. Bu sayısal modeller sistemi üç aşamadan oluşmaktadır: 1) yakın kıyı dalga özeliklerinin modellenmesi, 2) ilk aşamada elde edilen sonuçlar kullanılarak kıyı boyu kum taşınım hızının modellenmesi, 3) tahmin edilen kum taşınım hızları kullanılarak kıyı çizgisi değişiminin modellenmesi. Bu doğrultuda, öncelikle, NATO TU-WAVES Projesi veri

tabanından Manavgat Nehri ağzını etkileyen derin deniz dalga özellikleri, yıllık dalga gülünü de içeren, elde edildi. Daha sonra, yakın kıyı dalga modelleri REF/DIF1 ve SWAN kullanılarak yakın kıyı dalga özellikleri bulundu. REF/DIF1 dalga modeli sonuçlarının SWAN sonuçlarına göre daha olası bulunduğundan, üç saat aralıklı yakın kıyı referans dalga özellikleri zaman serisi dosyası REF/DIF1 sonuçları kullanılarak hazırlandı. Bu zaman serisi dosyası GENESIS'i çalıştırmakta kullanıldı. Manavgat Nehri ağzındaki kıyı çizgisi değişiminin sayısal modellemesinde son aşama taşınım parametreleri, k1 ve k2'nin belirlendiği kalibrasyon çalışması olmuştur. Kıyı çizgisi değişimi modelinin kalibrasyonunda kullanılacak kıyı çizgisi durumuna ait ölçümler bulunmadığından gözlemsel bir madde taşınım denklemi kullanılarak gerçekleştirilen kalibrasyon çalışması sonucunda k1 ve k2 yaklaşık olarak sırasıyla 0.516 ve 0.9 bulundu. Nehir ağzını kontrol eden koruma yapısı tamamlandığında, yapının arkasında kalan kıyı çizgisinin konumuna ait ölçümlerin kıyı çizgisi değişimi modelinin doğrulanmasında kullanılması ileride yapılması gereken bir çalışma olarak önerilmektedir.

Anahtar sözcukler: Yakın Kıyı Modellemesi, Kıyı Boyu Kum Taşıma Modellemesi, Kıyı Çizgisinin Değişme Modellemesi , Manavgat, , REF/DIF1, SWAN, GENESIS.

To:

A woman lightening my way, ...

My mother ...

ACKNOWLEDGMENTS

TABLE OF CONTENTS

LIST OF TABLES

TABLE

LIST OF FIGURES

Figure

LISTE OF SYMBOLS

$N(\sigma, \theta)$ action density spectrum

$E(\sigma, \theta)$ energy density spectrum

σ relative frequency

θ wave direction

c_x propagation velocity in x dimension

c_y propagation velocity in y dimension

c_σ propagation velocity in σ dimension

c_θ propagation velocity in θ dimension

$S(\sigma, \theta)$ source term

$S_{in}(\sigma, \theta)$ wind input source term

A   linear growth parameter

B   exponential growth parameter

$S_{ds,\,w}(\sigma,\theta)$ whitecapping

$\tilde{\sigma}$ mean frequency

$\tilde{k}$ mean wave number

Γ wave steepness dependent coefficient

$S_{ds,\,b}(\sigma,\theta)$ bottom friction

C_{bottom} bottom friction coefficient

$S_{ds,\,br}(\sigma,\theta)$ depth-induced breaking

$S_{ds.br.tot}$ mean rate of energy dissipation per unit horizontal area
        due to wave breaking

E_{tot} total wave energy

$\eta(x,y)$ surface displacement

C wave celerity

C_g group velocity

$h(x,y)$ local water depth

g   acceleration of gravity

$k(x,y)$ local wave number

h water depth

σ angular frequency of the waves

A   complex amplitude related to the water surface
        displacement

ω	dissipation factor
U	Ursell parameter
H	wave height
C_p	coefficient of permeability
Q_l	volume transport rate
I_l	immersed weight transport rate
ρ_s	mass density of the sediment grains
ρ	mass density of water
n	in-place sediment porosity
$\Delta\psi$	change in shoreline position
$\Delta\xi$	length of the shoreline segment
D_B	berm elevation
Dc	closure depth
q	line source or sink of sand
q_s	volume of sand added or removed per unit width of beach from shoreward side
q_0	volume of sand added or removed per unit width of beach from offshore side
Q	longshore sand transport rate
$\theta_{\sigma\beta}$	angle of breaking waves to the local shoreline
P	porosity of sand on the bed
$\tan\beta$	average bottom slope from the shoreline to the depth of active longshore sand transport
D_{LT}	depth of active longshore transport

γ	breaker index
$(H_{1/3})_b$	significant wave height at breaking
D_{LT0}	maximum depth of longshore transport
E_b	wave energy evaluated at the breaker line
C_{gb}	wave group speed at the breaker line
κ	breaker index
α_b	wave breaker angle relative to the shoreline
P_l	potential longshore sediment transport rate
I_l	immersed weight transport rate
$(H_b)_{rms}$	root mean square breaking wave height

CHAPTER 1

1. INTRODUCTION

1.1 DEFINITION OF THE PROBLEM

River mouths are very active coastal regions. The continuous sediment supply by the river and the movement by wave action cause the shoreline (the boundary between the sea and the land) to change its position in time and in space (Komar, 1976).

Processes occurring in the nearshore area of the sea are extremely dynamic, involving the combined action of waves, wave-induced currents, and sediment movement. The interaction of winds, waves, currents, tides, sediments, and other phenomena in the coastal zone trigger the coastal processes that are associated with sediment movement. The sediment motion causes shores to erode, accrete, or remain stable depending on the rates at which this sediment is supplied to and removed from the shore.

Sediment transport is a critical component to many coastal engineering problems; examples include sedimentation in navigational channels, sand transport in the littoral zone, and sediment resuspension during dredging or cable trenching and it is among the most important nearshore processes that control the beach morphology, and determines in large part whether shores erode, accrete, or remain stable.

An understanding of longshore sand transport is essential to coastal engineering design practice. This longshore movement of beach sediments is of particular importance since the transport can either be interrupted by any coastal structure like jetty, breakwater, etc., which block all or a portion of the longshore sediment transport. Sediment moving alongshore may also be captured by inlets and submarine canyons. Such interruptions of longshore sediment transport often pose problems to beaches located downcoast and threaten the usefulness of navigable waterways (channel, harbours, etc.). Using nearshore wave characteristics, longshore sand transport can be predicted and an estimation of nearshore sand budget can be performed. Therefore, establishing the nearshore wave climate is the starting step for estimating longshore sand transport rate.

Breaking waves in the nearshore zone are responsible for horizontal and vertical patterns of nearshore currents that move beach sediments. Sometimes this transport results only in a local rearrangement of sand into bars and troughs or into a series of rhythmic embayments cut into the beach. More serious impacts of this transport result from the extensive longshore displacements of sediments, possibly moving hundreds of thousands of cubic meters of sand along the coast each year (CEM-III, 1998).

Waves critically affect man in coastal regions, including the open coasts and adjacent continental shelves. Preventing beach erosion, designing and building coastal structures, designing and operating ships, providing marine forecasts, and coastal planning are examples of projects for which extensive information on wind-wave characteristics is crutial. This information may be either of statistical nature, derived from wave data covering a sufficiently long period of time (i.e. wave climate), or consists of merely daily predictions obtained from routine wave forecasting. The former

type of data is needed for planning, design and management purposes, whereas the later type is required for all daily coastal and marine operations such as offshore operations, shipping, sailing and coastal construction activities (Özhan and Abdalla, 1997).

The beach and nearshore zone of a coast are the regions where the forces of the sea act against the land. The beach is defined as the zone of unconsolidated sediments (e.g. sand and gravel) that extends from the uppermost limit of wave action to the low tide mark (Komar, 1976). In beach terminology, the nearshore zone is an indefinite zone extending seaward from the shoreline well beyond the breaker zone. Figure 1.1 shows the different zones of a beach area.
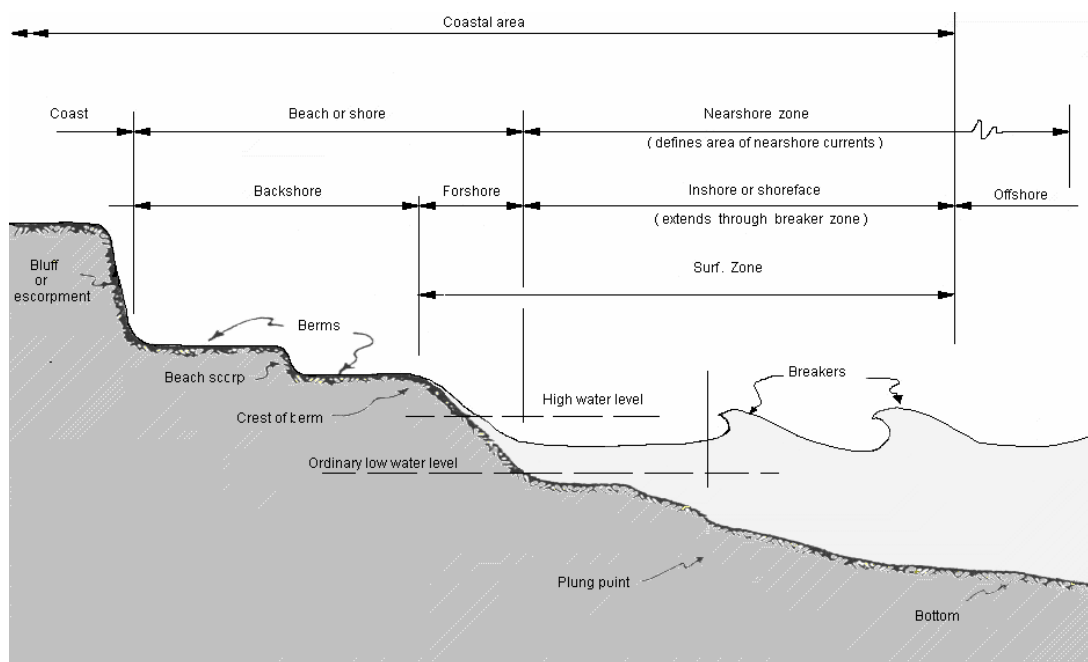
Figure 1.1 Visual definitions of terms describing a typical beach profile,
(SPM, 1984).

The important properties of sediment in coastal engineering can be placed into three groups: the size of the particles making up the sediment, the composition of the sediment, or the bulk characteristics of the sediments. In the geologist's size classification, sand grains are at least 16 times larger and may be more than 500 times larger in diameter than the largest clay particle (the same classification defines a particle as clay if it is less than 0.0039 mm.). In this thesis, only sand will be of our concern.

There are two modes of sediment transport: suspended sediment transport, in which sediment is carried above the bottom by the turbulent eddies of water, and bed-load sediment transport, in which the grains remain close to the bed and move by rolling and saltation. The former kind of transport is very difficult to be measured.

Sediment transport, which is defined as the movement of sediments in the nearshore zone by waves and currents, is divided into two general classes: transport parallel to the shore (longshore transport) and transport perpendicular to the shore (onshore-offshore transport).

Currents associated with a nearshore cell circulation generally act to produce only a local rearrangement of beach sediments. The rip currents of the circulation can be important in the cross-shore transport of sand, but there is minimal net displacement of beach sediments along the coast. The more important mode of transport is the longshore movement of sediments that is cuased by waves breaking obliquely to the coast and thus generating longshore currents that generally flow along extended distances. The resulting movement of beach sediment along the coast is referred to longshore sediment transport. Sediment transport can also be caused by currents generated due to the alongshore gradients in breaking wave heights,

4

commonly called diffraction currents. This transport manifests itself as movement of beach sediments towards structures that create these diffraction currents.

1.2   THE USE OF NUMERICAL MODELS FOR PREDICTION OF COSTAL CHANGES.

In the planning of projects located in the nearshore zone, numerical models that predict beach evolution has proven to be a powerful technique to assist in the selection of the most appropriate design. The models are essential for developing of the problem, organizing data, analyzing data and for solving the data under various circumstances.

In order to obtain a reliable wave climate, accurate input wave data is required. Main sources of wave data are visual observations, instrumental measurements and modelling. Visual observations are usually not accurate enough. The second source, instrumental measurements, is a reliable source of data and usually of sufficient accuracy. It usually gives estimates of spectra and other wave parameters. However measurements are very expensive and they only cover a local area for a limited duration of time. Numerical wave modelling is another source of data being used for hindcasting and forecasting of waves. This source is preferable since it is cheap and has no limitation on time and space coverage, provided that accurate data on wind fields are available.

In this study, REF/DIF1 and SWAN nearshore wave models were both used to obtain the nearshore wave characteristics that are the main input data to shoreline change models. One such model, the GENESIS shoreline

change model, which is a widely used model, was used to calculate the shore line changes around the Manavgat River mouth..

The wave atlas of the Turkish coasts which is the main result of the NATO TU-WAVES was used to obtain the deep water wave characteristics that are required as input data by the nearshore wave models.

The NATO TU-WAVES (Özhan and Abdalla, 1992, 1993a & 1993b and Özhan et al., 1995), is a major project that aims to find out the wave climate affecting the Turkish coastline as well as the whole Black Sea coasts. The project which includes systematic wave measurements, wave modelling and wave climate computations was carried out with partial support provided by the NATO Science for Stability (SfS) Program-Phase III.

Wave models can be classified according to their generation into four classes: zeroth, first, second and third generation models. However, there are other classification criteria in the literature according to several considerations. A model is considered as a decoupled model when the wave component is modelled to develop independently from other components. Otherwise it is considered as a coupled model. The group of decoupled models includes the first generation models in which the effect of non-linear interactions is not explicitly included. A model is referred to as a discrete spectral model if it combines the evolution of discrete wave components (several hundred wave components). A model follows the evolution of limited characteristic spectral parameters (usually not more than six) such as the peak frequency and the total energy, is called a parametrical model. This type of models can be used to simulate the "sea" conditions only (e.g not swell). Second generation models are basically in this group as proposed by

Hasselmann et al. (1976). When a parametrical model combines with a decoupled spectral model it is termed as a hybrid model.

Third generation models attempt to incorporate the state-of-the-art of the physics behind generation of sea waves into the basic radiative transfer equation governing the evolution of the wave spectrum, without any ad hoc assumptions regarding the spectral shape. These models are all based on the energy or action balance equation and are usually formulated to run on a spherical latitude-longitude grid. WAM (WAMDI Group, 1988) and METU3 (Abdalla, 1993) are examples of the third generation models.

1.3   SCOPE AND EXTEND OF THE PRESENT STUDY.

This research aims to develop a system of numerical models to present the shoreline changes around the mouth of Manavgat River. The system of numerical models has three components: 1) modelling of nearshore wave characteristics, 2) modeling of longshore sand transport rates using the results of the first component, 3) modeling of shoreline changes using the estimated sand transport rates.

Manavgat River, which is used for navigation by small recreation and local fishing boats, flows into the Mediterranean Sea at the southern coast of Turkey (Figure 1.2) near Manavgat Town which is located 6 km inland from river mouth.
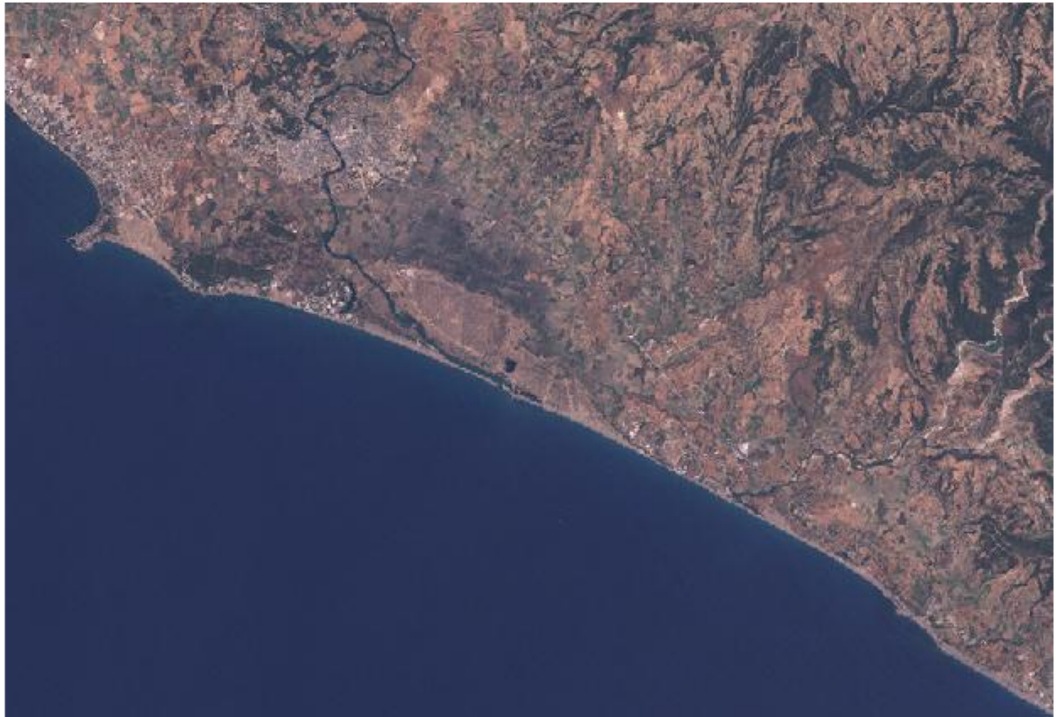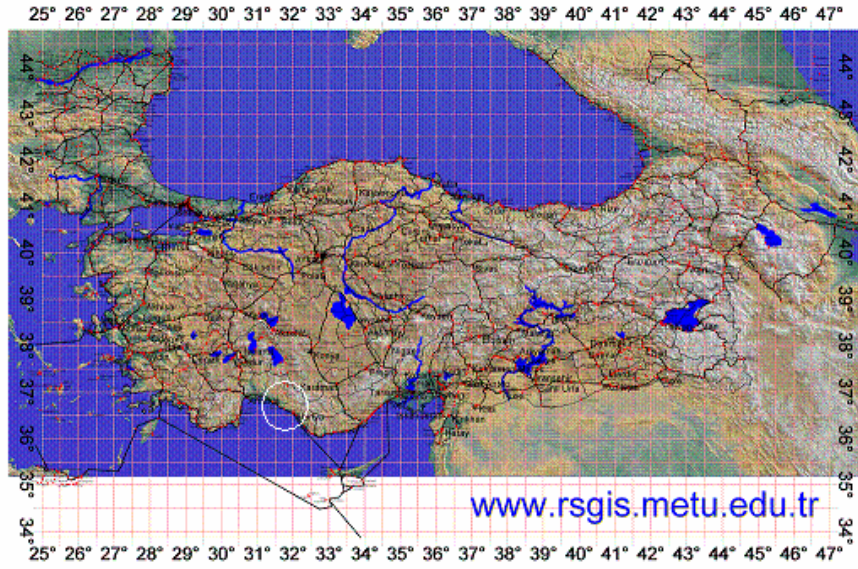
Figure 1.2 Location of the Manavgat River mouth

8

A dam constructed upstream 30 km. from the shoreline controls the river discharge that ranges from 20 m^3/sec to 1000 ^{3}/sec. There is no significant sediment input to the coast brought by the river because of the dam (Güler I., et al., 2003)

Unfortunately, there does not exit many bathymetric measurements of good quality, covering a long time period and large space. The most extensive bathymetric map available is the one that was prepared for an engineering project called "Manavgat su temin projesi". Sea depth measurements were taken for that project at 50 meter intervals over a sea area that covered 6400 m alongshore and 3300 m seaward. The reference point of this data set which is the location where a pipeline enters the sea is N36: 43.781 E031: 30.640 according to WGS-84 geodetic system coordinates, which was used without any coordinate correction.

During the period between 27.05.1996 and 10.02.2000, a jetty type structure with rubble mound section was built in order to fix and protect the mouth of the river. A preliminary study of the changes during that period was done. The results of this study are referred to in the third chapter.

As the first step, a literature search was to find out the models can be used. For nearshore wave models, it was found that SWAN and REF/DIF1 are the best applicable state-of-the art models. For estimating longshore sand transport rates, the most common method utilized is the wave energy flux method. Due to its wide use in many coastal change studies and its appropriateness for the studied area, the GENESIS model was chosen to predict the shoreline changes around the Manavgat River Mouth and to calculate longeshore sand transport rates.

CHAPTER 2

2. REVIEW OF RELEVANT LITERATURE

2.1. COASTAL NUMERICAL MODELING

Computers pervade the day-to-day work in the coastal engineering field. Every few years the computer power available to coastal engineers and scientists increases by an order of magnitude and quality. Along with this trend has come an increase in the demand for and use of computer-based calculation methods and numerical models to aid in solving complex coastal engineering problems. Several numerical models have been prepared for simulating a wide range of coastal processes such as wind, wave generation and propagation, nearshore currents, and sediment transport and beach change. Such modelling efforts are especially useful when there is a lack of measurements or observations in time and space.

2.1.1. Nearshore wave modeling

Waves provide an important energy source for forming beaches; sorting bottom sediments on the shore face; transporting bottom materials onshore, off-shore, and alongshore; and for causing many of the forces to which coastal structures are subjected (SPM, 1984).

Most ocean and sea waves are generated by winds that prevail offshore. The size of generated waves depend on three factors: wind speed, the duration of the wind, and the fetch length which is the distance over which the wind blows (Denny, 1988). As this wind-generated chaotic sea moves away from the generation area, their character changes. The waves organize into swells and tend to propagate in groups and their shape becomes more regular (e.g. sinusoidal). Because of the relatively simple shape and behavior of these waves traveling in very deep water, they can be described by what is known as linear wave theory. Linear wave theory has a number of assumptions; the most important for the modeling application discussed here is that linear wave theory assumes that wave height is small relative to water depth (Denny, 1988).

As waves travel from the deep ocean to shoreline, they undergo a number of transformations (propagation, dissipation and other transformations) , an understanding of which in the nearshore zone is essential during the investigation of any coastal phenomenon. These transformations can be expressed briefly as follow:

Propagation
− Shoaling

As waves enter the shallow water, they undergo a transformation starting from the location where they feel the bottom (at depth approximately one-half the deep-water wave length according the Airy, linear, theory). The wave celerity and length progressively decrease. The wave height first decreases slightly and increases very close to the shoreline. The wave period remains constant (as the number of waves is conserved). At water depths not far beyond the breaker zone, the wave trains consist of a series of peaked crests separated by relatively flat troughs, which finally they break.

- Refraction due to bottom and current variations

Variation in the wave velocity (celerity) occurs along the crest of a wave moving at an angle to underwater contours. The fact that the part of the wave in the deep water moves faster than the part in shallower water, causes the wave crest to bend for becoming more aligned with the contours. This bending effect is called refraction and depends on the ratio of water depth to wavelength (SPR, 1984). Refraction may also be caused by currents or any other phenomenon that cause one part of a wave to travel slower or faster than another part. Refraction by currents occurs when waves intersect the current at an angle and it depends on the initial angle between the wave crests and the direction of current flow, the characteristics of the incident waves, and the strength of the current.

Refraction determines the wave height in any particular water depth for a given set of incident deep-water wave conditions, results in a change in the wave energy distribution and contributes to the alteration of bottom topography by its effect on the erosion and deposition of beach sediments.

The dissipation of wave energy is caused by three different mechanisms:
- Dissipation by whitecapping (in deep water): whitecapping, or wave breaking in deep water, is primarily controlled by the steepness of the waves for which the waveform can remain stable. Waves reaching the limiting steepness begin to break and in so doing dissipate a part of their energy.
- Dissipation by depth-induced wave breaking: when waves moves into shoaling water, the limiting steepness which it can attain decreases, being a function of both the relative depth and the beach slope, perpendicular to the direction of wave advance. Then they break dissipating their energy.

– Dissipation by bottom friction: the bottom friction also causes waves to loose a part of their energy.

Redistribution of wave energy over the spectrum

In deep water, quadruplet wave-wave interactions dominate the evolution of the spectrum. They transfer wave energy from the spectral peak to lower frequencies (thus building their spectral energy causing the shift of the peak frequency to lower values) and to higher frequencies (where the energy is dissipated by whitecapping). In very shallow water, triad wave-wave interactions transfer energy from lower frequencies to higher frequencies often resulting in higher harmonics (Booji et al. 1999). The exact computation of the energy transfer due to both quadruplet and triad interactions, is computationally very expensive. Therefore, approximate parameterizations are usually implemented in practical wave models to include the effect of those interactions.

Diffraction, Reflection, and Wave Set-up

Diffraction of waves is the phenomenon in which energy is transferred laterally along the wave crest. It is most noticeable where an otherwise regular train of waves is interrupted by a barrier such as a breakwater or small island (SPM, 1984). Wave diffraction is especially important to engineers in the construction of breakwaters and other structures. Such structures cut off the wave energy creating a shadow zone, which is usually desired for harbouring boats.

Waves may be either partially or totally reflected from both natural and manmade barriers. Wave reflection may often be as important consideration as refraction and diffraction in the design of coastal structures, particularly for structures associated with harbour development.

Mass transport is induced by wave motion. When transported mass is halted by the shoreline, a current towards offshore is induced. The result of the computation based on the radiation stress concept show that the mean sea level falls below the still water level from offshore to the breaking point. This phenomenon is named set-down. In the surf zone, the mean sea level rises above the still water level. This phenomenon is called wave set-up.

There are currently several nearshore wave transformation models available for use in practical engineering and research problems. Generally, these models differ greatly with regard to the basic modeling approach, the selection of model inputs, as well as user control over the formulation of the model.

Most numerical wave models can be divided into two board classes: phase averaged and phase resolving (Kaihatu, 1997). Kaihatu (1997) describe phase averaged models as expressed in terms of the evolution of a conversed quantity such as wave energy and these models include WAM (Wave Model), SWAN (Simulating Waves Nearshore) and STWAVE. Phase resolving models are formulated in terms of the water free surface and are derived from the governing equations of fluid mechanics (Kaihatu, 1997). REFDIF and RCPWAVE are examples of phase resolving models.

Models in the phase averaging realm, such as WAM, SWAN, and STWAVE, are available for propagating waves over global distances to shelf regions; however their formulations do not include the fine-scale propagation effects that strongly influence the wave field in the nearshore region (Kaihatu, 1997). Phase resolving models such as RCPWAVE and REFDIF can offer physically consistent simulations of fine-scale variations in the nearshore area

due to bathymetric and current effects (Kaihatu, 1997). In this study, two nearshore waves models, SWAN and REF/DIF 1, were used.

Hsu at al. (1997) consider REF/DIF 1 to be the most complete model for combined refraction and diffraction. Other phase average models such as RCPWAVES were compared with laboratory and field data; and Kaihatu (1997) found REFDIF1 results were better. Additionally, RCPWAVE can not be used for locations with a complex bathymetry, such as islands or semi-enclosed coastal areas (Hsu et al., 1997). SWAN model, third-generation wave model to compute short-crested waves in coastal regions with shallow water and ambient currents, is based on the state-of the- art formulations and its results agree well with analytical solutions and laboratory observations and generalized field observations. For the reasons stated above SWAN and REF/DIF 1 were chosen as the wave models to calculate the nearshore wave characteristics.

2.1.1.1. SWAN model

Waves at the surface of the deep water can be well predicted with third-generation wave models that are driven by predicted wind fields (e.g. WAMDI group, 1988). These models are based on the energy or action balance equation and they are sometimes extended to the shelf seas by adding the finite-depth effects of shoaling, refraction and bottom friction. These models do not include the shallow-water effects of depth-induced wave breaking and triad wave-wave iteration; also the numerical techniques that are used are prohibitively expensive when applied to small-scale, shallow-water regions. Therefore they cannot be realistically applied to such regions. To solve this problem there are two alternatives seem to be available: the first is

to extend the approach of the energy or action balance equation by adding the required physical processes using other numerical techniques, the second is to exploit the alternative approach of the models based on mass and momentum balance equations. In Swan model, the depth-induced wave breaking and triad wave-wave iterations are added and in contrast to other third generation models, the numerical propagation scheme is implicit, which implies that the computations are more economic in shallow water.

The SWAN model is a phase-averaged, Eulerian numerical wave model to obtain realistic estimates of wave parameters of random and short-crested waves in coastal regions with shallow water from given wind, bottom, and current conditions. The model is based on the action balance equation with sources and sinks and it is based on the state-of the- art formulations.

Swan model accounts for the following wave propagation processes: propagation through geographic space, refraction due to bottom and current variations, shoaling due to bottom and current variations, blocking and reflection by opposing currents, and transmission through or blockage by sub-grid obstacles.

The following effects of wave generation and dissipation are implemented in SWAN, generation by wind action, dissipation by whitecapping, dissipation by depth-induced wave breaking, dissipation by bottom friction, and redistribution of wave energy over the spectrum by non-linear wave-wave interactions (both quadruplets and triads).

Diffraction is not modelled by the SWAN model. Therefore, it should not be used in areas where wave height variations are large within a horizontal scale of a few wavelengths. Reflections from rigid bodies not accounted for as

well. Because of this, the wave field computed by SWAN will generally not be accurate in the immediate vicinity of obstacles and certainly not in harbors. The depth and currents (if present) are input to SWAN. The depth variation due to wave effect and currents are not computed in SWAN. Wave induced set-up or wave-induced currents cannot be computed simultaneously with waves in SWAN but an approximate wave set-up is available for 1D cases. The propagation in SWAN is rather diffusive. SWAN should therefore not be used at scales larger than (roughly) 25 km.

Model Formulation

In SWAN, waves are described with the two-dimensional wave action density spectrum, even when strong non-linear phenomena dominate (e.g., in the surf zone). The spectrum that is considered here is the action density spectrum $N(\sigma,\theta)$, defined as $N(\sigma,\theta) = E(\sigma,\theta)/\sigma$, rather than the energy density spectrum $E(\sigma,\theta)$ since in the presence of currents, action density is conserved whereas energy density is not (e.g., Whitham, 1974). The independent variables are the relative frequency σ (as observed in a frame of reference moving with the action propagation velocity) and the wave direction θ (the direction normal to the wave crestline of each spectral component).

In SWAN, the evolution of the wave spectrum is described by the spectral action balance equation which for Cartesian coordinates is (e.g., Hasselmann et al., 1973):

$$\frac{\partial}{\partial t} N + \frac{\partial}{\partial x}(c_x N) + \frac{\partial}{\partial y}(c_y N) + \frac{\partial}{\partial \sigma}(c_\sigma N) + \frac{\partial}{\partial \theta}(c_\theta N) = \frac{S}{\sigma} \qquad (2.1)$$

17

The first term in the left-hand side of this equation represents the local rate of change of action density in time, the second and third terms represent propagation of action in geographical space (with propagation velocities c_x and c_y in x and y dimensions, respectively). The fourth term represents shifting of the relative frequency due to variations in depths and currents (with propagation velocity c_σ in σ dimension). The fifth term represents depth-induced and current-induced refraction (with propagation velocity c_θ in θ dimension). The expressions for these propagation speeds are taken from the linear wave theory (e.g., Whitham, 1974; Mei, 1983; Dingemans, 1997). The term S ($= S(\sigma, \theta)$) at the right hand side of the action balance equation is the source term in terms of energy density representing the effects of generation, dissipation and non-linear wave-wave interactions.

Transfer of wind energy to the waves is modeled in SWAN with the resonance mechanism of Phillips (1957) and the feedback mechanism of Miles (1957). The wind input source term is described as follows:

$$S_{in}(\sigma, \theta) = A + B \, E(\sigma, \theta)$$

(2.2)

In which A is the linear growth parameter due to the resonance mechanism and B is the exponential growth parameter due to the feedback mechanism. The effect of currents on wave generation due to wind input is accounted for in SWAN by using the apparent local wind speed and direction.

The dissipation term of wave energy is represented by the summation of three different contributions:

− $S_{ds,w}(\sigma, \theta)$, whitecapping, which is represented by the pulse-based model of Hasselmann (1974). Reformulated in terms of wave number

18

(rather than frequency) so as to be applicable in finite water depth (cf. the WAMDI group, 1988), this expression can be written as:

$$S_{ds,w}(\sigma,\theta) = -\Gamma \; \widetilde{\sigma} \frac{k}{\widetilde{k}} E(\sigma,\theta)$$

(2.3)

where $\widetilde{\sigma}$ and $\widetilde{k}$ denote the mean frequency and the mean wave number respectively and the coefficient Γ is a wave steepness dependent coefficient.

- $S_{ds,b}(\sigma,\theta)$, bottom friction: Three bottom friction models have been selected for this program. Those models are the empirical model of JONSWAP (Hasselmann et al., 1973), the drag law model of Collins (1972) and the eddy-viscosity model of Madsen et al. (1988). The formulations for these bottom friction models can all be expressed by the following general form:

$$S_{ds,b}(\sigma,\theta) = -C_{bottom} \frac{\sigma^2}{g^2 \sinh^2(kd)} E(\sigma,\theta)$$

(2.4)

in which C_{bottom} is a bottom friction coefficient.

- $S_{ds,br}(\sigma,\theta)$, depth-induced breaking. The process of depth-induced wave breaking is still poorly understood and little is known about its spectral modeling. However, the total dissipation (i.e. integrated over the whole spectral space) due to this type of wave breaking can be well modeled with the dissipation of a bore applied to the breaking waves in a random field. In SWAN model the bore based model of Battjes and Janssen (1978) is

used to model the energy dissipation due to depth-induced breaking which is given as:

$$S_{ds,br}(\sigma,\theta) = -\frac{S_{ds.br.tot}}{E_{tot}} E(\sigma,\theta)$$

(2.5)

where $S_{ds.br.tot}$ is the mean rate of energy dissipation per unit horizontal area due to wave breaking and E_{tot} is the total wave energy.

In SWAN the computations of energy transfer due to quadruplet wave-wave interactions are carried out using the Discrete Interaction Approximation (DIA) of Hasselmann et al. (1985) as it is the case for the deep water third generation models such as WAM (WAMDI group, 1988) and METU3 (Abdalla, 1991). For the triad wave-wave interactions The Lumped Triad Approximation (LTA) of Eldeberky (1996), which is a slightly adapted version of the Discrete Triad Approximation of Eldeberky and Battjes (1995) is used in SWAN (Booji et al., 1999).

2.1.1.2. REF/DIF 1 Model

REF/DIF1 is represents a new group of water wave models that have significantly improved accuracy in comparison to previous models. Until recently, only very approximate models existed which relied on ray tracing techniques and excluded diffraction. These models had difficulties modeling waves propagation over complex bathymetries. REF/DIF1 is a weakly non-linear combined refraction and diffraction model that models waves on a uniform grid, thus avoiding many of the shortcomings in ray tracing techniques (Kirby and Dalrymple, 1994). Some explanation of wave

propagation and transformation as waves approach the shore will clarify the modeling procedure.

The weakly nonlinear combined refraction and diffraction model described here (REF/DIF 1) is based on Stokes expansion of the water wave problem and includes the third order correction to the wave speed. The wave height is known to second order (Liu and Tasy, 1984).

The problem of water waves propagating over irregular bathymetry in arbitrary directions is a three-dimensional problem and involves complicated nonlinear boundary condition. In one horizontal dimension, sophisticated models by Chu and Mei (1970) and Djordjev and Redkopp (1978) predict the behavior of Stokes waves over slowly varaying bathymetry. In order to simplify the problem in three dimensions, Berkhoff (1972), noted that the important properties of linear progressive water waves could be predicted by a weighted vertically integrated model. Berkhoff's equation is known as the mild slope equation. It is written in terms of the surface displacement $\eta(x, y)$.

$$\nabla_h.(CC_g\nabla_h\eta) + \sigma^2 \frac{C_g}{C}\eta = 0$$

(2.6)

here,

$C = \sqrt{(g/k)\tanh kh}$, the wave celerity,

$C_g = C\{1 + 2kh/\sinh 2kh\}/2$, the group velocity,

$h(x, y)$, the local water depth, g is the acceleration of gravity, $k(x, y)$ local wave number, h is the water depth, σ angular frequency of the waves given by:

$$\sigma^2 = gk \tanh kh \qquad (2.7)$$

For the linear mild slope equation, Radder (1979) developed a parabolic model, which had several advantages over the elliptic form presented by Berkhoff. Booij (1981) also developed a splitting of elliptic equation, enables the parabolic model to handle waves propagating within   of the assumed direction. This procedure has been used in the previous versions of REF/DIF 1 model (up to 2.3).

In contrast to the mild slope model which is valid for varaying bathymetry, researchers in the area of wave diffraction were developing models for constant bottom applications. For example Mei and Truk, (1980) developed a simple parabolic equation for wave diffraction. Their equation is

$$\frac{\partial A}{\partial x} = \frac{i \partial^2 A}{2k \partial y^2} \qquad (2.8)$$

where A is a complex amplitude related to the water surface displacement by

$$\eta = A e^{i(kx-\sigma t)} \qquad (2.9)$$

Yue and Mie, 1980, developed a nonlinear form of Mei and Truk equation, wich accurately predicts the propagation of third order Stokes wave.

Kirby (1983), using a Lagrangian approach, and Kirby and Dalrymple (1983a), with a multiple scales technique, developed the predecessor to the REF/DIF 1 model which bridged the grape between the nonlinear diffraction models and the linear mild slope equation and can be written in several forms (hyperbolic for time depending applications and elliptic for steady state problems) depending on the application (Kirby and Dalrymple, 1994).

Booij (1981), using Lagrangian approach, developed a version of the mild slope equation including the influence of current. Later a nonlinear correction and the ability to handle strong currents were added by Kirby and Dalrymple (1983a) (the equation can be seen in (Kirby and Dalrymple, 1994)). Kirby (1986a) derived again the mild slope equation including the influence of currents for a wide angle parabolic approximation, which allows the study of waves with large angles of wave incidence with respect to the x axis. In the present version of REF/DIF 1 the equation has been extended to include the more accurate minimax approximation (Kirby, 1986b) for the present version of REF/DIF 1. This equation is given by

$$
(C_g + U)A_x - 2\Delta_1 V A_y + i(\bar{k} - a_0 k)(C_g + U)A
$$
$$
+ \left\{ \frac{\sigma}{2}\left(\frac{C_g + U}{\sigma} \right)_x - \Delta_1 \sigma \left(\frac{V}{\sigma} \right)_y \right\} A + i\Delta' \left[(p - V^2)\left(\frac{A}{\sigma} \right)_y \right]_y
$$
$$
- i\Delta_1 \left\{ \left[UV\left(\frac{A}{\sigma} \right)_y \right]_x + \left[UV\left(\frac{A}{\sigma} \right)_x \right]_y \right\}
$$
$$
+ \frac{i\sigma k^2}{2} D|A|^2 A + \frac{\omega}{2} A + \frac{-b_1}{k} \left\{ \left[(p - V^2)\left(\frac{A}{\sigma} \right)_y \right]_{xy} + 2i\left(\sigma V\left(\frac{A}{\sigma} \right)_y \right)_x \right\}
$$
$$
+ b_1 \beta \left\{ 2i\omega U\left(\frac{A}{\sigma} \right)_x + 2i\sigma V\left(\frac{A}{\sigma} \right)_y - 2UV\left(\frac{A}{\sigma} \right)_{xy} + \left[(p - V^2)\left(\frac{A}{\sigma} \right)_y \right]_y \right\}
$$
$$
- \frac{i}{k} b_1 \left\{ (\omega V)_y + 3(\omega U)_x \right\}\left(\frac{A}{\sigma} \right)_x - \Delta_2 \left\{ \omega U\left(\frac{A}{\sigma} \right)_x + \frac{1}{2}\omega U_x\left(\frac{A}{\sigma} \right) \right\}
$$
$$
+ ik\omega U(a_0 - 1)\left(\frac{A}{\sigma} \right) = 0 \tag{2.10}
$$

where

$$
\beta = \frac{k_x}{k^2} + \frac{\left(k\left(p - U^2 \right) \right)_x}{2k^2 \left(p - U^2 \right)} \tag{2.11}
$$

23

$$\Delta_1 = a_1 - b_1 \tag{2.12}$$

$$\Delta_2 = 1 + 2a_1 - 2b_1 \tag{2.13}$$

$$\Delta' = a_1 - b_1 \frac{\overline{k}}{k} \tag{2.14}$$

and ω is a dissipation factor. The coefficients a_0, a_1 and b_1 depend on the aperture width to specify minimax approximation;

in Kirby (1986) : $a_0 = 1$, $a_1 = -0.5$, and $b_1 = 0$

in Radder`s approximation: $a_0 = 1$, $a_1 = -0.75$, and $b_1 = -0.25$

and in Kirby (1986b) : $a_0 = 0.994733$, $a_1 = -0.890065$, and $b_1 = -0.451641$

in the previous equations, the dissipation relationship relating the angular frequency of the wave, the depth and the wave number is changed to reflect the Doppler shift due to current. The new form of eq. (2.7) is

$$\left(\omega - kU^2\right) = gk \tanh kh \tag{2.15}$$

where

$$\omega = \sigma + kU \tag{2.16}$$

Assumptions in REF/DIF model:

The REF/DIF 1 model, in parabolic form, has a number of assumptions inherent in it. These assumptions are as following:

1. Mild slope. The mathematical derivation of the model equations assumes that the variation in the bottom occur over distances which are long in comparison to a wave length. For a linear model, Booij (1983) for bottom slopes up to 1:3 the mild slope model was accurate

and for steeper slopes it still predicted the trends of wave height changes correctly (Kirby and Dalrymple, 1994).

2. Weak nonlinearity. Strictly the model is based on a Stokes perturbation expansion and therefore is restricted to applications where Stokes waves are valid, unless the Stokes-Hedges nonlinear model dispersion relationship is selected. A measure of nonlinearity is the Ursell parameter which is given as

$$U = HL^2 / h^3 \qquad (2.17)$$

when is exceeds 40, Stokes solution is no longer valid.
In this case, a heuristic dispersion relationship developed by Hedges (1976) is used. In shallow water this relationship matches that of a solitary wave. This relationship is

$$\sigma^2 = gk \tanh\left(kh\left(1 + |A|/h\right)\right) \qquad (2.18)$$

This hybrid model is discussed in more detail in Kirby and Dalrymple (1986). There are, as a result of the different dispersion relationships possible three options in REF/DIF 1 : (1), a linear model, (2), a Stokes-to- Hedges nonlinear model and (3), a Stokes model.

3. The wave direction is confined to a sector ±70° to the principal assumed wave direction, due to the use of the minima wide angel parabolic approximation of Kirby (1986b) (Kirby and Dalrymple, 1994).

Energy dissipation:

Energy dissipation in the model occurs in a number of ways depending on the situation being modeled. The linear form of the mild slope equation with dissipation (w, the dissipation factor) is:

$$\frac{\partial A}{\partial x} = \frac{i\partial^2 A}{k\partial y^2} + wA$$

(2.19)

where the factor w is given depending on the nature of energy dissipation as :

- for laminar surface and bottom boundary layers

the surface film damping :

$$w = \frac{\sigma k \sqrt{(v/2\sigma)}(1-i)}{\tanh kh}$$

(2.20)

the boundary layer damping at bottom:

$$w = \frac{2\sigma k \sqrt{(v/2\sigma)}(1-i)}{\sinh 2kh}$$

(2.21)

- for turbulent boundary layer (using Darcy-Weisbach friction factor)

$$w = \frac{2\sigma k f |A|(1-i)}{2\pi \sinh 2kh \sinh kh}$$

(2.22)

- for porous bottoms, for a given coefficient of permeability Cp:

$$w = \frac{gkC_p(1-i)}{\cosh^2 kh}$$

(2.23)

-

Wave breaking:

The dissipation due to wave breaking is given in REF/DIF 1 due to Kirby and Dalrymple (1986a) as

$$w = \frac{KC_g \left(1 - (\gamma h / H)^2\right)}{h}$$

(2.24)

Where K and γ are empirical constants equal to 0.017 and 0.4 respectively, Kirby and Dalrymple (1994). Here the wave height is, $H = 2|A|$.

Wave climate:

The REF/DIF is typically used with monochromic waves trains propagating in one given direction. The model can also be used with several waves with different directions at a given frequency.

In REF/DIF directional spread is used with a given frequency component, and not for continuous distribution of frequencies as in true directional spectrum. At the present time the REF/DIF 1 model can only calculate waves at a single frequency, and per calculation. The problem of computing the shoreward evolution of directional spectrum of refracting, diffracting and breaking waves has resently been addressed in a new model called REF/DIF S. this model is essentially an enhancement to REF/DIF 1 which allows for the simultaneous computation of many wave components on a large vectorizing computer. Since the amount of computer power required to run REF/DIF S in full spectral mode is enormous, the single component model REF/DIF still be supported and developed, Kirby and Dalrymple (1994).

Numerical development:

The parabolic model is conveniently solved in finite difference form. The numerical solution is based on Crank-Nicholson Technique using forward difference level in x, but centered at $i+1/2$, central difference in y $0(\Delta^2 x, \Delta^2 y)$ using very efficient tridiagonal solver.
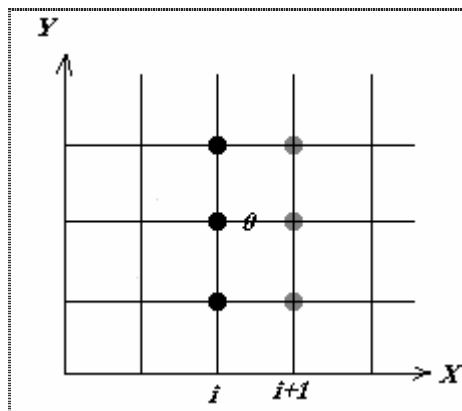
Figure 2.1 Crank-Nicholson numerical solution grid

The model subroutine level can be seen in the schemes below:
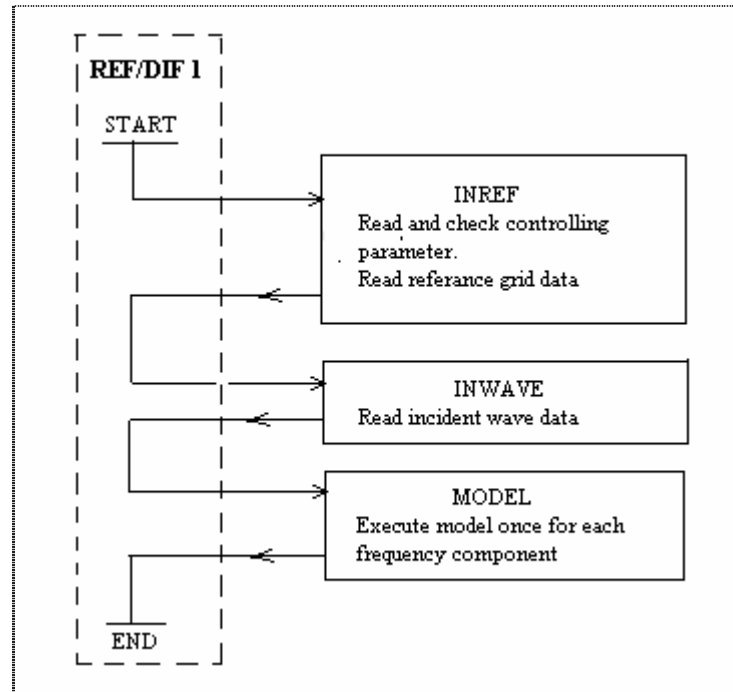
Figure 2.2 REF/DIF 1: model subroutine level

2.1.2.   Sediment Transport Modelling

Obliquely approaching and breaking waves in the nearshore zone combines with various horizontal and vertical patterns of other nearshore currents to transport beach sediments. Sometimes this transport results only in a local rearrangement of sand into bars and troughs or into a series of rhythmic embayments cut into the beach. More serious impacts of this transport result from the extensive longshore displacements of sediments, possibly moving hundreds of thousands of cubic meters of sand along the coast each year (CEM-III, 1998).

In practice, the longshore sediment transport rate can be expressed as the volume transport rate Q_l or as an immersed weight transport rate I_l related to the volume transport rate by

$$I_l = (\rho_s - \rho)g(1-n)Q_l \qquad (2.6)$$

where

ρ_s = mass density of the sediment grains

ρ = mass density of water

g = acceleration due to gravity

n = in-place sediment porosity.

There are several approaches to predict the longshore transport rate. The most commonly used approach is the energy flux method. The second approach, which is suggested by Watson (1980,1982), is based on the longshore transported current. According to this approach the longshore sediment transport calculation is carried out using the breaking-wave-driven longshore current model of Longuet-Higgins (1970). Potential longshore sand transport rates can be also calculated using the wave climate data when available. As an example, the Wave Information Study (WIS) hindcast wave estimates which are given for intermediate to deep water depths is used in the calculation of potential longshore transport in the USA. The littoral drift rose is a useful tool for explaining longshore transport trends along a section of shoreline where the shoreline profile is mild and bottom contours are reasonably parallel to the shoreline. These methods (current, the use of wave climate data, and littoral drift rose methods) are explained in detail in the second chapter of the CEM-III (1998).

2.1.2.1. Wave Energy Flux Method

In 1938, Munch Peterson was the first who related the rate of sand transport to the energy flux of wave in deep water in conjunction with harbour studies on the Danish coast. Later on many studies were made to find out the relation between longshore sediment transport and the wave energy flux (mentioned in CEM-III, 1998).

According to this method, the potential longshore sediment transport rate is correlated with the longshore component of wave energy flux by the following formula:

$$P_l = (E_b C_{gb}) \sin \alpha_b \cos \alpha_b \qquad (2.25)$$

where E_b is the wave energy evaluated at the breaker line, which is given as

$$E_b = \frac{\rho g H_b^2}{8} \qquad (2.26)$$

and C_{gb} is the wave group speed at the breaker line,

$$C_{gb} \cong \sqrt{g d_b} = \left(g \frac{H_b}{\kappa} \right)^{\frac{1}{2}} \qquad (2.27)$$

in which κ is the breaker index H_b / d_b. α_b, is the wave breaker angle relative to the shoreline. The term $(E_b C_{gb})$ is the "wave energy flux" evaluated at the

breaker zone. According to this approach, the immersed weight transport rate, I_l, is given as:

$$I_l = KP_l \qquad (2.28)$$

in which K is an empirical dimensionless coefficient. By using Equations 5.2, 5.3 and 5.4 in Equation 5.5, it can be written as:

$$I_l = K \left(\frac{\rho g^{\frac{3}{2}}}{16\kappa^{\frac{1}{2}}} \right) H_b^{\frac{5}{2}} \sin(2\alpha_b) \qquad (2.29)$$

and the volume transport rate, Q_l, can be found as,

$$Q_l = K \left(\frac{\rho \sqrt{g}}{16\kappa^{\frac{1}{2}}(\rho_s - \rho)(1-n)} \right) H_b^{\frac{5}{2}} \sin(2\alpha_b) \qquad (2.30)$$

Originally, the coefficient K is defined assuming that the root mean square breaking wave height $(H_b)_{rms}$ is utilised. Shore Protection Manual (1984) gives a value of K based on computations utilising the significant wave height as, $K_{SPM.sig} = 0.39$ which corresponds to the root mean square wave related value of $K_{SPM.rms} = 0.92$. The literature provides a wide-range of K values. Recent works suggest the dependence of K on the size of sand particles and the beach slope.

2.1.3. Shoreline Change Modelling

Beach erosion, accretion and changes in the offshore bottom topography occur naturally and artificially due to engineering in coastal zone which influences the sediment movement along and across the shore, changing the beach plan shape and depth contours.

In the planning of projects located in the nearshore zone, prediction of beach evaluation with numerical models has proven to be a powerful technique to assist in the selection of the most appropriate design. The models are essential for the developing of the problem, organizing the data, analyzing the data and for solving the data under various circumstances. Beach models can be classified as follows:

Analytical models of shoreline change:

Analytical models are closed form mathematical solutions of a simplified differential equation for shoreline change. Because of the many idealizations needed to obtain a closed-form solution, particularly the requirement of constant wave in space and time, analytical models are too crude for use in planning or design phase, except possibly in preliminary stage of project scooping.

Profile erosion models:

This type of model is used mostly for the evaluation of beach change on the upper profile produced by storms and for the initial adjustment of beach fills to wave action. This type of models is simplified by omitting the

longshore transport processes. For example, longshore process is assumed as constant so that only one profile at a time along the coast is treated.

Shoreline change models:

This type of modelling enables the calculation of the evolution of the shoreline under a wide range of beach, coastal structure, wave, and initial and boundary conditions, which may vary in space and time, as appropriate. The profile shape is assumed to remain constant, in principle, landward and seaward movement of any contour could be used in the modelling to represent beach position change. Thus, this type of model is sometimes referred to as a "one-contour line" model or, simply, "one-line" model. Since the mean shoreline position (zero-depth contour) or similar datum is conveniently measured, the representative contour line is taken to be the shoreline. Longshore sand transport together with lateral boundary conditions on each of the two ends of the model grid are the dominant causes of beach change in the shoreline change model.

Schematic 3-D Models:

Three-dimensional beach change models describe bottom elevation changes, which can vary in both horizontal (cross-shore and longshore) directions. Therefore, the fundamental assumptions of constant profile shape used in shoreline change models and constant longshore transport in profile erosion models are removed. However the achivement of this goal is limited by the capability to predict wave climate and sediment transport rates. Perlin and Dean (1978) extended the "two-line model" of Bakker (1968) to an n-line model in which depths were restricted to monotonically decrease with

distance offshore for any particular profile. Schematized 3-D beach change models have not yet reached the stage of wide application due to complexity.

Fully 3-D Models:

Waves, currents, sediment transport, and changes in bottom elevation are calculated point by point in small areas defined by a horizontal grid placed over the region of interest. This kind of models requires special expertise and use of powerful computers.

2.1.3.1. GENESIS model

The shoreline change numerical model is the only general purpose engineering model presently available for wide application in simulating long-term evolution of the beach plan shape. With the development of GENESIS, the potential of the shoreline change model has reached a stage where it can be operated without expertise in numerical modelling. Briefly basic assumptions of shoreline change modelling are:

- The beach profile shape is constant.
- The shoreward and seaward limits of the profile are constant.
- Sand is transported alongshore by the action of breaking waves.
- The detailed structure of the nearshore circulation is ignored.
- There is a long-term trend in shoreline evolution.
- The beach profile moves parallel to it self so that it translates shoreward or seaward without changing its shape in the course of eroding and accreting (Pelnard-Considere, 1959 referring to GENESIS Report). If the profile shape does not change, any point on it to specify the location of the entire profile with respect to a baseline (one-line model).

Sand is transported along shore between two well-defined limiting elevation on the profile. The shoreward limit is located at the top of active berm and the seaward limit is located at the location where no significant depth changes occur which is called depth of profile closer as stated in "GENESIS, Report 1, Technical References". These limits are used to determine the perimeter of a beach cross-sectional area by which the changing in volume, leading to shoreline change, can be computed.

The transport rate formula contained in Version 2 of GENESIS describes longshore sand transport produced solely by incident waves. It does not describe transport produced by tidal currents, wind, or other forcing agents, indicating that the model should not be used if breaking waves are not the dominant mechanism for transport sand alongshore.

GENESIS does not account for the full vertical and horizontal water and sand circulation, making it incapable, for example, of describing transport by rip currents, undertow or return flow, or other 3-D fluid and transport processes.

The assumption that there must be a long-term trend in shoreline evolution means that a boundary condition or some other systematic process, for example, a river discharge, or a regular change in the wave pattern such as produced by a detached breakwater, dominates the beach change.

- *Governing equations for shoreline change*

The equation governing shoreline change is formulated by conservation of the sand volume. The y-axis points offshore and the x-axis is oriented

parallel to the trend of the coast (distance alongshore). The related terms in the equation (1), which is the governing equation of shoreline change, are as follows:

Δy: the change in shoreline position.

Δx: the length of the shoreline segment.

D_B: berm elevation.

D_C: the closure depth.

q: line source or sink of sand ($q = q_s + q_0$).

q_s: volume of sand added or removed per unit width of beach from shoreward side.

q_0: volume of sand added or removed per unit width of beach from offshore side.

As $\Delta t \longrightarrow 0$ the governing equation for the rate of shore line position is:

$$\frac{\partial y}{\partial t} + \frac{1}{(D_B + D_C)} \left[\frac{\partial Q}{\partial x} - q \right] = 0 \tag{2.31}$$

In order to solve Equation (2.31), the initial shoreline position over the full reach to be modelled, boundary conditions on each end of the beach, and values for Q, q, D_B, and D_C must be given.

- *Sand transport rates*

Longshore sand transport

The empirical predictive formula for the longshore sand transport rate used in GENESIS (GENESIS Report 1)is:

$$Q = (H^2 C_g)_b \left[a_1 \sin 2\theta_{bs} - a_2 \cos \theta_{bs} \frac{\partial H}{\partial x} \right]_b \qquad (2.32)$$

where;

H= wave height

Cg = wave group speed given by linear wave theory

b= subscript denoting wave breaking condition

θ_{bs} = angle of breaking waves to the local shoreline

The non-dimensional parameters a_1 and a_2 are given as:

$$a_1 = \frac{k_1}{16(\rho_s / \rho - 1)(1 - P)(1.416)^{5/2}}$$

and (2.33)

$$a_2 = \frac{k_2}{8(\rho_s / \rho - 1)(1 - p)\tan \beta (1.416)^{7/2}}$$

where;

k_1, k_2 = empirical coefficient, treated as a calibration parameter

ρ_s = density of sand (taken to be 2.65 103 kg/m3 for quartz sand)

ρ = density of water (1.03 10^3 kg/m3 for seawater)

p = porosity of sand on the bed (taken to be 0.4)

$\tan \beta$ = average bottom slope from the shoreline to the depth of active longshore sand transport.

The first term in Equation (2.32). corresponds to the "CERC formula" described in the SPM (1984) and accounts for longshore sand transport produced by obliquely incident breaking waves. The second term in Equation 2 is not part of the CERC formula and is used to describe the effect of another generating mechanism for longshore sand transport, the longshore

gradient in breaking wave height. In fact normally this term is small comparing to the first one but it gains importance when existence of a structure causes diffraction.

k_1 and k_2 coefficients are called as the "transport parameters" in calibration of the model. k_1 varies between 0.1 –1 and k_2 varies between 0.5 – 1.5 times of k_1 (GENESIS Report 2).

- *Empirical parameters*

Depth of longshore transport

The width of the profile over which longshore transport takes place under a given set of wave conditions is needed to estimate the amount of sand (percentage of total) bypassing occurring at groins and jetties. Since the major portion of alongshore sand movement takes place in the surf zone, this distance is approximately equal to the width of the surf zone, which depends on the incident waves, principally the breaking wave height.

In Version 2 of GENESIS, a quantity called "the depth of active longshore transport, " D_{LT} is defined and set equal to the depth of breaking of the highest one-tenth waves at the updrift side of the structure.

$$D_{LT} = \frac{1.27}{\gamma} \left(H_{1/3} \right)_b \tag{2.34}$$

1.27 = conversion factor between one-tenth highest wave height and significant wave height,

γ = breaker index, ratio of wave height to water depth at breaking,

$\left(H_{1/3}\right)_b$ = significant wave height at breaking.

GENESIS uses another characteristic depth, termed the "maximum depth of longshore transport" D_{LT0} to calculate the average beach slope $\tan_\beta$ appearing in Equation (2.33). The quantity D_{LT0} is calculated as:

$$D_{LT0} = \left(2.3 - 10.9 H_0\right)\frac{H_0}{L_0} \tag{2.35}$$

Equation (2.35) was introduced by Hallermeier (1983) to estimate an approximate annual limit depth of the littoral zone under extreme waves (GENESIS Report 1).

Average profile shape and slope

It is assumed that the profile moves parallel to itself. However, to determine the location of breaking waves alongshore and to calculate the average nearshore bottom slope used in the longshore transport equation, a profile shape must be specified. For this purpose, the equilibrium profile shape deduced by Bruun (1954) and Dean (1977) is used (GENESIS Report 1):

$$D = Ay^{2/3} \tag{2.36}$$

in which D is the water depth, and A is an empirical scale parameter.

The scale parameter A has been shown by Moore (1982) (GENESIS Report1, Technical Reference) to depend on the beach grain size d_{50} (d_{50} expressed in mm and units of A of $m^{1/3}$):

$$A = 0.41(d_{50})^{0.84}, d_{50} \prec 0.4$$
$$A = 0.23(d_{50})^{0.32}, 0.4 \le d_{50} \prec 10.0$$

(2.37)

$$A = 0.23(d_{50})^{0.28}, 10.0 \le d_{50} \prec 40.0$$
$$A = 0.46(d_{50})^{0.11}, 40.0 \le d_{50}$$

The average nearshore slope $\tan\beta$ for the equilibrium profile defined by equation (2.36) is calculated as:

$$\tan\beta = \left(\frac{A^3}{D_{LT0}}\right)^{1/2}$$

(2.38)

Depth of closure

The depth of closure is the seaward limit beyond which the profile does not exhibit significant change in depth and it is difficult to determine this parameter to small bathymetric changes. It is recommended that both bathymetry surveys and equation 2.35 to be used to check the consistency of values obtained. GENESIS uses an average closure depth for the entire model (GENESIS Report 1).

It is recommended that both bathymetry (profile) surveys and Equation 5 (Hallermeier, 1983) be used as a check of the consistency of values obtained. On an open-ocean coast, the depth of closure is not expected to show significant longshore variation, since the wave climate and sand characteristics would be similar. However, in the case of the existence of large structures such as long jetties or break waters, the wave climate changes due to sheltering effects of that the depth closure will may be smaller. This kind of assumption is not counted in GENESIS since it is accepted that the depth closure is same everywhere.

- *Wave calculation*

Offshore wave information can be obtained from either a hindcast calculation, or from an actual wave gage. Wave data are input to the model at a fixed time interval, typically in the range of 6 to 24 hr. The wave height and direction at the gage must be transformed to breaking at intervals alongshore for input to GENESIS. Monochromatic wave models hold the wave period constant in this process.

The modelling system GENESIS is composed of two major submodels. One submodel calculates the longshore sand transport rate and shoreline change. The other submodel is a wave model that calculates, under simplified conditions, breaking wave height and angle alongshore as determined from wave information given at a reference depth offshore. This submodel is called the internal wave transformation model, as opposed to another, completely independent, external wave transformation model which can be optionally used to supply nearshore wave information to GENESIS. The availability and reliability of wave data as well as the complexity of the nearshore bathymetry should be used to evaluate which wave model to apply.
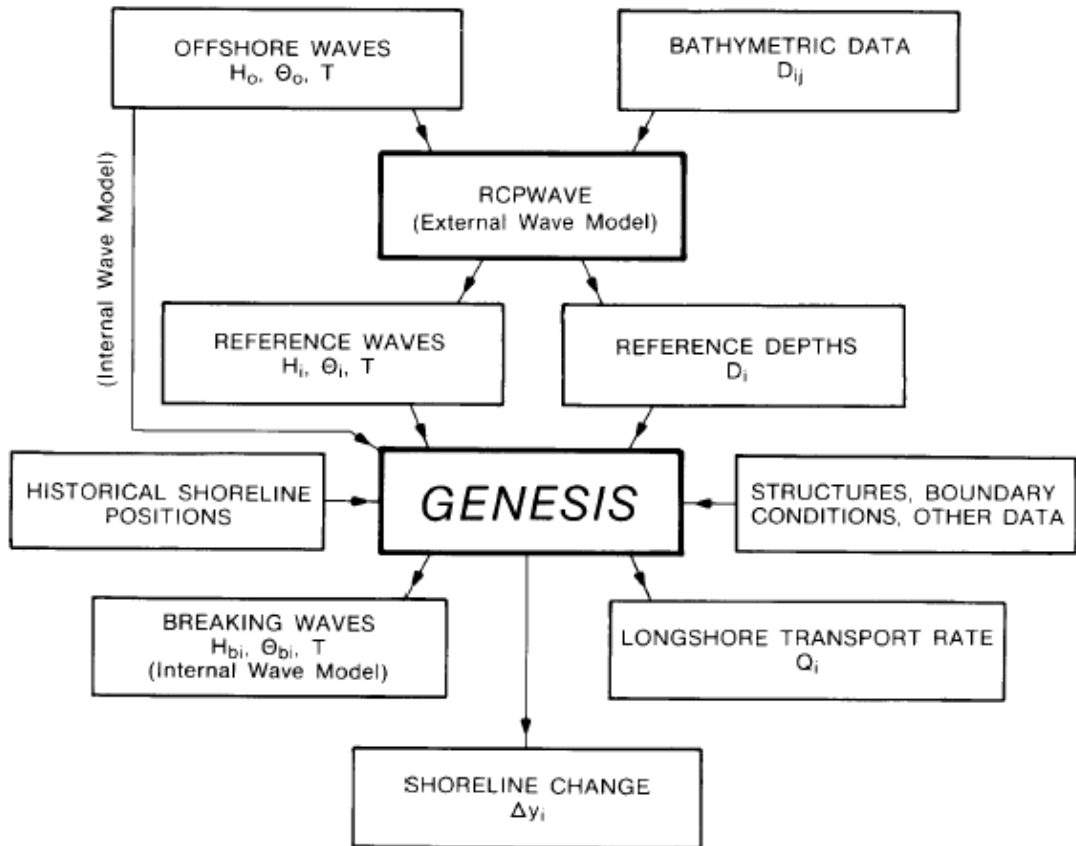
Figure 2.3 GENESIS, RCPWAVE, and the overall calculation flow

- *Grid system*

In GENESIS calculated quantities along the shoreline are discretized on a staggered grid in which shoreline positions y_i are defined at the centre of the grid cells ("y-points") and transport rates Qi at the cell walls ("Q-points"), as shown in Figure 2.4. The left boundary is located at grid cell 1, and the right boundary is at cell N. In total there are N values of the shoreline position, so the values of the initial shoreline position must be given at N points. There are N+l values of the longshore sand transport rate since N+l cell walls enclose the N cells; values of the transport rate at boundaries must

be specified (Q_1 and Q_{n+1}). GENESIS will calculate the remaining values. Since Q_1 is a function of the wave conditions all wave conditions are calculated at Q-points. The tips of structure are located at Q-points. Beach fills; river discharges and other sand sources and sinks are located at y-points.
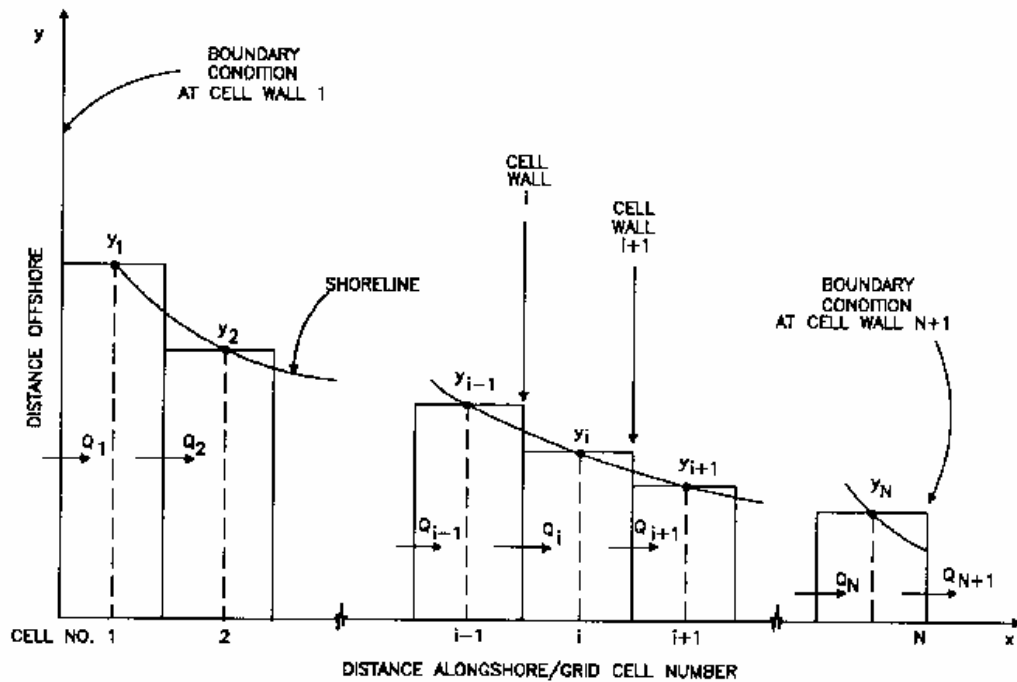
Figure 2.4 Finite difference staggered grid for GENESIS

- *Numerical solution scheme*

In order to describe realistic structure and shoreline configurations, including waves that vary alongshore with time, Equation 1 most be solved numerically. The allowable grid spacing and time step of a finite difference numerical solution of partial differential equation such as Equation 1 depend on the type of solution scheme. Under certain idealized conditions and simplification it is easy to examine the dependence of the solution on the

time and space steps. The main assumption is θ_{bs} in Equation 2 is small, therefore:

Sin $\theta_{bs} = 2\theta_{bs}$. It is also assumed that θ_b does not change with x. Also for simplicity, the line source or sink (q) is omitted from Equation 1 and after some mathematical manipulations Equation 1 can be written as:

$$\frac{\partial y}{\partial t} = (\varepsilon_1 + \varepsilon_2)\frac{\partial^2 y}{\partial x^2} \tag{2.39}$$

where;

$$\varepsilon_1 = \frac{2k_1}{(D_B + D_c)}(H^2 C_g)_b \tag{2.40}$$

and

$$\varepsilon_2 = \frac{k_2}{(D_B + D_c)}\left(H^2 C_g \cos\theta_{bs}\frac{\partial H}{\partial x}\right)_b \tag{2.41}$$

The numerical stability of the calculation scheme is governed by:

$$R_s = \frac{\Delta t(\varepsilon_1 + \varepsilon_2)}{(\Delta x)^2} \tag{2.42}$$

Equation (2.31) can be solved by either an explicit or an implicit solution scheme. If solved using an explicit scheme, the new shoreline position for each of the calculation cells depends only on values calculated at the previous time step. The main advantages of the explicit scheme are easy programming. A major disadvantage is, however, preservation of stability of

the solution, imposing a severe constraint on the longest possible calculation time step for given values on model constants and parameters.

If equation (2.31) is solved using implicit scheme in which the new shoreline position depends on values calculated on the old, as well as the new, time step. The main advantage of the implicit scheme is that it is stable for very large values of Rs. The disadvantages of the implicit solution scheme are that the program, boundary conditions, and constraints become more complex, as compared with the explicit scheme. These disadvantages are, however, not considered to be major when compared with its advantage. Roughly speaking, for values of Rs less than 10, the numerical error equalled the magnitude of R~ expressed as a percentage. Above the value of 10, the error increased at a greater than linear rate with Rs . GENESIS calculates the value of Rs at each time step at each grid point alongshore and determines the maximum value. If Rs > 5 for any grid point, a warning is issued (GENESIS Report 1).

CHAPTER 3

3.   PRESENTATION AND DISCUSSION OF RESULTS

Ref/Dif 1, (Kirby and Dalrymple, 1994) and SWAN (Booji N. et. al., 1999) wave models were used to simulate wave propagation over the bathymetry of the sea bottom offshore the Manavgat River mouth for obtaining the nearshore wave conditions to be used as input data for the GENESIS model in order to estimate the shoreline changes.

3.1   Input Data

Necessary input data for Ref/Dif 1, SWAN, and GENESIS models are described in this part with explanation of the important features related to Manavgat case.

3.1.1   REF/DIF 1 Input Data

Ref/Dif 1 is a representative of a new group of water wave models that have significantly improved accuracy in comparison to previous models. Until recently, only rough approximate models, which relied on ray tracing techniques and excluded diffraction,were available. These models had

problems with modeling waves propagation over complex bathymetries. Ref/Dif 1 is a weakly nonlinear parabolic refraction and diffraction model. The weak nonlinearity of Ref/Dif 1 results from a Stokes perturbation expansion, in which wave heights are calculated to the second order while wave phase speed is corrected to the third order (Kirby and Dalrymple, 1994). Stokes theory is not accurate for shallow water conditions, so a Hedges dispersion relationship is incorporated into Ref/Dif 1. Kirby and Dalrymple (1986) combined the Stokes and Hedges theories to cover the range of deep to shallow water. The Stokes-Hedges hybrid solution was used in the Ref/Dif 1 calculations for this study.

REF/DIF 1 is based on the parabolic mild slope equation that includes two major assumptions. The first is Berkhoff's mild slope equation, which is so named because it assumes a slowly varying bathymetry. However, Booij (1983) found that for bottom slopes up to 1V:3H the mild slope model accurately simulated wave characteristics, and for steeper slopes, it still predicted the trends of wave height changes and reflection coefficients correctly. The bathymetry utilized in this study can be characterized as consisting of mild slopes and therefore does not pose a problem.

The second assumption involves the parabolic approximation, or Radder's approximation, of the mild slope equation that reduces a boundary value problem to an initial value problem where only the initial condition and the two lateral conditions need to be specified (Kaihatu, 1997). One important consequence of the parabolic approximation is that waves can only propagate in the forward direction. Therefore, slightly reflected waves are included while waves reflected into the opposite direction of wave

propagation are neglected. For this study, wave reflection is minimal and can be neglected.

REF/DIF 1 inputs include a bathymetry grid, initial wave height and period, and other model characteristics such as a closed or open boundary and bottom boundary damping. In this study, open boundary conditions were used to minimize model boundary effects. Turbulent bottom boundary damping was implemented, since it provides the best approximation of bottom damping under natural conditions.

3.1.1.1 Wave Data

The nearshore wave data are required as input boundary condition for the GENESIS shoreline model. However to obtain these data, deep water wave data are the main input to the nearshore wave models in addition to other data such as bathymetric and current data. The necessary deep-water wave data for this study are obtained form the Wave Atlas of the Turkish coasts (Özhan and Abdalla, 1999), which is the main result of the a major project aimed to find out the wave climate affecting the Turkish coastline as well as the whole Black Sea coasts called The NATO TU-WAVES (Özhan and Abdalla, 1992, 1993a & 1993b and Özhan et al., 1995, 1999). This project was supported from the NATO Science for Stability (SfS) Program-Phase III. The basic results of the wave climate computations at the Manavgat river mouth location (36.500N, 31.30^0 E) are shown in the Figure 3.1.
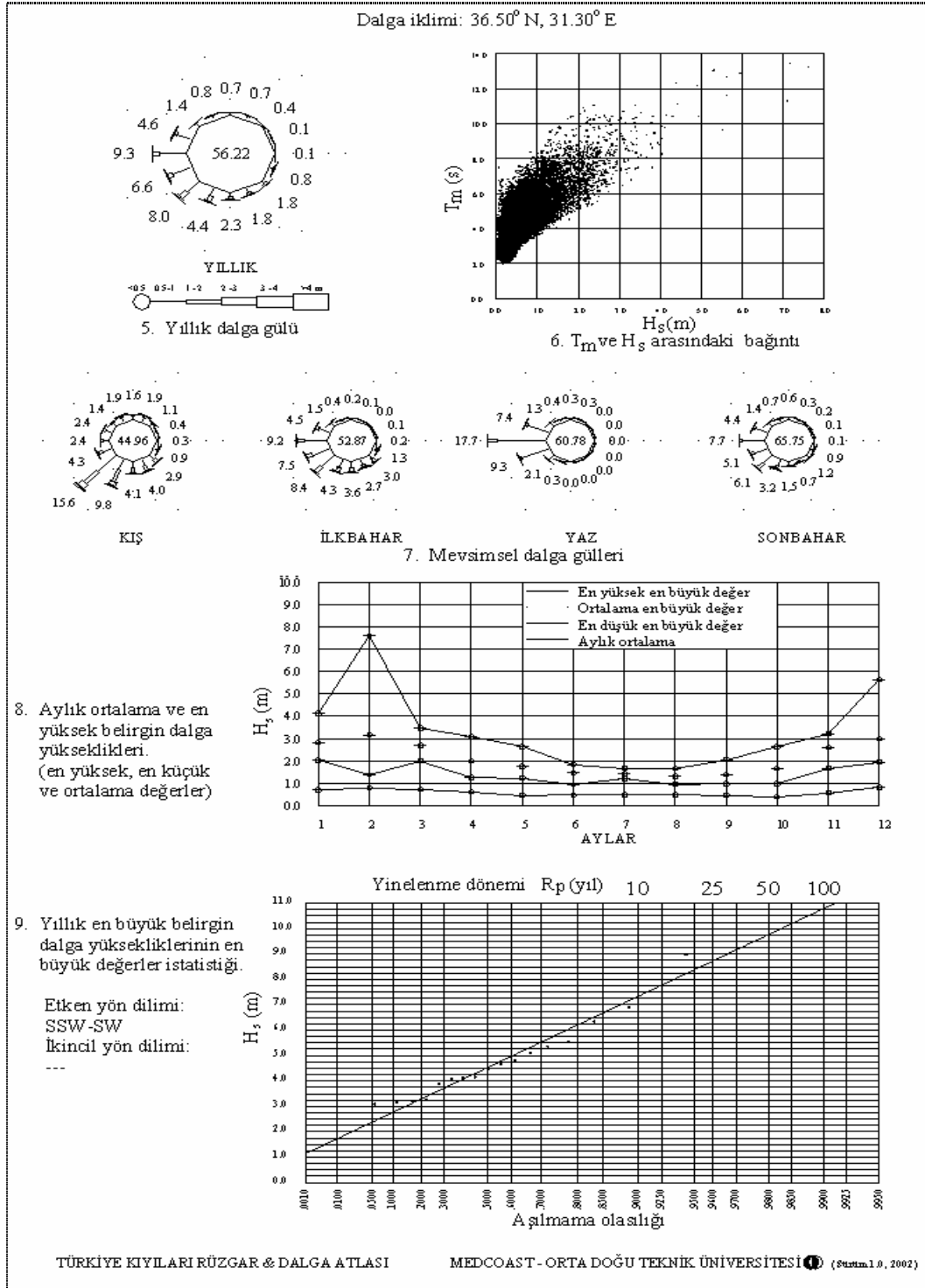
Figure 3.1. Wave Atlas's page for the wave climate of the Manavgat River mouth.

Figure 3.1 shows the following information available for the Manavgat River mouth:

- The annual wave rose, which provides the directional distribution of the average occurrence percentages of various significant wave height (H_s) levels during the whole year.

- Significant wave height-mean wave period scatter diagram, which presents the relation between the significant wave height H_s and the mean wave period T_m (both measured). In this study it is recommended to use the lower part of this scatter as the upper part corresponds to swell waves, and the lower represents the sea waves.

- Seasonal wave roses, they are similar to the annual wave rose except for the time representation. Each rose represents the directional distribution of the average occurrence percentages of different significant wave height H_s levels during one of the four seasons.

- Monthly mean and monthly maximum significant wave heights. In this graph, the monthly mean significant wave height H_s is given as the average of all significant wave heights occurred in a given month during a time interval of 8 years (September 1991-July 1999). It is important to keep in mind that in the calculation of sediment transport we need the $\overline{(H_s^2)}$ not the $(\overline{H_s})^2$ and $(\overline{H_s})^2 \leq \overline{(H_s^2)}$. Also the monthly the largest (maximum) wave height during the same period and the lowest (minimum) are given.

- The last item in the Figure 3.1 is the extreme value statistics for significant wave heights, in which the annual peak significant wave height H_s value are plotted on Gumbel paper by assuming that the annual maxima follow the Gumbel distribution.

The shoreline adjacent to the Manavgat River makes an angle of 23 degree with the east direction as it is shown in Figure 3.2 in which the directions and heights of waves affecting the river mouth can be clearly seen. As it is observed from the figure not all segments of the wave rose affect the Manavgat coastal area since some directions point offshore. Table 3.1 shows waves with their percentages that are used in the calculations.

Table 3.1 shows the waves affecting the studied area with their heights, periods, percentages, and directions. The wave heights were taken as the average values of each wave height band. The corresponding wave periods were found from the significant wave height-mean wave period scatter diagram (Figure 3.1). The occurrence percentages were calculated by dividing the number of waves of each band by the total waves number recorded.
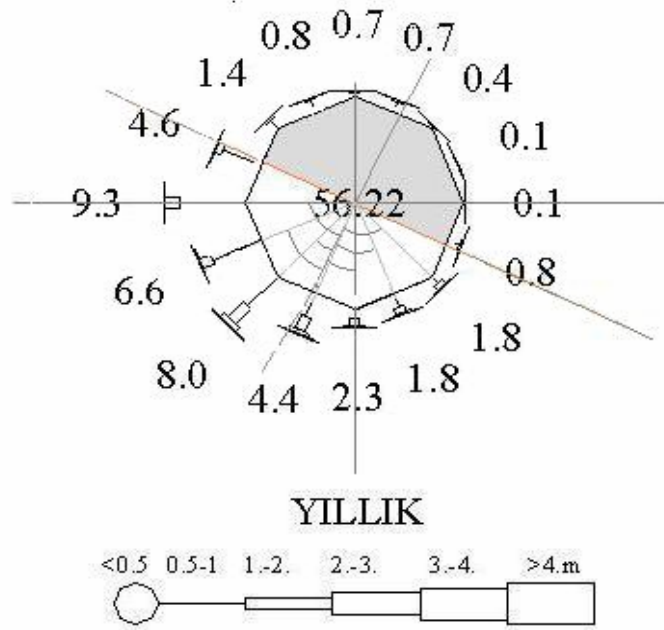
Figure 3.2. The part of the annual wave rose that affects the Manavgat coastal area.

Table 3.1 Deep-water waves affecting the Manavgat River mouth.

DIR	CALM%	0.5-1 (0.75 m) T=4sec	1.-2. (1.5 m) T=6sec	2.-3. (2.5 m) T=7.5sec	3.-4. (3.5 m) T=9sec	>4. (4.5 m) T=10.2sec	DIR-PER	REF/DIF DIR.
E	56.22	0.0973998	0.0465825	0	0	0	0.1	not included
ENE	56.22	0.1270433	0.0084696	0.0042348	0	0	0.1	not included
NE	56.22	0.2498518	0.1058694	0	0	0	0.4	not included
NNE	56.22	0.4658254	0.1736258	0.0127043	0	0	0.7	not included
N	56.22	0.5208774	0.1312781	0.0127043	0	0	0.7	not included
NNW	56.22	0.6521555	0.1778606	0.0127043	0	0	0.8	not included
NW	56.22	1.1476243	0.2625561	0.0127043	0	0	1.4	not included
WNW	56.22	3.7604811	0.8681291	0.0211739	0	0	4.6	not included
W	56.22	7.5251969	1.6981452	0.0677564	0	0	9.3	-67
WSW	56.22	5.1283137	1.3127806	0.114339	0	0	6.6	-44.5
SW	56.22	4.7175404	2.5112222	0.5928686	0.1270433	0.0423478	8	-22
SSW	56.22	2.0538664	1.7489625	0.4615906	0.0804607	0.0338782	4.4	0.5
S	56.22	1.2873719	0.7876683	0.1990345	0.0127043	0	2.3	23
SSE	56.22	0.9147116	0.7622597	0.1651563	0.0042348	0	1.8	45.5
SE	56.22	0.9739985	0.6733294	0.1016346	0.0211739	0	1.8	68
ESE	56.22	0.4997036	0.2413822	0.0338782	0.0042348	0	0.8	not included

3.1.1.2 Bathymetric Data

A good quality bathymetric data, covering a sufficiently long time period and large space, is not available around the Manavgat river mouth. The only available somewhat comprehensive bathymetric data was compiled as a part of "Manavgat su temin projesi". The water depth measurements covered a sea area 6400 m alongshore and 3300 m seaward with 50 m space intervals. The reference point of this set of data, the place where the pipe which provide fresh water to the offshore terminal in that project enters the sea, is N36: 43.781 E031: 30.640 according to the WGS-48 geodetic system coordinates that were used without any coordinate correction.

Depth measurements were carried out for the period between 8th and 24th July 1992 by taking the mean water level as datum by the Echo Sounder device. Transducer depth correction was made (Manavgat Su temin projesi batimetri raporu). These measurements indicate that the water depths increase almost linearly (with almost constant slope away from the coast). The rate of increase in front of the Manavgat river mouth is relatively faster (with a steeper slope) as seen in Figure 3.3.
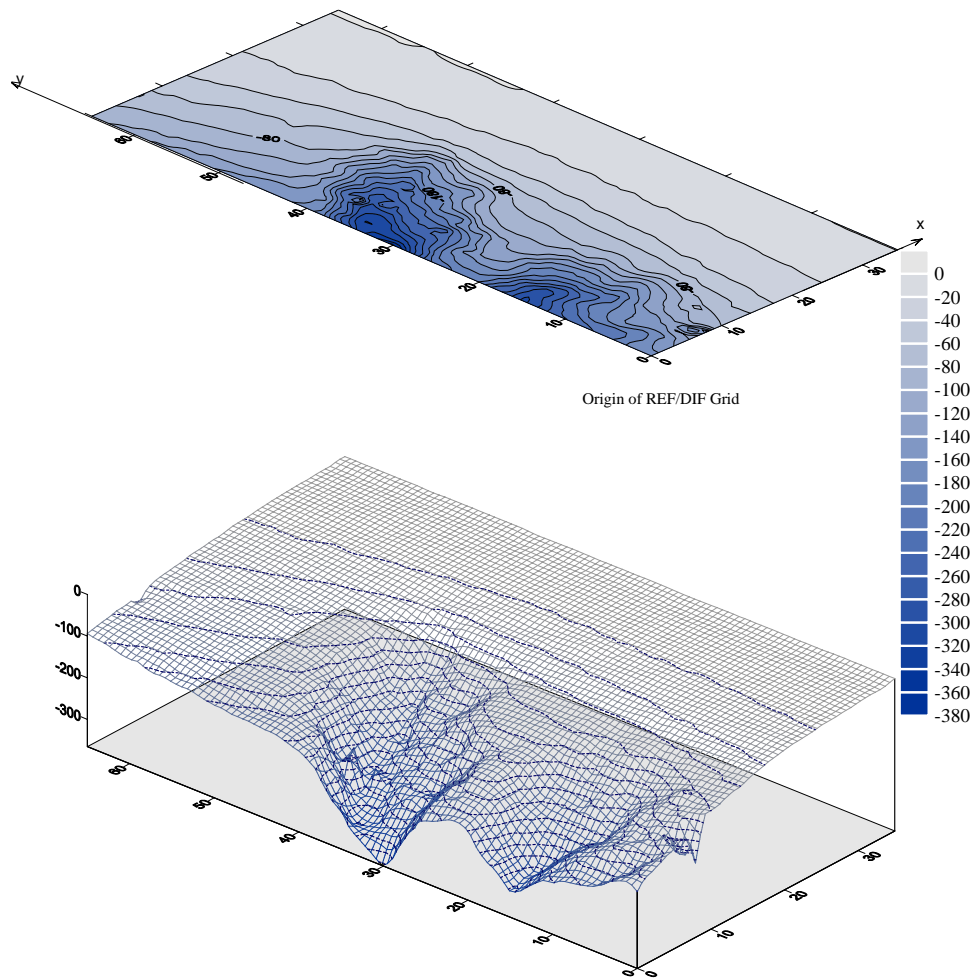
Figure 3.3 Bathymetric map offshore the Manavgat River mouth

As it is mentioned in the Ref/Dif 1 user manual, the origin of Ref/Dif domain is always chosen to be the lower right-hand corner of the domain

with the x-axis pointing in the propagation direction and the y-axis pointing towards left. The origin of the Ref/Dif domain used in this study is shown in the Figure 3.3.

Some simple bathymetric maps were also available covering the period between 27.05.1996 and 10.02.2000 during and after the construction of a coastal structure (jetty type with rubble mound) that has been built in order to fix and protect the mouth of the river. A study was carried out to investigate the shoreline changes around the mouth of Manavgat River by digitizing those maps. From that study it can be seen that the river mouth moved about 144 m. westward. The width of the mouth changed from 150 m. with approximately about 1 m. water depth to 47 m. with almost 3-3.5 m. water depth. There was deposition almost in the all studied area and the shoreline behind the protection structure (in the east side) moved about 40 m. seaward as it is seen in the figures provide in appendix A.

In order to operate the Ref/Dif 1 model over a certain bathymetry, several files need to be created. The main input files for Ref/Dif 1 are the file called param.h (which must be created in order to store the dimension of the grid -see used param.h in appendix B), a file including information about the bathymetry grid with reasonable space interval called refdat.dat, and a file including the wave data and other needed input data called indat.dat .

The square grid used in this study was a 141 by 255 cell with space increments of 25x25 m. . However when the model did not give good results in the case of relatively small waves, a part of this grid was dropped (the part being in the deep water part) and a grid of 61 by 255 cells with 25 m. interval was utilized. The refdat.dat files can be seen in appendix B.

The indat.dat file contains all the information needed to control the operations of the program, and all of the input wave data. The data is arranged in several lists and put in the indat.dat file using the namelist convention. These different namelist groups are defined according to the following namelist statement: Ingrid, inmd, fnames, waves1a, waves1b, waves1c, and waves2. The definition of each input variable of the namelist groups are briefly listed bellow with the values that have been used in running REF/DIF for Manavgat grid.

Ingrid namelist

- mr, nr are grid dimensions with maximum values are ixr, iyr respectively (ixr, iyr values are given in param.h). In the trail runs of REF/DIF 1 it has been seen that the model does not complete the operation as the water depth is so deep for some waves so that the bottom does not affect them.. After some trial runs, the selected grid dimensions, mr and nr, according to wave heights and period are listed in the table below:

Table 3.2 Grid dimensions and incoming wave heights and periods used in REF/DIF 1

mr	nr	H (m.)	T (sec.)
141	255	4.5	10.2
141	255	3.5	9
61	255	2.5	7.5
61	255	1.5	6
61	255	0.75	4.2

- iu switch for the physical units iu=1, MKS; iu=2 English
- ntype, nonlinearity, ntype=1 linear, ntype=1 composite model, and ntype=2 stokes wave model.
- Icur, input current data, icur=0, no currents input, iccur=1, currents input. For Manavgat grid icur=0 as there is no current affecting the Manavgat river mouth (Güler I, 1996)
- ibc is the boundary condition switch. ibc=0 closed boundaries, ibc=1, open boundaries.
- dxr, dyr are the reference grid x-spacing and y-spacing, which are assumed to be uniform over the entire reference grid.
- dt is the depth tolerance value.
- ipace, nd: ispace is controlling subdivisions; ispace=0 program attempts its own x subdivisions. ispace =1, user specifies x subdivisions. nd is the number of y subdivisions.
- iff(1), iff(2), iff(3) are dissipation switches iff(1)=1 turning on turbulent boundary layer; iff(2)=1 turn on porus bottom damping; iff(3)=1 turn on laminar boundary layers. In case on no damping, all values equal zero.
- Isp, user-grid specification, isp=0 switch to no sub grid to be read; isp=1 sub grid will be read.
- Iinput, specifies whether the program or user will generate the first row of complex amplitude A value. Iinput=1 the program will sepecify it, iinput=2 user specifies A in an external data file wave.dat.
- ioutput, specifies the last complex amplitude A are to be stored in owave.dat . ioutput=2 turns the option on and ioutput=1 skips it.

inmd namelist group

- md(ixr): if ispace=1 the x-direction subdivisions are inserted here and the array md must be dimensioned according to the value of ixr in param.h.

fnames namelist group

This group includes the input and output file names. These names are listed in the table bellow, and it is important to know that the files in italic underlined font are the files needed in our case.

Table 3.3 Inputs and out put files of REF/DIF 1

No:	name	information included in the file
filename1	*refdat.dat*	*grid data*
filename2	*outdat.dat*	*old standard output data file*
filename3	subdat.dat	user-specified subgrids
filename4	wave.dat	user-specified complex amplitude on first row (iinput=2)
filename5	owave.dat	complex amplitude on last row (iouput=2
filename6	surface.dat	complex amplitude data for constructing an image of water suface
filename7	bottomu.dat	bottom velocity
filename8	*angle.dat*	*calculated wave directions at reference grid points*
filename9		not used at present dummy name
filename10	refdif1.log	run logo for REF/DIF 1program
filename11	*height.dat*	*calculated wave heights at reference grid points*
filename12	sxx.dat	Sxx components at reference grid locations
filename13	sxy.dat	Sxy components at reference grid locations
filename14	asyy.dat	Syy components at reference grid locations
filename15	*depth.dat*	*tide correlated depths at grid points*

If iinput=1 the rest of indat.dat is as follows:

waves1a namelist group

- iwave switch for wave filed type. Iwave=1 discrete components. Iwave=2 directional spreading model.
- Nfreqs is the number of frequency components to be run whos maximum value is ncomp in parm.h.

For iwave=1

waves1b namelist group

- freqs: wave period for each frequency component.
- Tide: tidal offset.
- nwaves number of wave component for each frequency.
- amp: amplitude for each component wave.
- dir: direction in degrees relative to x axis for wave.

For iwave=2

waves1c namelist group

- thet0: the central direction for model spectrum.
- freqs. Tide as above.
- edens: variance density for each component.
- nwavs: directional spreading factor
- nseed: seed value for the number generator (between 0 and 9999).

For iinput=2

waves2 namelist group

- freqin, tidein: wave period and tide offset for the single frequency component.

In the case of Manavgat River mouth domain, indat.dat file was prepared by using iwave=1 (descrete wave components) as it was difficult to get full directional spreading model.

An example of indat.dat is given in the appendix B.

3.1.2 SWAN Input data

Cycle III of SWAN is a stationary and optionally non-stationary model formulated in Cartesian (recommended for small scales) or spherical (small scales and large scales) coordinates. The stationary mode should be used only for waves with a relatively short residence time computational area under consideration i.e. the travel time of the waves through the region should be small compared to the time scale of the geophysical conditions (wave boundary conditions, wind, and storm surge) (Ris, et. al., 1998). In Manavgat case, the travel time of the waves through the grid is small compared to the time scale of the wave and wind conditions, and hence the stationary mode is used in runs with the SWAN model.

In order to run SWAN model, the user needs to prepare some files such as the sea bed topography file that includes the water depth values over the input grid points, current and wind files, and SWAN input file which should be with .swn extension. This file should be edited according to the commands given in SWAN.edit file. An example of that file, including all needed input data is available in the SWAN user's manual.

In the Manavgat case, the SWAN input file is Manavgat.swn. The sea bed topography file is Manavgat.dat and it is similar in format to refdat.dat.

However, there was no need in SWAN to make the subdivision externally as that can be done by choosing a computational grid finer than input grid. In Manavgat.dat, the space increments in x and y directions were 100 m. However, the space increment used in the model was 25 m. in both directions. Another input file is Manavgat.loc which includes the locations where wave characteristics are required. This was prepared in such a way that comparison with Ref/Dif 1 results could easily be done.

The most important commands of the SWAN input file will be explained below with the reasonable values for Manavgat river mouth case used in Manavgat.swn.

- *Start-up commands*

    PROJECT defines a number of strings to identify the SWAN run (project name ect) in the print and plot file. In this study project name is 'Manavgat'.

    SET: sets values of certain general parameter ([level] [nor] [depmin] [maxmes] [maxerr] [grav] [rho] [inrhog] [hsrerr]) such as increase in water level, direction of North with respect to the x-axis, threshold depth, maximum number of error messages, error level, gravitational acceleration, water density, a term indicate whether the user requires output based on variance or based on true energy, the relative difference between the user imposed significant wave height and the significant wave height computed by SWAN, and the type of used grids. All used parameters are the same as default values of swan except the direction of x-axis with north which is [nor]=113^{0} for the Manavgat case.

MODE: requests a stationary / non-stationary or 1D-mode / 2D-mode of SWAN. For the Manavgat project, the default option of SWAN was used (which is stationary, two-dimensional).

COORD: to choose between Cartesian and spherical coordinates.

- *general commands*

    TEST: requests the output of intermediate results for testing purposes.

    POOL: requests the status of computer memory.

- *commands for model description*

    a-Commands for computational grid:

    CGRID: defines the type of computational grid (REGULAR or CURVILINEAR) and its dimensions. In the Manavgat case, the computational grids was chosen to be the same with the input grid. For regular grids like that used in the Manavgat case, these dimensions are: [xpc] [ypc] [alpc] [xlenc] [ylenc] [mxc] [myc]. CGRID commend also includes CIRCLE and SECTOR options which indicate that the spectral directions cover the full circle or only a sector from that circle. In the Manavgat project, the computational grid is regular with origin of the x and y coordinates xpc=0, ypc=0, and direction of the positive x-axis of the computational grid alpc=0. length of the computational grid in x and y directions are xlenc=6500 m. and ylenc=3500 m. number of meshes in computational grid in x and y directions are mxc=65, myc=35. SECTOR option has been chosen as only spectral wave directions in a limited directional sector are considered; the range of this sector is given by [dir1]=-25^0 and [dir2]=205^0. 45^0 has been add to each side of incoming wave sector to avoid some errors mentioned in the SWAN manual. The number of meshes in θ-space has been chosen to be mdc=36. Lowest discrete

frequency that is used in the calculation in Hz is flow=0.04, whereas the highest is fhigh=1. [msc] which is one less than the number of frequencies, defines the grid resolution in frequency- space between the lowest and the highest discrete frequency (msc=40). Figure 3.4 shows the coordinates of the origin [xpc] and [ypc], the orientation [alpc] and the grid point numbering of the computational grid with respect to the problem coordinates system.

READGRID: reads a curvi-linear computational grid.
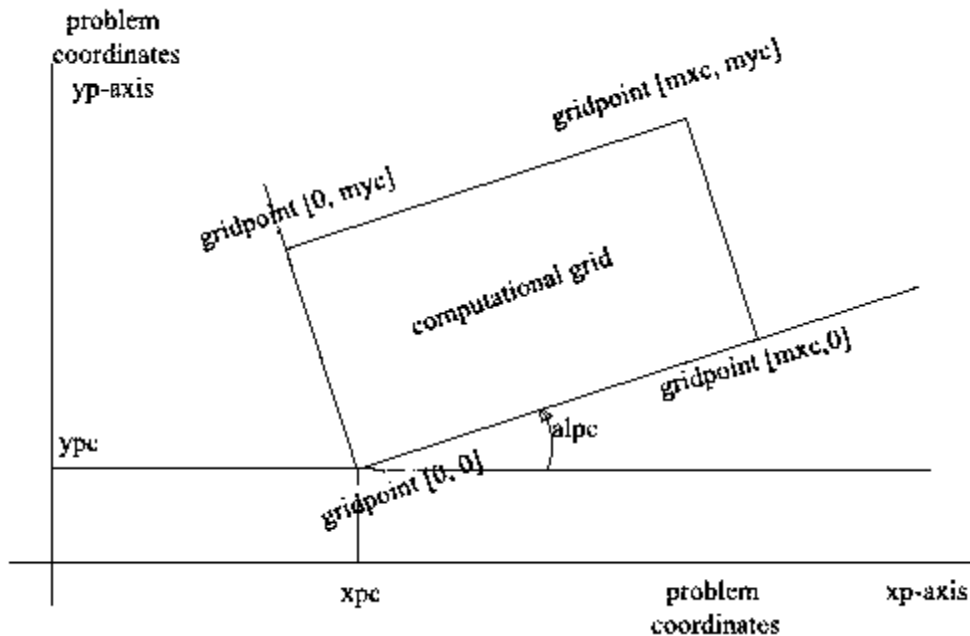
Figure 3.4 Orientation and coordinates of the origin of computational grid of SWAN with respect to the problem coordinate system.

b-Commands for input fields:

INPGRID: defines dimension of input bottom, water level, current, friction and wind fields' grids, which can be different from each other.

In the Manavgat case, the input grid is regular and have the following data: [xpinp]=0, [ypinp]=0, [alpinp]=0 [mxinp]=65, [myinp]=35, [dxinp]=100 and [dyinp]=100. Also this command includes information about the file of input grid such as

READINP: reads input fields

WIND activates constant wind option.

c- Commands for boundary/initial conditions:

BOUND defines boundary conditions for the computational spatial grid. BOUNDPAR1: defines the shape of the spectra whether it is JONSWAP (default), PM (Pierson-Moskowitz), GAUSS (a Gaussian-shaped frequency spectrum), and BIN where energy is located in one frequency bin. This commands also determine the type of wave period (MEAN, or PEAK) that will be used. DSPR ,option for expressing the width of the directional distribution (the distribution function itself is $\cos^m(\theta - \theta_{peak})$, is also included in this commend expressed as power or degrees.

BOUNDPAR2: defines parametric spectra at the boundary. It consists of two parts, the first part defines the boundary side or segment where the spectra will be given and the second part defines the spectral parameters ([hs] [per] [dir] [dd]) of these spectra. [dd], coefficient of directional spreading; $\cos^m\theta$ distribution is assumed and it is interpreted as the directional standard deviation in degrees if the option DEGREES is chosen in the command BOUNDPAR1 or it is interpreted as the power m. for the Manavgat case deep wave data obtained from the NATO-TU waves is calculated using Janswap spectra with m=2 (MS=2). From the numerical relation between [MS] and the one-sided directional spread of the waves (DSPR) that is

available in SWAN user manual the value of DSPR can be found to be DSPR=31.5 degrees when MS=2.

BOUNDSPEC: defines spectra at boundary when it is consisted of two parts.

BOUNDNEST1: this command is used when the SWAN nested boundary conditions are used.

BOUNDNEST2: this command is used when the WAM nested boundary conditions are used.

BOUNDNEST3: this command is used when the WAVEWATCH III nested boundary conditions are used.

INITIAL This command can be used to specify the initial values for a stationary or non-stationary computation.

d- Commands for physics:

GEN: SWAN first-, second- or third-generation physics (GEN1, CEN2, CEN3), In the Manavgat case, SWAN's default option was used (stationary, two-dimensional).

BREAKING: activates dissipation by depth-induced wave breaking.

FRICTION: activates dissipation by bottom friction.

TRIAD: activates three wave-wave interactions.

OBSTACLE: defines characteristics of sub-grid obstacles.

SETUP: activates the computation of the wave-induced set-up.

OFF: deactivates certain physical processes.

e- Commands for numerics

PROP: to choose the numerical propagation scheme.

NUMERIC: sets some of the numerical properties of SWAN.

- *Output: commands*

a- Commands for output locations:

FRAME defines an output frame (a regular grid).

GROUP defines an output group (for regular and curvi-linear grids).

CURVE defines an output curve.

RAY defines a set of straight output lines (rays).

ISOLINE defines a depth- or bottom contour (for output along that contour).

POINTS defines a set of individual output points.

NGRID defines a nested grid.

LINE defines a set of lines in plots.

SITES defines a set of place names in plots.

b- Commands to write or plot output quantities:

These commands control the output and plot properties and can be seen in the SWAN user manual. However they are briefly listed below.

QUANTITY: defines properties of output quantities.

BLOCK: requests a block output (geographic distribution).

TABLE: requests writing of a table (set of locations).

SPECOUT: requests spectral output.

NESTOUT: requests spectral output for subsequent nested computations.

PLOT: requests plotting of a figure.

- *Compute, hotfile and stop commands*

    COMPUTE starts a computation.

    HOTFILE stores results for subsequent SWAN run.

    STOP end of user's input.

    An example of Manavgat.swn is available in appendix B.

3.1.3   GENESIS Input ata

GENESIS calculates shoreline change due to spatial and temporal differences in longshore transport rate as produced by breaking waves (CEM, 1998) and has been applied to predict shoreline response for the design of numerous coastal engineering projects.

The GENESIS model requires an input wave condition to set the offshore boundary condition for the study area. The model employs an internal wave model, RCPWAVE, (with the assumption of straight and parallel contours) to propagate these waves to the shoreline. However, an external wave model can also be used (Ref/Dif 1 and SWAN in the Manavgat case) to propagate these waves to a nearshore reference depth, at which the GENESIS model reads the wave data. After reading the input data from the external wave model, the internal wave model is used between the reference depth and the shoreline to calculate the breaking wave conditions at each model grid cell. Shoreline change along the coastline is computed in the time domain as a function of breaking wave characteristics.

GENESIS is operated through use of seven input data files (see Figure 3.6) including data on the shoreline and the wave conditions and other needed parameters. These input data files and parameters are explained in the following sections.

- Wave input

SWAN and REF/DIF models were used to find out the nearshore wave characteristics at a reference depth of 12 m. of the 35 different incoming waves (5 wave heights with different 7 incoming wave angles as it is seen in table 3.3). Three different points where chosen with depth of almost 12 m. to find out wave boundary condition needed to run GENESIS. The first one is at the beginning of the boundary, the next is at the middle and the third point located close to the end of the boundary. Nearshore wave model's results at those points have been taken and a comparison has been made to find out the wave boundary condition obtained to run GENESIS. As it will be explained in the next chapter, it has been found that the differences between nearshore wave heights of these three points are small enough to consider a constant nearshore boundary condition in runs of GENESIS using the wave characteristics at the middle point of reference line.

The GENESIS model requires a time series wave input (i.e., height, direction and period) for the model simulations. Assuming that the wave boundary condition are constant over GENESIS boundary and using the nearshore wave model results and accuracy of them, a time serious wave input file with time step of 3 hours was prepared by means of a Fortran program written by Dr. Karim Rakha (see appendix C). GENESIS nearshore wave input file compiled by that program, waves.dat , is available in the appendix C for further uses.

- Model grid

In order to run GENESIS a coordinate system and grid covering the region of the project, and measured shoreline positions, locations and configurations of structures and beach fills, and other topographic and geometric information should be chosen. A one-dimensional model grid of 6500 m. legth of shoreline (66 grid cells, each 100 m. long), was used. The shoreline positions in that grid were taken as shown in Figure 3.5.

GENESIS is operated through use of few input data files, as illustrated in Figure 3.6. Input and output file names consist of five letters with the three-letter extension. This extension should be the same for all input files and it is ".dat" in the Manavgat case.
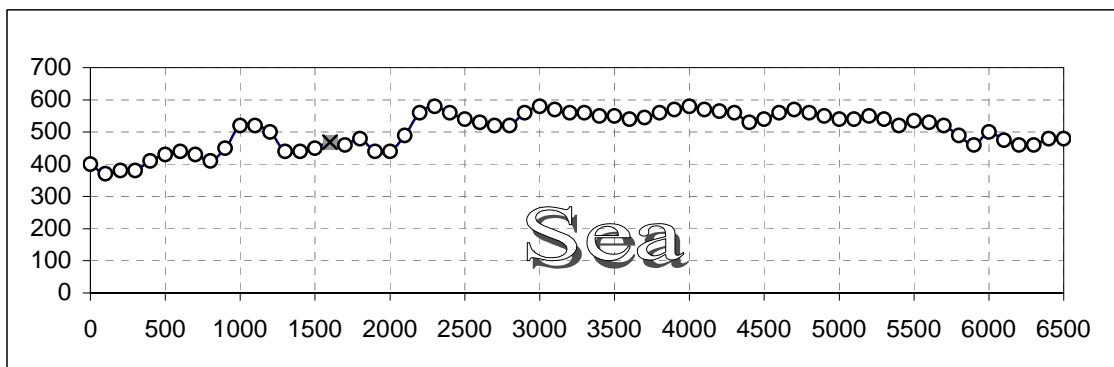
Figure 3.5 Manavgat shoreline and GENESIS coordinate.
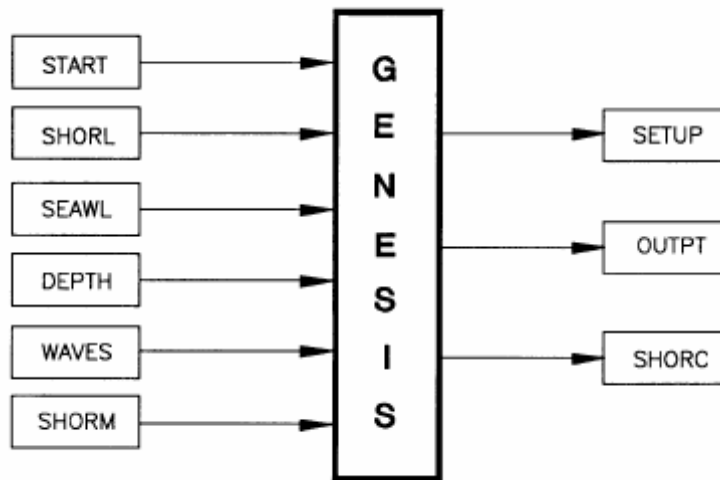
Figure 3.6 Schematic input and output file structure of GENESIS

(Hanson, and Kraus, 1989).

- GENESIS input files

1- shorl file:

    The input file shorl.dat holds the position of the shoreline used by GENESIS at the start of calculation. Positions of the shoreline are given in the units (meter) selected at Line A.2of the START file and are measured from the baseline (x-axis). shorl.dat used in this study is as follows:

```
 ---------------------------------------------------------------------------------
INITIAL SHORELINE POSITION OF 920724; CELL SPACING (DX=100 m)
THESE DATA WERE OBTAINED FROM THE "Manvgat Su temin projesi,24-july-1992"
STARTING AT ALONGSHORE POSITION X=0. AND ENDING AT X=6500.
****************************************************************
400.0  370.0  380.0  380.0  410.0  430.0  440.0  430.0  410.0  450.0
```

```
520.0  520.0  500.0  440.0  440.0  450.0  474.0  460.0  480.0  440.0
440.0  490.0  560.0  580.0  560.0  540.0  530.0  520.0  520.0  560.0
580.0  570.0  560.0  560.0  550.0  550.0  540.0  545.0  560.0  570.0
580.0  570.0  565.0  560.0  530.0  540.0  560.0  570.0  560.0  550.0
540.0  540.0  550.0  540.0  520.0  535.0  530.0  520.0  490.0  460.0
500.0  475.0  460.0  460.0  480.0  480.0
```

2- shorm file:

The input file shorm.dat holds the position of the measured shoreline to be reproduced in the procedure of calibrating or verifying the model. GENESIS calculates a number called the "calibration/verification error" (CVE) as the average of the absolute difference between the calculated shoreline position (held in SHORC) and the measured shoreline position (held in SHORM) at each grid point (Hanson, 1987).

If the modeler specifies at line A.4 in the START file that only a portion of the shoreline will be used in the simulation, then only that segment of the shoreline between and including the boundary cells is loaded from shorl, (initial shoreline file). However, the shoreline positions must be given for the full range of the calculation grid (NN points), as GENESIS will load positions of the shoreline subsection with reference to the original, full grid (Hanson, 1987). In the Manavgat case, only initial shoreline positions are available from "Manavagt Su Temin Projesi" and as GENESIS does not work without shorm file, this file was prepared by using the same initial shoreline as thee measured shoreline.

72

3- seawl file:

The input file seawl.dat holds the positions of one or more seawalls or effective seawalls with respect to the baseline and specified in the proper length units. If a seawall is not specified, an effective seawall is placed at -9999 m or ft (depending on units selected) by GENESIS, and SEAWL is not read (Hanson, and Kraus, 1989).

4- depth:

this file is not needed in the Manavgat case as the nearshore wave file has been prepared for GENESIS so that the program will run using technique similar to that described by Bodge, Creed and Raichle (1995).

5- Waves file:

this file includes deep waves characteristics when the external RCPWAVE nearshore wave model is used. However it includes the reference time serious nearshore wave characteristics when the near shore wave data are obtained from running other programs. In the Manavgat case, the deep water wave data were sorted into 35 direction and period bins and were used to obtain the nearshore wave conditions for those bins. Afterwards, a three-hour time series nearshore wave input file (i.e., height, direction and period) was prepared for the model simulations.

6- Start file:

The input file start.dat contains the instructions that control the shoreline change simulation and is the principal interface between the modeler and GENESIS. After preparing start file for a project, only a few

quantities in it will need to be changed during the course of calibration and verification.

Start file contains requests for information in a series of lines arranged in sections according to general subject. These sections are model setup, waves, beach, non-diffracting groins, diffracting groins and jetties, groins and jetties, detached breakwaters, seawalls, beach fills, bypassing, and comments. Model setup section is related to model grid and measurements, while the waves section includes commands related to wave treatment and measurements. Inputs related to these two sections were already explained above.

In the beach section, the effective grain size, average berm height and closure depth should be given. For the Manavgat case, it is mentioned in (Güler, 1996) that two different values of median grain size were found from two different analyses. The first one, which was found by the Yüksel Proje team, is 1 mm. The other, which was obtained by the Istanbul Technical University, was 3.7 mm. In this study the effective grain size is used to be 1 mm as this value was also used in the Yuksel Proje's work around the river mouth. For another value of the grain size, one should change the grain size given in the line c.1 in start.dat file. Berm height was used as 1.0 m (Güler, 1996). By using Equation 2.35 and information available in (Güler, 1996) the closure depth was taken as 9m.

While dealing with sections related to groins some important points should be explained. First one is: As there are no groins or jetties at the cell wall 1 or N+1, the boundary will be treated as a pinned beach allowing sand

to freely cross it from both sides. The second is: when modeling the grid cell relater to the river mouth, the mouth is treated as non-diffracting (does not extend beyond average width of surf zone) groin with zero permeability supposing the river flow prevents sands from passing. The modeling of the river mouth cell after totally finishing the protection structure that is controlling, is explained in the discussion part.

Other sections and the data used are clearly seen in start.dat file that wasprepared for modeling the Manavgat case as it is shown below :

```
 --------------------------------------------------------------------------------
              ********************************************************
              *    INPUT FILE START.DAT TO GENESIS VERSION 3.0    *
              ********************************************************
A--------------------------- MODEL SETUP ------------------------------A
A.1  RUN TITLE
   manavgat river mouth
A.2  INPUT UNITS (METERS=1; FEET=2): ICONV
   1
A.3  TOTAL NUMBER OF CALCULATION CELLS AND CELL LENGTH: NN, DX
   66    100
A.4  GRID CELL NUMBER WHERE SIMULATION STARTS AND NUMBER OF CALCULATION
     CELLS (N = -1 MEANS N = NN): ISSTART, N
   1    66
A.5  VALUE OF TIME STEP IN HOURS: DT
   3
A.6  DATE WHEN SHORELINE SIMULATION STARTS
     (DATE FORMAT YYYYMMDD: 1 MAY 1992 = 19920501): SIMDATS
   920724
A.7  DATE WHEN SHORELINE SIMULATION ENDS OR TOTAL NUMBER OF TIME STEPS
     (DATE FORMAT YYYYMMDD: 1 MAY 1992 = 19920501): SIMDATE
   990724
A.8  NUMBER OF INTERMEDIATE PRINT-OUTS WANTED: NOUT
   1
A.9  DATES  OR  TIME STEPS  OF INTERMEDIATE PRINT-OUTS
```

(DATE FORMAT YYYYMMDD: 1 MAY 1992 = 19920501, NOUT VALUES): TOUT(I)

960724

A.10 NUMBER OF CALCULATION CELLS IN OFFSHORE CONTOUR SMOOTHING WINDOW
(ISMOOTH = 0 MEANS NO SMOOTHING, ISMOOTH = N MEANS STRAIGHT LINE.
RECOMMENDED DEFAULT VALUE = 11): ISMOOTH

11

A.11 REPEATED WARNING MESSAGES (YES=1; NO=0): IRWM

1

A.12 LONGSHORE SAND TRANSPORT CALIBRATION COEFFICIENTS: K1, K2

0.5   1

A.13 PRINT-OUT OF TIME STEP NUMBERS? (YES=1, NO=0): IPRINT

1

B------------------------------ WAVES --------------------------------B

B.1 WAVE HEIGHT CHANGE FACTOR. WAVE ANGLE CHANGE FACTOR AND AMOUNT (DEG)
(NO CHANGE: HCNGF=1, ZCNGF=1, ZCNGA=0): HCNGF, ZCNGF, ZCNGA

1 1 0

B.2 DEPTH OF OFFSHORE WAVE INPUT: DZ

12

B.3 IS AN EXTERNAL WAVE MODEL BEING USED (YES=1; NO=0): NWD

0

B.4 COMMENT: IF AN EXTERNAL WAVE MODEL IS NOT BEING USED, CONTINUE TO B.9

B.5 NUMBER OF SHORELINE CALCULATION CELLS PER WAVE MODEL ELEMENT: ISPW

4

B.6 NUMBER OF HEIGHT BANDS USED IN THE EXTERNAL WAVE MODEL TRANSFORMATIONS
(MINIMUM IS 1, MAXIMUM IS 9): NBANDS

1

B.7 COMMENT: IF ONLY ONE HEIGHT BAND WAS USED CONTINUE TO B.9

B.8 MINIMUM WAVE HEIGHT AND BAND WIDTH OF HEIGHT BANDS: HBMIN, HBWIDTH

0   0

B.9 VALUE OF TIME STEP IN WAVE DATA FILE IN HOURS (MUST BE AN EVEN MULTIPLE
OF, OR EQUAL TO DT): DTW

3

B.10 NUMBER OF WAVE COMPONENTS PER TIME STEP: NWAVES

1

B.11 DATE WHEN WAVE FILE STARTS (FORMAT YYYYMMDD: 1 MAY 1992 = 19920501): WDATS

910901

C------------------------------ BEACH --------------------------------C

C.1 EFFECTIVE GRAIN SIZE DIAMETER IN MILLIMETERS: D50

1.0

C.2 AVERAGE BERM HEIGHT FROM MEAN WATER LEVEL: ABH

1

C.3 CLOSURE DEPTH: DCLOS

  9

C.4 ANY OPEN BOUNDARY? (NO=0, YES=1): IOB

  0

C.5 COMMENT: IF NO OPEN BOUNDARY, CONTINUE TO D.

C.6 TIME BASE IN BOUNDAY MOVEMENT SPECIFICATION(S)?
  (SIMULATION PERIOD = 1, DAY = 2, TIME STEP = 3): ITB

  1

C.7 OPEN BOUNDARY ON LEFT-HAND SIDE? (NO=0, YES=1): IOB1

  1

C.8 COMMENT: IF A GROIN ON LEFT-HAND BOUNDARY, CONTINUE TO C.10

C.9 BOUNDARY MOVEMENT PER TIME BASE ON LEFT-HAND BOUNDARY, IN SYSTEM OF
  UNITS SPECIFIED IN A.2 (PINNED BEACH => YC1 = 0): YC1

  0

C.10 OPEN BOUNDARY ON RIGHT-HAND SIDE? (NO=0, YES=1): IOBN

  1

C.11 COMMENT: IF A GROIN ON RIGHT-HAND BOUNDARY, CONTINUE TO D.

C.12 BOUNDARY MOVEMENT PER TIME BASE ON LEFT-HAND BOUNDARY, IN SYSTEM OF
  UNITS SPECIFIED IN A.2 (PINNED BEACH => YCN = 0): YCN

  0

D----------------------- NON-DIFFRACTING GROINS -------------------------D

D.1 ANY NON-DIFFRACTING GROINS? (NO=0, YES=1): INDG

  1

D.2 COMMENT: IF NO NON-DIFFRACTING GROINS, CONTINUE TO E.

D.3 NUMBER OF NON-DIFFRACTING GROINS: NNDG

  1

D.4 GRID CELL NUMBERS OF NON-DIFFFRACTING GROINS (NNDG VALUES): IXNDG(I)

  17

D.5 LENGTHS OF NON-DIFFRACTING GROINS FROM X-AXIS (NNDG VALUES): YNDG(I)

  280

E----------------- DIFFRACTING (LONG) GROINS AND JETTIES -----------------E

E.1 ANY DIFFRACTING GROINS OR JETTIES? (NO=0, YES=1): IDG

  0

E.2 COMMENT: IF NO DIFFRACTING GROINS, CONTINUE TO F.

E.3 NUMBER OF DIFFRACTING GROINS/JETTIES: NDG

  0

E.4 GRID CELL NUMBERS OF DIFFFRACTING GROINS/JETTIES (NDG VALUES): IXDG(I)

E.5 LENGTHS OF DIFFRACTING GROINS/JETTIES FROM X-AXIS (NDG VALUES): YDG(I)

E.6 DEPTHS AT SEAWARD END OF DIFFRACTING GROINS/JETTIES(NDG VALUES): DDG(I)

77

F----------------------- ALL GROINS/JETTIES ------------------------------F

F.1 COMMENT: IF NO GROINS OR JETTIES, CONTINUE TO G.

F.2 PERMEABILITIES OF ALL GROINS AND JETTIES (NNDG+NDG VALUES): PERM(I)

   0

F.3 IF GROIN OR JETTY ON LEFT-HAND BOUNDARY, DISTANCE FROM SHORELINE
   OUTSIDE GRID TO SEAWARD END OF GROIN OR JETTY: YG1

   0

F.4 IF GROIN OR JETTY ON RIGHT-HAND BOUNDARY, DISTANCE FROM SHORELINE
   OUTSIDE GRID TO SEAWARD END OF GROIN OR JETTY: YGN

   0

G----------------------- DETACHED BREAKWATERS --------------------------G

G.1 ANY DETACHED BREAKWATERS? (NO=0, YES=1): IDB

   0

G.2 COMMENT: IF NO DETACHED BREAKWATERS, CONTINUE TO H.

G.3 NUMBER OF DETACHED BREAKWATERS: NDB

   0

G.4 ANY DETACHED BREAKWATER ACROSS LEFT-HAND CALCULATION BOUNDARY
   (NO=0, YES=1): IDB1

   0

G.5 ANY DETACHED BREAKWATER ACROSS RIGHT-HAND CALCULATION BOUNDARY
   (NO=0, YES=1): IDBN

   0

G.6 GRID CELL NUMBERS OF TIPS OF DETACHED BREAKWATERS
   (2 * NDB - (IDB1+IDBN) VALUES): IXDB(I)

G.7 DISTANCES FROM X-AXIS TO TIPS OF DETACHED BREAKWATERS
   (1 VALUE FOR EACH TIP SPECIFIED IN G.6): YDB(I)

G.8 DEPTHS AT DETACHED BREAKWATER TIPS (1 VALUE FOR EACH TIP
   SPECIFIED IN G.6): DDB(I)

G.9 TRANSMISSION COEFFICIENTS FOR DETACHED BREAKWATERS (NDB VALUES):
TRANDB(I)

H---------------------------- SEAWALLS -------------------------------H

H.1 ANY SEAWALL ALONG THE SIMULATED SHORELINE? (YES=1; NO=0): ISW

   0

H.2 COMMENT: IF NO SEAWALL, CONTINUE TO I.

H.3 GRID CELL NUMBERS OF START AND END OF SEAWALL (ISWEND = -1 MEANS
   ISWEND = N): ISWBEG, ISWEND

```
   1    66
```

I---------------------------- BEACH FILLS -----------------------------I

I.1 ANY BEACH FILLS DURING SIMULATION PERIOD? (NO=0, YES=1): IBF

   0

I.2 COMMENT: IF NO BEACH FILLS, CONTINUE TO K.

I.3 NUMBER OF BEACH FILLS DURING SIMULATION PERIOD: NBF

   0

I.4 DATES OR TIME STEPS WHEN THE RESPECTIVE FILLS START
   (DATE FORMAT YYYYMMDD: 1 MAY 1992 = 19920501, NBF VALUES): BFDATS(I)

I.5 DATES OR TIME STEPS WHEN THE RESPECTIVE FILLS END
   (DATE FORMAT YYYYMMDD: 1 MAY 1992 = 19920501, NBF VALUES): BFDATE(I)

I.6 GRID CELL NUMBERS OF START OF RESPECTIVE FILLS (NBF VALUES): IBFS(I)

I.7 GRID CELL NUMBERS OF END OF RESPECTIVE FILLS (NBF VALUES): IBFE(I)

I.8 ADDED BERM WIDTHS AFTER ADJUSTMENT TO EQUILIBRIUM CONDITIONS
   (NBF VALUES): YADD(I)

J---------------------------- BYPASSING -------------------------------J

J.1 ANY BYPASSING OPERATIONS DURING SIMULATION PERIOD? (NO=0, YES=1): IBP

   0

J.2 COMMENT: IF NO BYPASSING OPERATIONS, CONTINUE TO K.

J.3 READ BYPASSING RATES FROM A FILE OR SPECIFY BELOW?
   (FILE=1, BELOW=2): IBPF

   2

J.4 COMMENT: IF BYPASSING OPERATIONS ARE SPECIFIED BELOW, CONTINUE TO J.8
   -- BYPASSING OPERATIONS SPECIFIED IN SEPARATE DATA FILE --

J.5 DATE OR TIME STEP WHEN BYPASS DATA FILE STARTS AND ENDS, RESPECTIVELY
   (FORMAT YYYYMMDD: 1 MAY 1992 = 19920501): QQDATS QQDATE

   0   0

J.6 CELL NOS. WHERE BYPASS FILE STARTS AND ENDS, RESPECTIVELY: IQQS, IQQE

   0   0

J.7 COMMENT: END OF BYPASS DATA FILE SECTION. CONTINUE TO K.
   -- BYPASSING OPERATIONS SPECIFIED IN THIS FILE --

J.8 NUMBER OF BYPASSING OPERATIONS DURING SIMULATION PERIOD: NBP

   1

J.9 DATES OR TIME STEPS WHEN THE RESPECTIVE OPERATIONS START
   (DATE FORMAT YYYYMMDD: 1 MAY 1992 = 19920501, NBP VALUES): BPDATS(I)

J.10 DATES OR TIME STEPS WHEN THE RESPECTIVE OPERATIONS END

(DATE FORMAT YYYYMMDD: 1 MAY 1992 = 19920501, NBP VALUES): BPDATE(I)

J.11 GRID CELL NUMBERS OF START OF RESPECTIVE OPERATIONS (NBP VALUES): IBPS(I)

J.12 GRID CELL NUMBERS OF END OF RESPECTIVE OPERATIONS (NBP VALUES): IBPE(I)

J.13 BYPASSING RATES AS TOTAL AVERAGE VOLUME PER HOUR (CY/HR OR M3/HR,

ACCORDING TO UNITS GIVEN IN A.2) FOR RESPECTIVE OPERATIONS

(NBP VALUES): QBP(I)

K----------------------------- COMMENTS -------------------------------K

* ALL COORDINATES MUST BE GIVEN IN THE "TOTAL" GRID SYSTEM

* ONE VALUE FOR EACH STRUCTURE, TIP ETC. ESPECIALLY IMPORTANT FOR

COMBINED STRUCTURES, E.G., TWO DBW'S WHERE THE LOCATION WHERE THEY

MEET HAS TO BE TREATED AS TWO TIPS.

* ANY GROIN CONNECTED TO A DETACHED BREAKWATER MUST BE REGARDED AS

DIFFRACTING

* CONNECTED STRUCTURES MUST BE GIVEN THE SAME Y AND D VALUES WHERE THEY

CONNECT

* IF DOING REAL CASES, THE WAVE.DAT FILE MUST CONTAIN FULL YEARS DATA

* DATA FOR START OF BEACH FILL IN SPACE AND TIME SHOULD BE GIVEN IN

INCREASING/CHRONOLOGICAL ORDER. DATA FOR END OF BEACH FILL MUST

CORRESPOND TO THESE VALUES, AND NOT NECESSARILY BE IN INCREASING ORDER.

* DON'T CHANGE THE LABELS OF THE LINES SINCE THEY ARE USED TO IDENTIFY

THE LINES BY GENESIS.

---------------------------------- END ----------------------------------

 ----

3.2   Results

Annual wave rose offshore the Manavgat river mouth was used to obtain the deep-water wave characteristics to be employed as input wave data in order to find out the nearshore wave conditions. Than by using the calculated nearshore wave data, a time serious reference wave file with a time interval of three hours was prepared for use in the computations with the GENESIS program. An important step in this numerical shoreline change modeling of Manavgat River mouth was the calibration procedure in which the "transport parameters" k_1 and k_2 were determined.

3.2.1   Nearshore Wave Modelling

3.2.1.1 REF/DIF 1

Deep-water wave data listed in the Table 3.1, (35 different wave parameter bins), were used to run REF/DIF1 model. An indat.dat file was prepared as it was mentioned above and shown in the Appendix B. The GENESIS shoreline model requires the nearshore wave data at a reference depth (12 m depth in the Manavgat case). Three locations at the GENESIS reference depth were chosen. One is located at the beginning of the grid, the second at the middle and the last one at the end.

Table 3.4 REF/DIF 1 model results for the Manavgat River mouth.

	deep		water	max Hb	over grid	first	location	second	location	third	location
%	theta	h	t	H b	angle b	hnear	angle-n	hnear	angle-n	hnear	angle-n
7.5252	-67	0.75	4.2	0.8951	2.3321			0.7383	10.482		
5.1283	-44.5	0.75	4.2	0.9647	-5.803			0.7337	22.879		
4.7175	-22	0.75	4.2	0.8964	-7.637	0.7296	-21.36	0.7336	-21.51	0.7369	-21.47
2.0539	0.5	0.75	4.2	0.9143	0.7196	0.7329	-0.211	0.7379	-2.702	0.7407	0.4999
1.2874	23	0.75	4.2	0.9631	-5.81	0.7304	22.322	0.734	22.348	0.7365	22.37
0.9147	45.5	0.75	4.2	0.9239	-7.938			0.7313	-22.23		
0.974	68	0.75	4.2	0.886	-2.644			0.7389	-10		
1.6981	-67	1.5	6	2.1915	-23.25			1.3218	-47.09		
1.3128	-44.5	1.5	6	1.7749	-21.98			1.3894	-37.48		
2.5112	-22	1.5	6	1.7313	-8.987	1.3776	-19.83	1.3487	-20.17	1.4326	-19.94
1.749	0.5	1.5	6	1.8184	0.9017	1.4237	0.9417	1.4661	0.8176	1.4623	0.4589
0.7877	23	1.5	6	1.7877	10.536	1.3305	21.078	1.3337	22.105	1.4444	20.972
0.7623	45.5	1.5	6	2.0507	33.493			1.4069	39.116		
0.6733	68	1.5	6	2.3488	-36.78			1.3442	48.047		
0.0678	-67	2.5	7.5	2.8183	-32.42			2.1371	-42.6		
0.1143	-44.5	2.5	7.5	3.0041	-25.78			2.0477	-33.7		
0.5929	-22	2.5	7.5	3.0892	-14.46	2.3482	-18.91	2.1506	-18.33	2.5097	-18.09
0.4616	0.5	2.5	7.5	3.0823	2.0699	2.5287	0.774	2.505	1.6433	2.5466	0.416
0.199	23	2.5	7.5	3.0284	16.645	2.235	18.676	2.1088	20.495	2.6181	19.16
0.1652	45.5	2.5	7.5	2.8767	36.553			2.1444	36.295		
0.1016	68	2.5	7.5	3.5084	41.896			2.1986	46.515		
0	-67	3.5	9	3.7506	-24.47			2.6843	-36.74		
0	-44.5	3.5	9	4.0117	-20.01			2.7115	-28.83		
0.127	-22	3.5	9	4.4743	-14.23	3.2836	-16.91	3.2367	-15.47	3.3245	-15.76
0.0805	0.5	3.5	9	4.3859	0.3151	3.5693	1.2158	3.722	0.7746	3.6958	0.366
0.0127	23	3.5	9	4.0516	15.881	3.3668	15.291	3.0671	18.087	3.7069	16.957
0.0042	45.5	3.5	9	3.9756	26.476			2.7874	30.435		
0.0212	68	3.5	9	3.8226	33.324			2.6321	39.557		
0	-67	4.5	10.2	4.9135	-24.78			3.1079	-32.08		
0	-44.5	4.5	10.2	5.1932	-23.92			3.2773	-26.07		
0.0423	-22	4.5	10.2	5.5106	-16.4	4.3469	-13.94	4.3979	-13.68	4.4636	-14.55
0.0339	0.5	4.5	10.2	5.872	0.3117	4.9887	1.3771	4.6706	2.2978	5.3129	0.3419
0	23	4.5	10.2	5.3545	11.915	4.9146	14.61	4.1698	15.492	4.9809	15.666
0	45.5	4.5	10.2	5.3687	30.486			3.56	27.966		
0	68	4.5	10.2	4.9884	40.406			3.3762	35.753		

Table 3.4 includes the results of REF/DIF1 runs at three selected location for 35 deep wave direction and period bins affecting the Manavgat river mouth. From the table, it can be seen that the differences between the wave heights at the chosen locations are small enough (see Figure 3.7) so that a constant boundary condition can be used for the GENESIS runs.

From Table 3.4, the differences in the wave heights were calculated. These are shown in Table 3.5. From Table 3.5, it is clearly seen that the wave height differences are in order of a few centimeters except for the wave of 4.5m. height with wave angle of 23 degrees, which already has zero accuracy. Figure 3.7 shows these differences in wave height according to incoming deep-water wave height and direction along GENESIS reference depth. As these differences can be neglected, a constant time serious nearshore wave boundary condition can be used I GENESIS shoreline model.
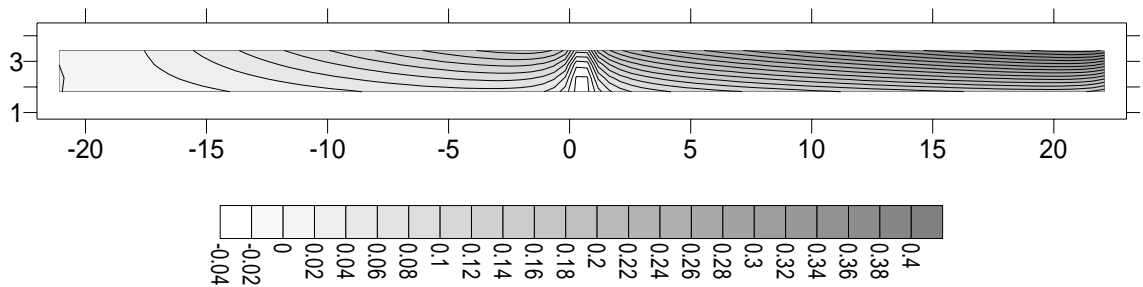
Figure 3.7 Difference in the wave heights according to incoming deep-water wave height and direction along the GENESIS reference depth
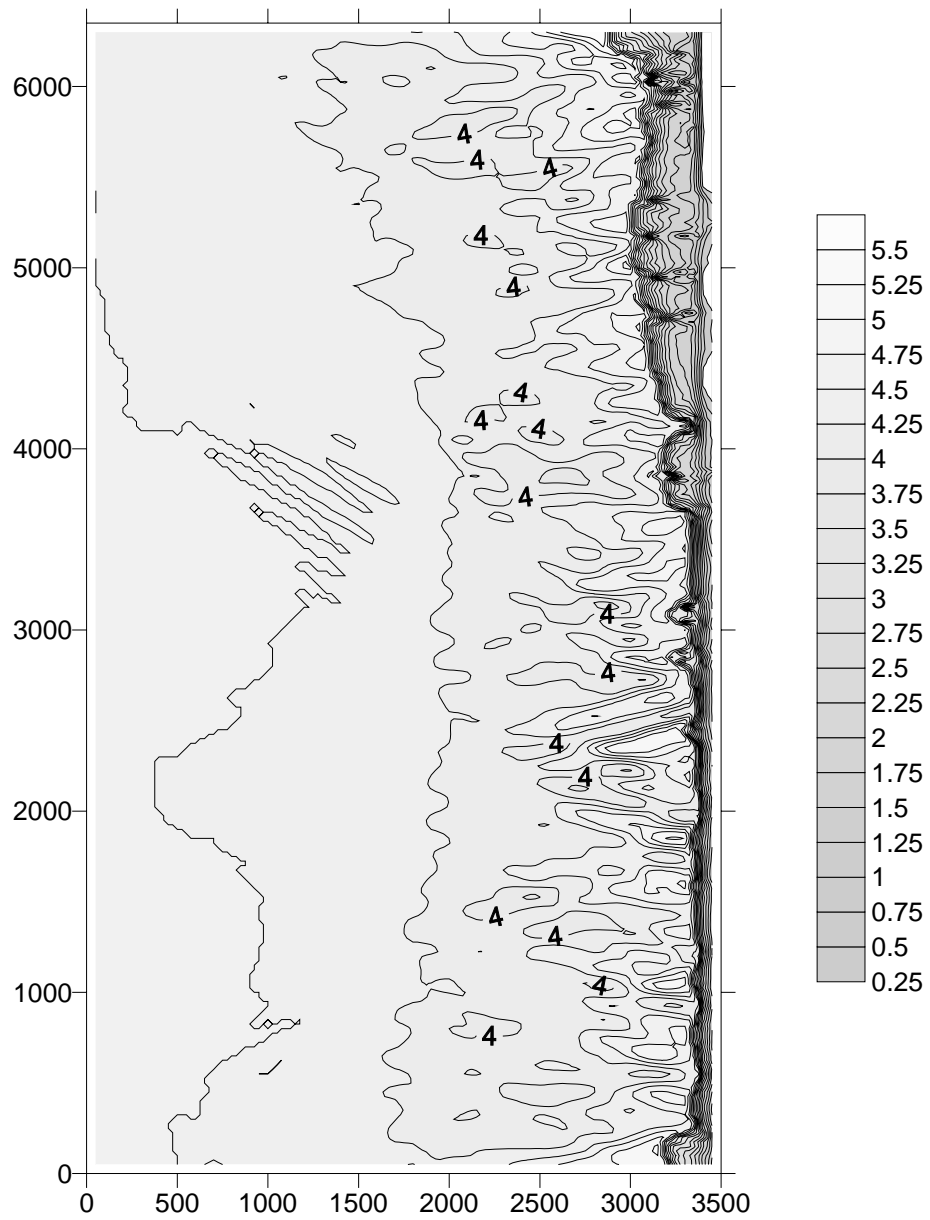
Figure 3.8 Nearshore wave field for the offshore wave of H=4.5m., T=10.2
sec., and θ=0.5^0 (REF/DIF 1).

3.2.1.2 SWAN

In this study, SWAN model, which is based on the spectral wave action balance equation, has been also used to obtain nearshore wave data. Then a comparison between SWAN model's results and the results of REF/DIF1 model, which can be considered as propagation model, has been made.

In order to run SWAN model, deep-water wave data listed in the Table 3.1 were used. A manavgat.swn file was prepared for each deep-water wave characteristics as it was expressed above and seen in the example given in Appendix B. to make comparison with REF/DIF1 the point of reference depth located at the middle of bathymetric grid was considered. Table 3.5 shows the results of SWAN runs at that location and the differences between the m and those resulted from REF/DIF1 runs. Figure 3.9 illustrate the nearshore wave filed for two incoming deep-water wave conditions (H=4.5m., T=10.2sec., q=0.50 and H=3.5m., T=9 sec., q=0.50).

Figure 3.10 shows the differences in wave height between SWAN and REF/DIF1 for each incoming deep-water wave height in seven direction bins. It can be seen from the figure that REF/DIF 1 gives greater values of wave height than those given by SWAN. Figure 3.11 shows the differences in wave direction between SWAN and REF/DIF1 for each incoming deep-water wave height in seven direction bins. It can be seen from the figure that REF/DIF 1 gives greater absolute values of wave angle than the absolute values given by SWAN.

Table 3.5 Comparison of the SWAN results with those of REF/DIF 1

deep	water			SWAN			ref /dif		ref/dif	-swan
a/ref	a/swan	h	t	hnear	angle-near		hnear	angle-near	Hr-Hsw	ar-as
-67	157	0.75	4.2	0.41328	114.492	-24.492	0.7383	10.4823	0.325	34.974
-45	135	0.75	4.2	0.5292	105.95	-15.95	0.7337	22.8791	0.2045	38.829
-22	112	0.75	4.2	0.61111	97.372	-7.372	0.7336	-21.506	0.1225	-14.13
0.5	89.5	0.75	4.2	0.63744	90.193	-0.193	0.7379	-2.7023	0.1005	-2.509
23	67	0.75	4.2	0.60572	82.941	7.059	0.734	22.3484	0.1283	15.289
45.5	44.5	0.75	4.2	0.5194	74.232	15.768	0.7313	-22.232	0.2119	-38
68	22	0.75	4.2	0.40143	65.761	24.239	0.7389	-10.003	0.3375	-34.24
-67	157	1.5	6	0.79752	110.788	-20.788	1.3218	-47.09	0.5243	-26.3
-45	135	1.5	6	1.02512	103.342	-13.342	1.3894	-37.478	0.3643	-24.14
-22	112	1.5	6	1.18477	96.121	-6.121	1.3487	-20.166	0.1639	-14.04
0.5	89.5	1.5	6	1.23621	90.118	-0.118	1.4661	0.8176	0.2299	0.9356
23	67	1.5	6	1.17411	84.056	5.944	1.3337	22.1048	0.1596	16.161
45.5	44.5	1.5	6	1.00583	76.75	13.25	1.4069	39.1159	0.4011	25.866
68	22	1.5	6	0.77454	69.463	20.537	1.3442	48.0466	0.5697	27.51
-67	157	2.5	7.5	1.34579	107.385	-17.385	2.1371	-42.604	0.7913	-25.22
-45	135	2.5	7.5	1.73418	100.965	-10.965	2.0477	-33.695	0.3135	-22.73
-22	112	2.5	7.5	2.00421	94.95	-4.95	2.1506	-18.331	0.1464	-13.38
0.5	89.5	2.5	7.5	2.09147	89.962	0.038	2.505	1.6433	0.4135	1.6053
23	67	2.5	7.5	1.9865	84.931	5.069	2.1088	20.4952	0.1223	15.426
45.5	44.5	2.5	7.5	1.70256	78.897	11.103	2.1444	36.2946	0.4418	25.192
68	22	2.5	7.5	1.30929	72.786	17.214	2.1986	46.5145	0.8893	29.301
-67	157	3.5	9	2.07272	102.568	-12.568	2.6843	-36.741	0.6116	-24.17
-45	135	3.5	9	2.65251	97.831	-7.831	2.7115	-28.83	0.059	-21
-22	112	3.5	9	3.04008	93.593	-3.593	3.2367	-15.469	0.1966	-11.88
0.5	89.5	3.5	9	3.15643	89.945	0.055	3.722	0.7746	0.5656	0.7196
23	67	3.5	9	2.98319	86.202	3.798	3.0671	18.0873	0.0839	14.289
45.5	44.5	3.5	9	2.54711	81.746	8.254	2.7874	30.4354	0.2403	22.181
68	22	3.5	9	1.95428	77.253	12.747	2.6321	39.5566	0.6778	26.81
-67	157	4.5	10	2.66444	102.566	-12.566	3.1079	-32.083	0.4435	-19.52
-45	135	4.5	10	3.40899	97.828	-7.828	3.2773	-26.07	-0.1317	-18.24
-22	112	4.5	10	3.90529	93.59	-3.59	4.3979	-13.678	0.4926	-10.09
0.5	89.5	4.5	10	4.05331	89.944	0.056	4.6706	2.2978	0.6173	2.2418
23	67	4.5	10	3.83256	86.203	3.797	4.1698	15.4924	0.3372	11.695
45.5	44.5	4.5	10	3.27365	81.748	8.252	3.56	27.9658	0.2864	19.714
68	22	4.5	10	2.51221	77.255	12.745	3.3762	35.7526	0.864	23.008
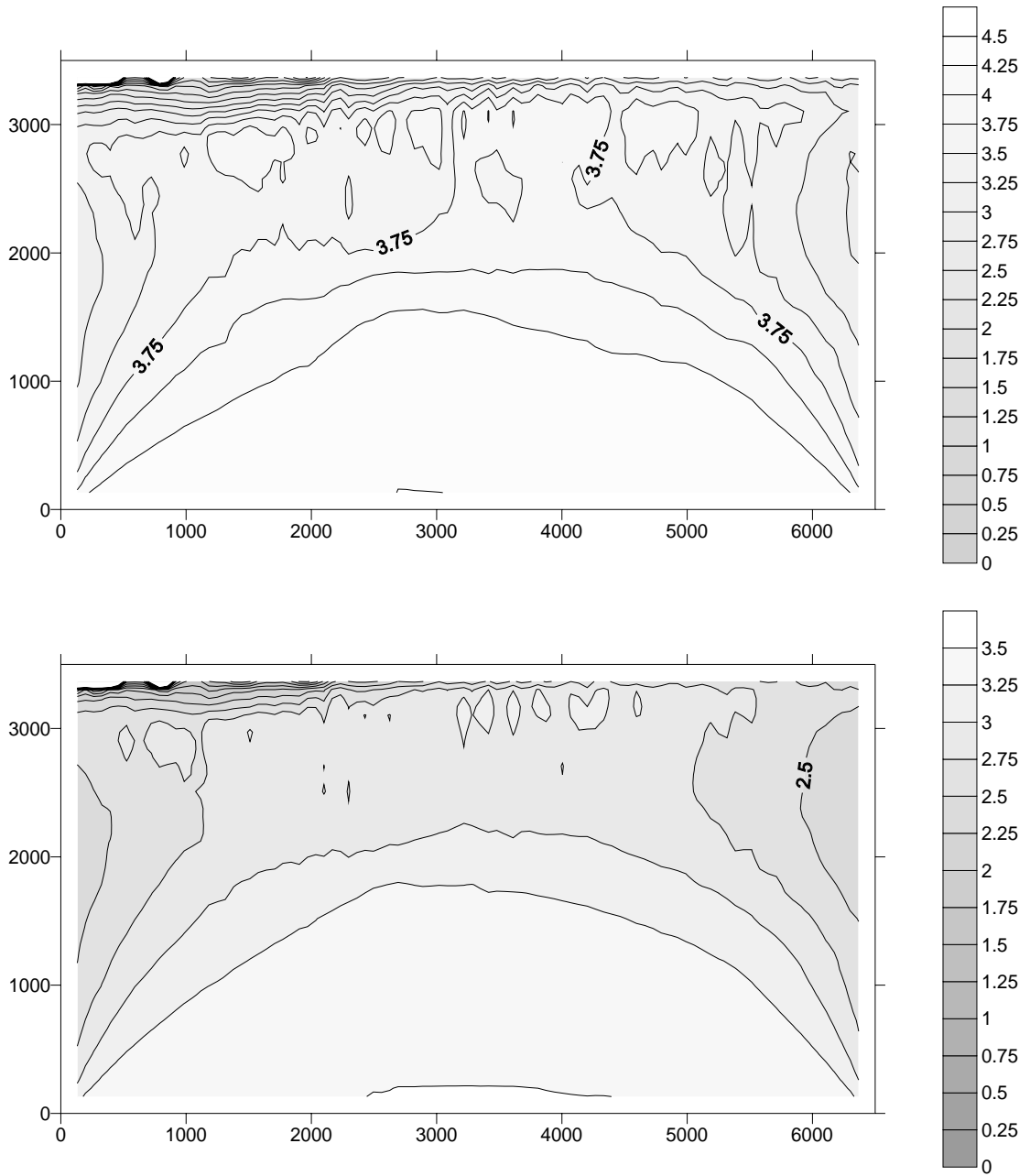
Figure 3.9 Nearshore wave field for the offshore wave of H=4.5m., T=10.2 sec., and θ=0.5^0 and the wave of H=3.5m., T=9 sec., and θ=0.5^0 (SWAN)
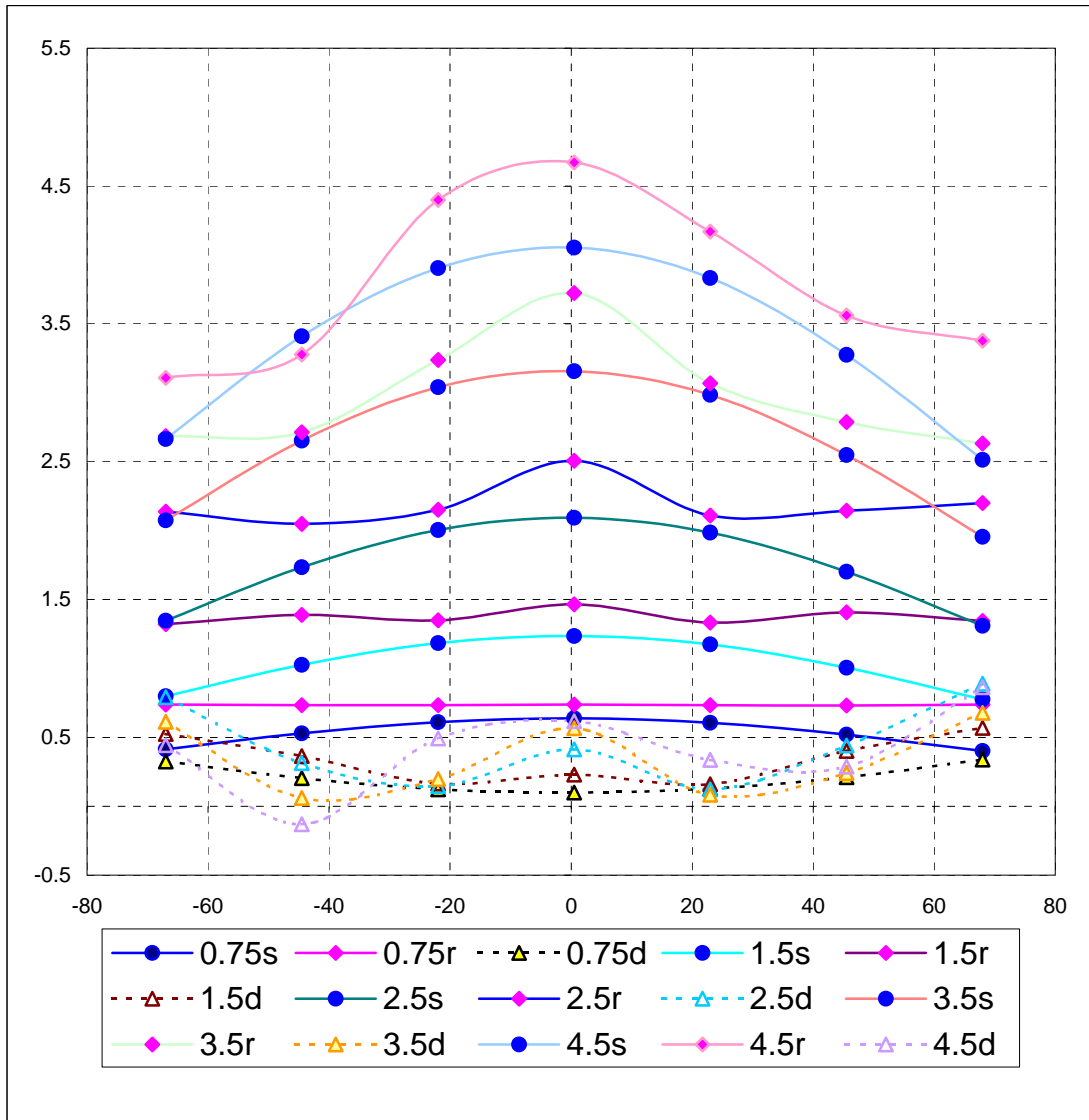
Figure 3.10 Comparison of REF/DIF1 and SWAN wave heights at the
GENESIS reference line.
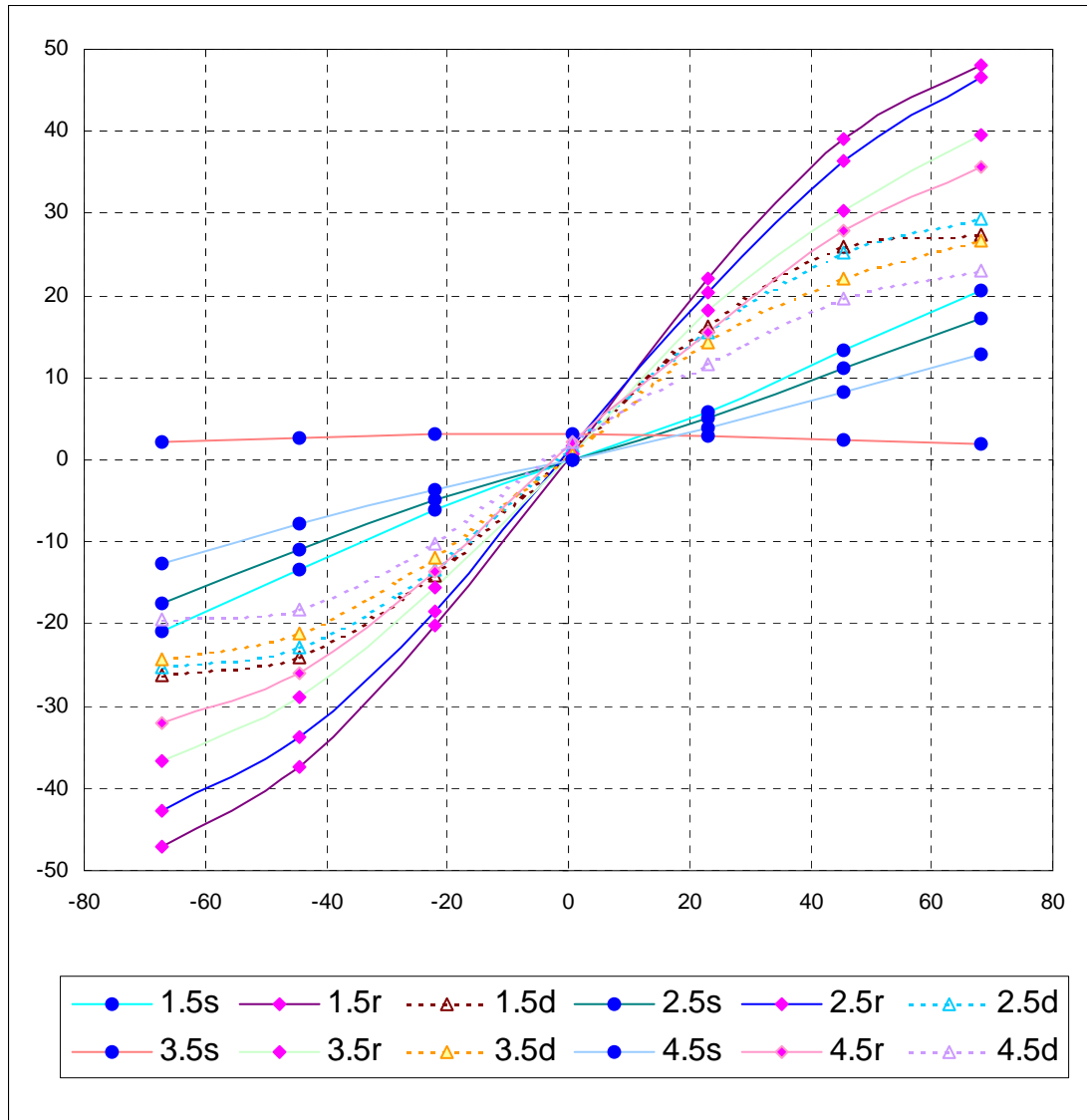
Figure 3.11 Comparison of REF/DIF1 and SWAN wave angles at the GENESIS reference line.

3.2.2 Longshore Sediment Transport

The last step of the modelling is the shoreline change, which has been carried out by using the GENESIS model (GENEralized Model for SImulating Shoreline Change).

3.2.2.1 GENESIS

In this section, the results of GENESIS model, which is designed to simulate long-term shoreline responses that are produced by spatial and temporal changes in longshore sand transport, will be explained. In order to simulate the shoreline changes by using the GENESIS model, the following procedure has to be followed. Firstly, data collection for the studied area is required. This step was explained previously. The second step is to setup the model. Thirdly, calibration and verification the model, which are both essential steps, must be carried out before running the model as the last step in order to get the model outputs.

In order to setup the model, the required input files (shorl.dat, shorm.dat, seawl.dat, waves.dat, and start file) were prepared as it was explained in the part of input data. The model GENESIS "VERSION 3.0 DEC 1995" was used with the help of "Shoreline Modeling System", SMS, which must be available under C drive of the PC.

3.2.2.1.1 Model Calibration and Verification

Before GENESIS can be used for quantitative estimation of shoreline changes, the capability of the model to provide reliable estimates of shoreline evolution at the site must be demonstrated through calibration and verification.

Model calibration refers to the process of adjusting the model coefficients so that optimal agreement between the measured and calculated values is obtained. In the present study, the model calibration indicates the adjustment of the sediment "transport parameters", $k1$ and $k2$ in order to provide the best agreement between the calculated and measured shoreline positions. Different suggestions of $k1$ and $k2$ values are available in literature. Some of these are listed in Table 3.6.

Table 3.6 Some suggestions for the "transport parameters", $k1$ and $k2$.

k1	k2	Reference
0.77		Komar and Inman (1970)
0.58-0.77	(0.5-1) k1	Hanson and Kraus (1989)
0.1-1	(0.5-1.5) k1	Gravens, Kraus, and Hanson (1991)

The lack of long-term shoreline observations, which should be more than one year according to Hanson and Kraus 1989, and the limited data on existing structures in the area (except the controlling structure), made it difficult to perform the model calibration and verification. Therefore,

calibration could be approximately done by using different techniques such as measured sand transport rates, empirical estimations, or local measurements.

3.2.2.1.1.1   Calibration by using Kampius's Empirical Formula

There exist no measurements of the shoreline position in the study area, which can be used for calibration and verification. For good calibration and verification, three measured shorelines must be available. One of these is used as the initial shoreline, the other to calibrate the model and the last to verify the calibrated model.

For the Manavgat case, the model was calibrated by using the estimated longshore sediment rates from the Kamphuis (1991) formula (mentioned in Abul-Azm, and Rakha, 1997). After calculating Q_s from the Kamphuis formula as shown in Table 3.7, different values of k1 and k2 (within ranges mentioned in Table 3.6) were used to calculate Q_s from the GENESIS model during 4 years (till 1996). As it is shown in Table 3.8, k1=0.516 and k2= 0.9 are the values that provide the best fit to the results obtained from the Kamphuis formula. These values were used in simulating shoreline changes around the Manavgat River mouth. Figure 3.11 shows the shoreline position of 1996 compared with initial shoreline in 1992.

Table 3.7 Estimation of longshore sediment transport rates by using the empirical formula of Kamphius.

Estimation of Qs for Manavgat using Kampuis' empirical formula.						
Beach slope = 0.0181, D50 = 1mm, Angle with north =113						
Angle	Average Ho	Breaker Angle	Hb (Aces)	T	q_s Kamphuis	Prob	Q_S Kamphuis
-67	0.75	2.3321	0.8951	4.2	-27174.4529	7.525196917	-2044.9
-44.5	0.75	5.8033	0.9647	4.2	-54357.843	5.128313712	-2787.6
-22	0.75	7.637	0.8964	4.2	-55172.2809	4.717540442	-2602.8
0.5	0.75	0.7196	0.9143	4.2	14010.76951	2.05386635	287.8
23	0.75	5.8097	0.9631	4.2	54213.03123	1.287371898	697.9
45.5	0.75	7.9377	0.9239	4.2	59948.90463	0.914711612	548.4
68	0.75	2.6443	0.886	4.2	28703.90714	0.973998475	279.6
-67	1.5	23.254	2.1915	6	-1034000.09	1.698145168	-17558.8
-44.5	1.5	21.9849	1.7749	6	-660593.082	1.312780554	-8672.1
-22	1.5	8.9866	1.7313	6	-386388.718	2.511222156	-9703.1
0.5	1.5	0.9017	1.8184	6	108338.61	1.74896248	1894.8
23	1.5	10.5357	1.7877	6	451540.7133	0.787668332	3556.6
45.5	1.5	33.493	2.0507	6	1044380.267	0.762259676	7960.9
68	1.5	36.7752	2.3488	6	1404325.632	0.673329381	9455.7
-67	2.5	32.4249	2.8183	7.5	-2729298.55	0.067756416	-1849.3
-44.5	2.5	25.7838	3.0041	7.5	-2843350.81	0.114338951	-3251.1
-22	2.5	14.4553	3.0892	7.5	-2250768.05	0.592868637	-13344.1
0.5	2.5	2.0699	3.0823	7.5	715925.5896	0.461590582	3304.6
23	2.5	16.6451	3.0284	7.5	2334230.012	0.199034471	4645.9
45.5	2.5	36.5529	2.8767	7.5	2939844.498	0.165156263	4855.3
68	2.5	41.8962	3.5084	7.5	4474212.95	0.101634624	4547.3
-67	3.5	24.4704	3.7506	9	-5694266.61	0	0.0
-44.5	3.5	20.0068	4.0117	9	-5920709.58	0	0.0
-22	3.5	14.2319	4.4743	9	-6153853.63	0.127043279	-7818.1
0.5	3.5	0.3151	4.3859	9	616209.4097	0.080460744	495.8
23	3.5	15.8812	4.0516	9	5356046.089	0.012704328	680.4
45.5	3.5	26.4764	3.9756	9	6619959.081	0.004234776	280.3
68	3.5	33.3241	3.8226	9	6656578.847	0.02117388	1409.5
-67	4.5	24.7775	4.9135	10.2	-11856645.1	0	0.0
-44.5	4.5	23.9165	5.1932	10.2	-13036693.9	0	0.0
-22	4.5	16.4024	5.5106	10.2	-12162701.8	0.04234776	-5150.6
0.5	4.5	0.3117	5.872	10.2	1324014.114	0.033878208	448.6
23	4.5	11.9151	5.3545	10.2	9629939.709	0	0.0
45.5	4.5	30.4856	5.3687	10.2	15384959.05	0	0.0
68	4.5	40.4064	4.9884	10.2	14285563.96	0	0.0
						34.11959007	-29433.0
					Q_s between 1992-1996= -117731.81 m^3/ year		

Table 3.8 Calibration of "transport parameters", k1 and k2.

k1	k2	Q GENESIS
0.5	1	-1.09E+05
0.6	1.2	-1.59E+05
0.54	1.08	-1.29E+05
0.54	0.8	-1.29E+05
0.52	0.8	-1.19E+05
0.518	0.8	-1.18E+05
0.516	**0.9**	**-1.17E+05**
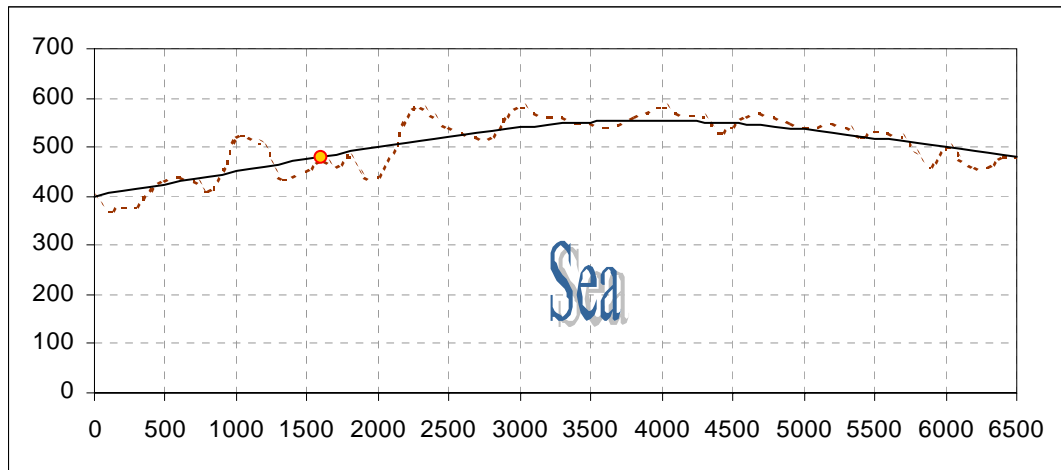
Figure 3.12 The final shoreline shape calculated by using the "transport

parameters" k1=0.516 and k2=0.9 (1996)

3.2.2.1.1.2   Verification of the Model

Verification could be performed by using the shoreline displacement behind the controlling structure (between 27.05.1996 and 10.02.2000) which was found to be about 40 m., so that the model calibration and verification step could be finished. In the Manavgat case, the structure controlling the river mouth is an impermeable non-diffracting jetty (groins as well as jetties that do not extend beyond the average width of the surf zone are treated as non-diffracting structures that interrupt the movement of sand alongshore). The mouth is treated as an impermeable non-diffracting groin, so the model should be able to simulate the shoreline position after the construction of the structure. The shoreline displacement at the mouth that was found from the maps prepared by Yuksel Project could be used for verification of the model. However, the measurements could not be used in this stage for two reasons. Firstly, the structure had not been totally finished at the time of the measurement. Secondly, the area was not yet stable (in equilibrium). Thus the vales of k1 and k2 that were found from the model calibration by using Kampiues' formula are accepted as the final transport parameters for this stage. However, it is recommended to verify the model in the future by taking reliable measurements of the shoreline along the study area.

GENESIS was run for the Manavgat River mouth area for the year of 1996 when the controlling jetty designed by Yuksel Project was started to be built, and also for the period of 2006 to 2036 in order to show the future behaviour of the shoreline. It should be pointed out that the first and the last few cells of the modelled area should not be used since suitable locations for boundaries were not available (for example rocky part of the shore).

The output files of GENESIS for 1996, and 2006 are available in Appendix B. However, the out put file for 2036 has not been included in that Appendix as it is too long. Figures 3.13-3.15, Figures 316-3.18 and Figures 3.19-3.21 show the shoreline positions, shoreline changes, transports rate for years 1996, 2006, and 2036. Figure 3.22 illustrates the shoreline positions for 1996, 2006, and 2036 all together.
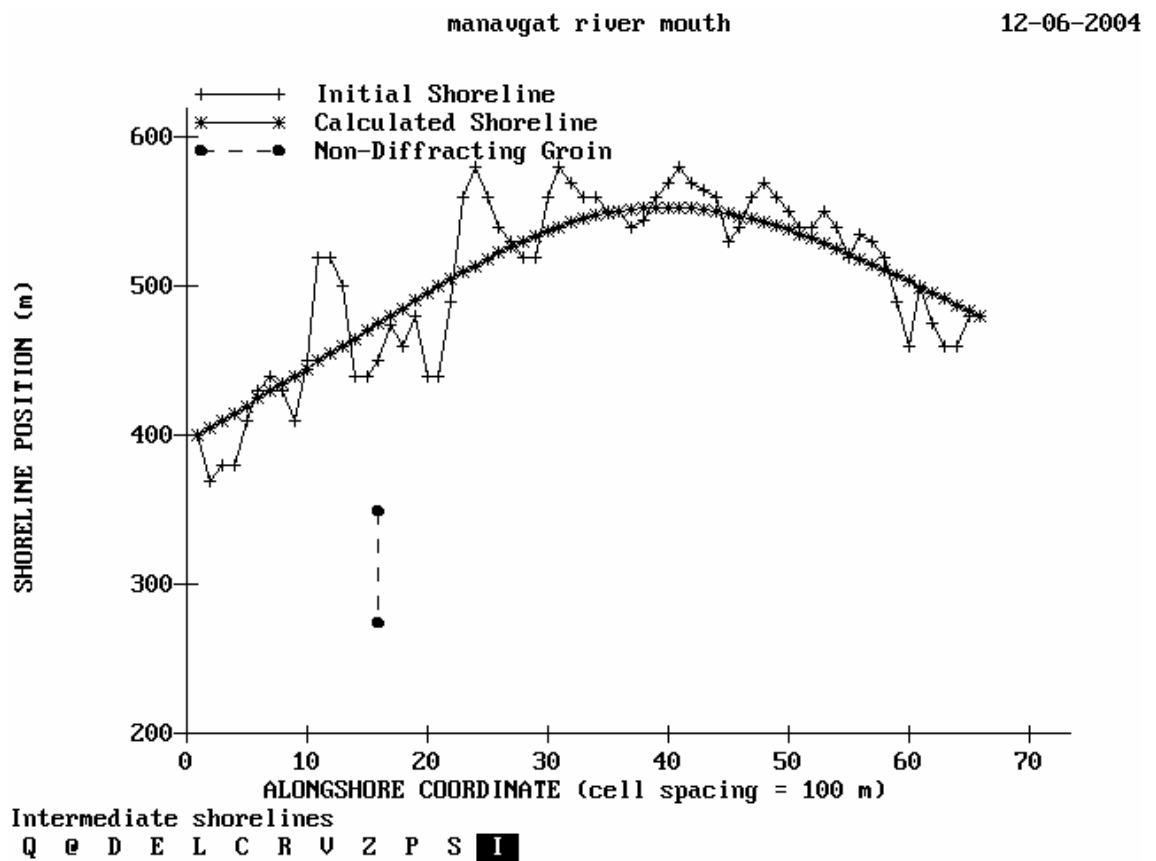
Figure 3.13 The shoreline positions (1996)
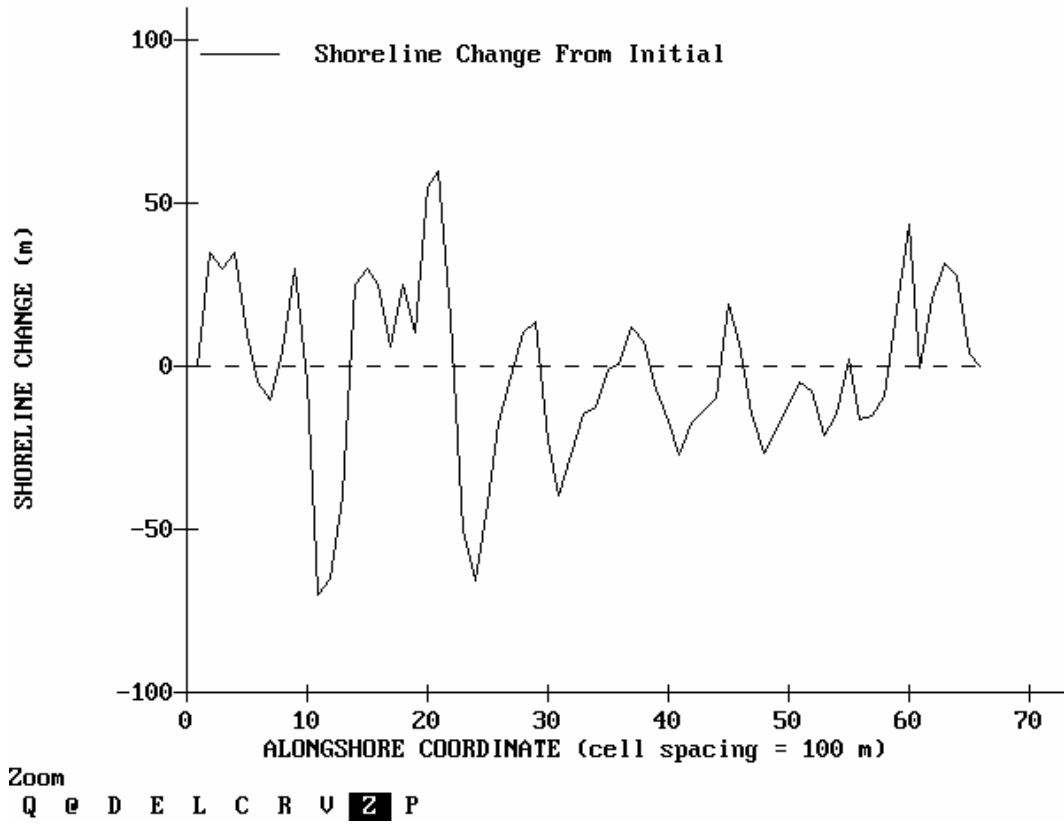
Figure 3.14 Shoreline changes (1996)
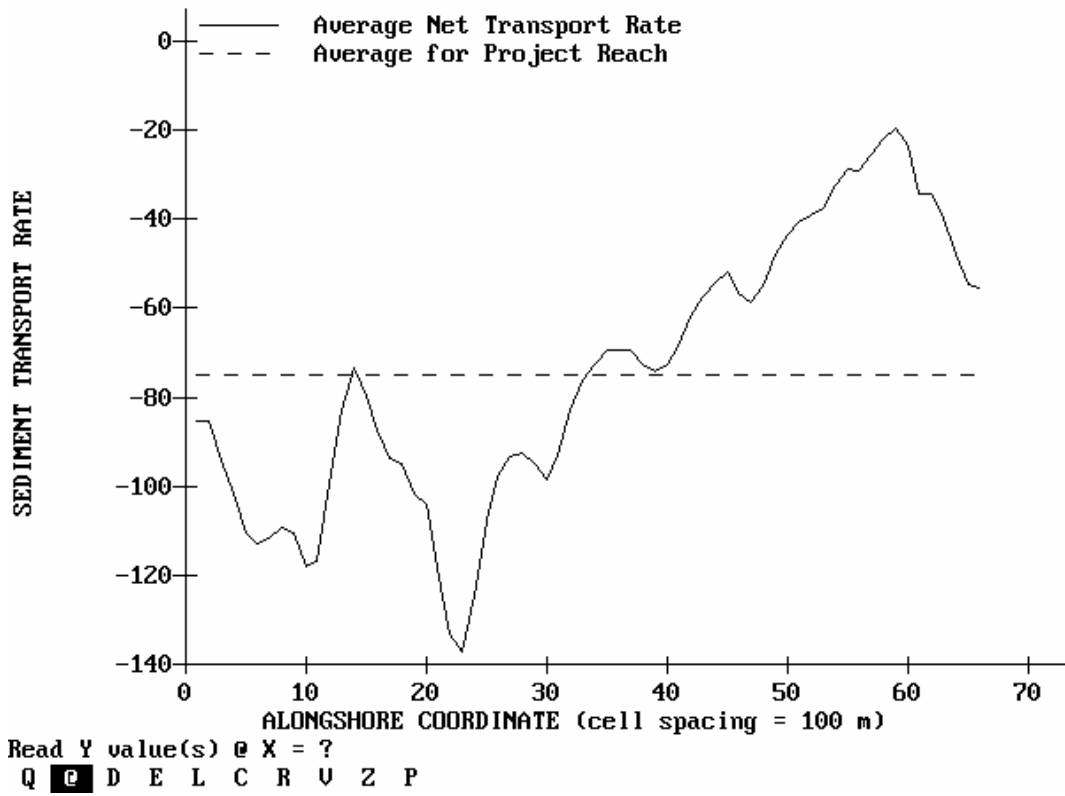
Figure 3.15 Sand transport rates in thousand cubic meters per year. (1996)
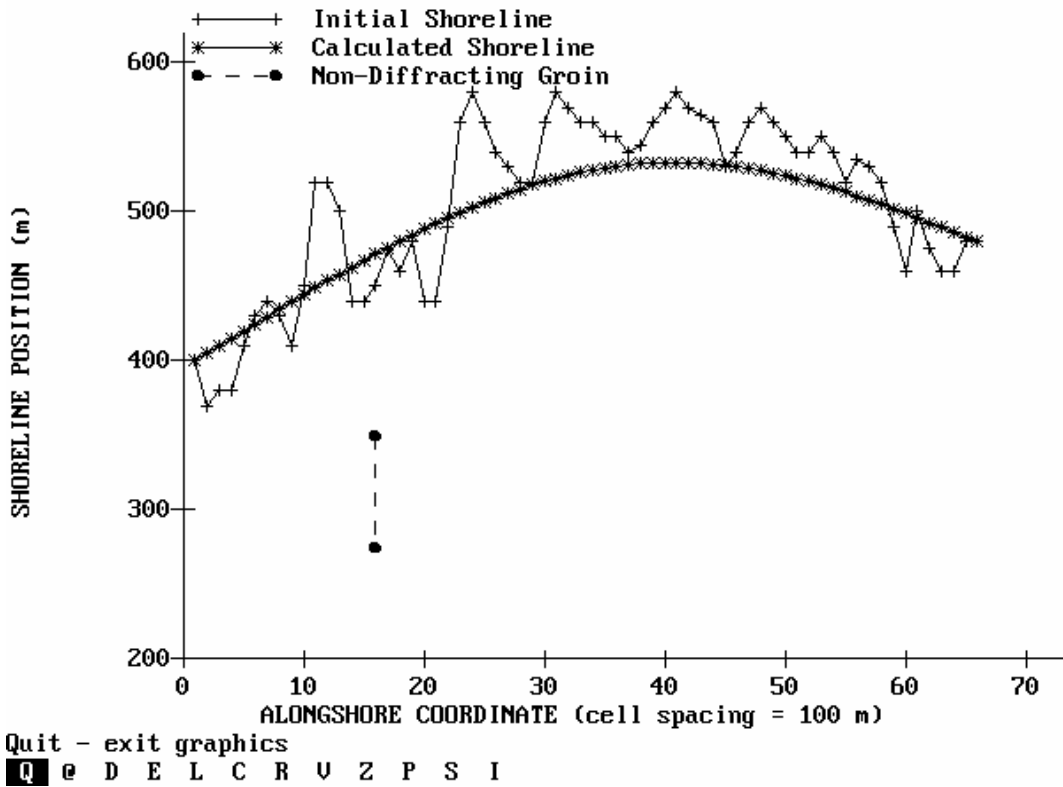
Figure 3.16 Shoreline positions (2006)
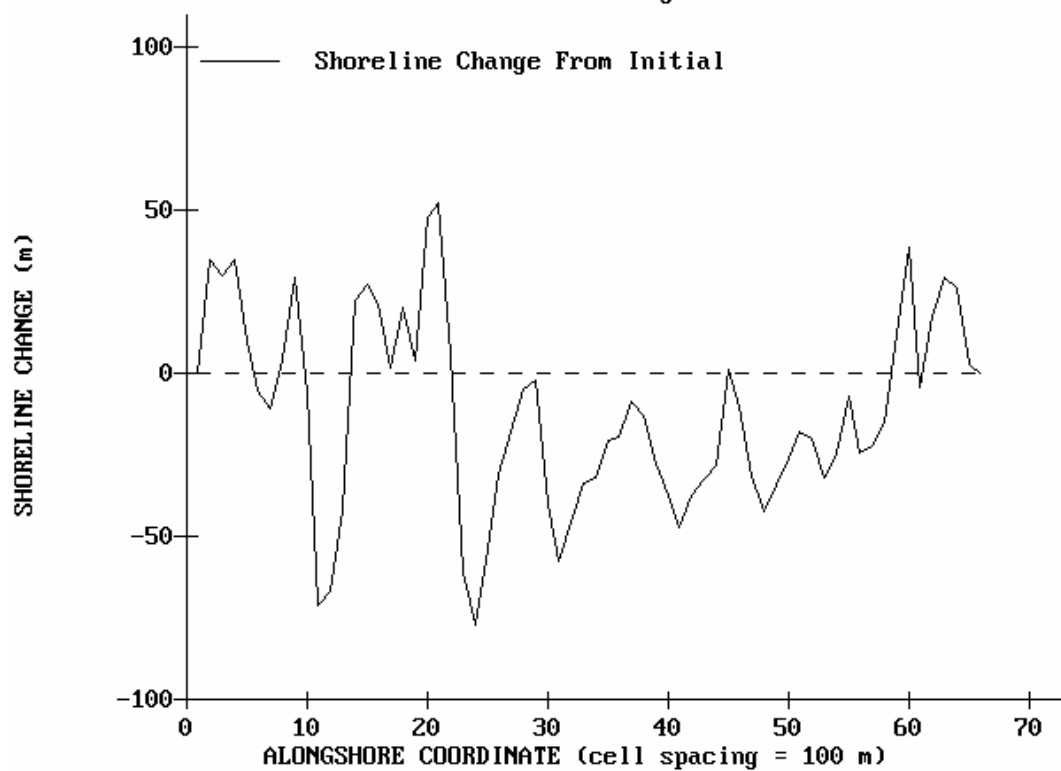
Figure 3.17 Shoreline changes (2006)
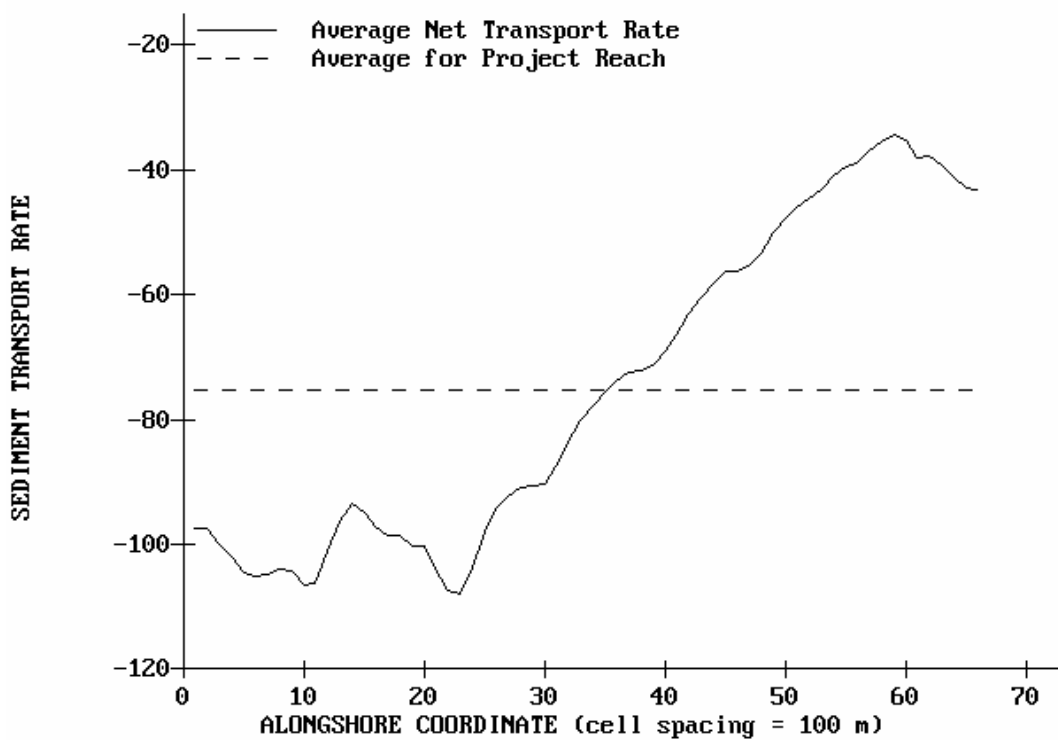
Figure 3.18 Sand transport rates in thousand cubic meters per year. (2006)
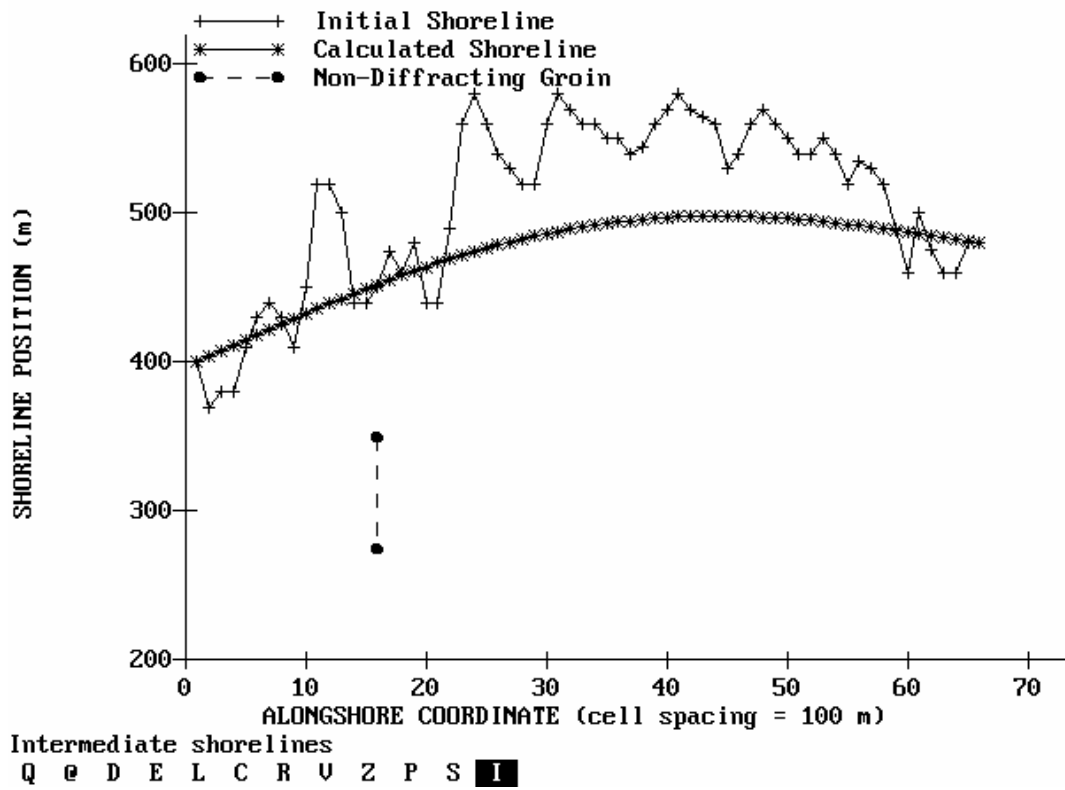
Figure 3.19 Shoreline positions (2036)
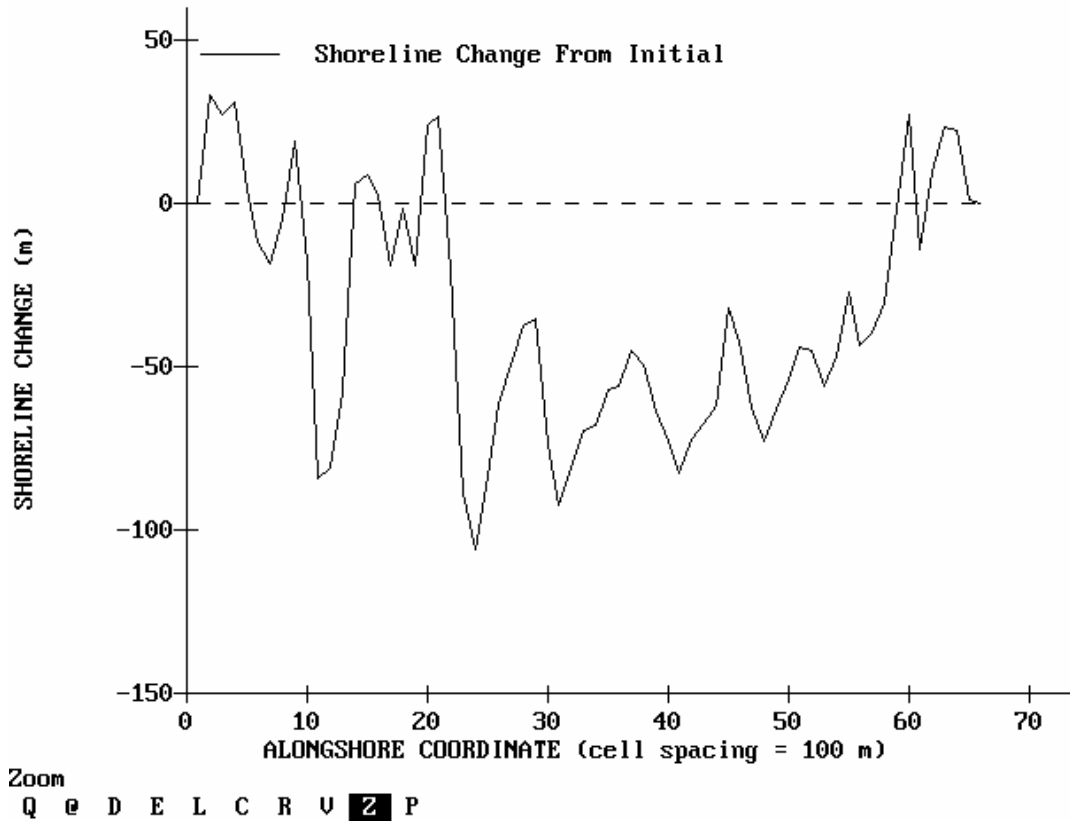
Figure 3.20 Shoreline changes (2036)
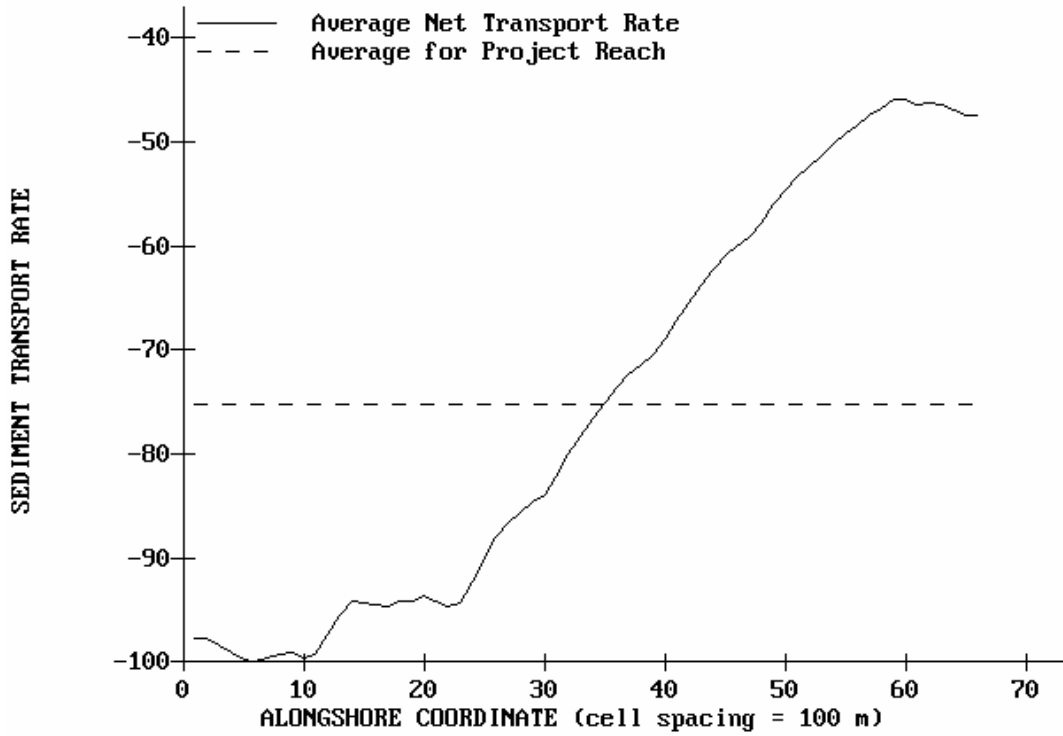
Figure 3.21 Sand transport rates in thousand cubic meters per year. (2036)
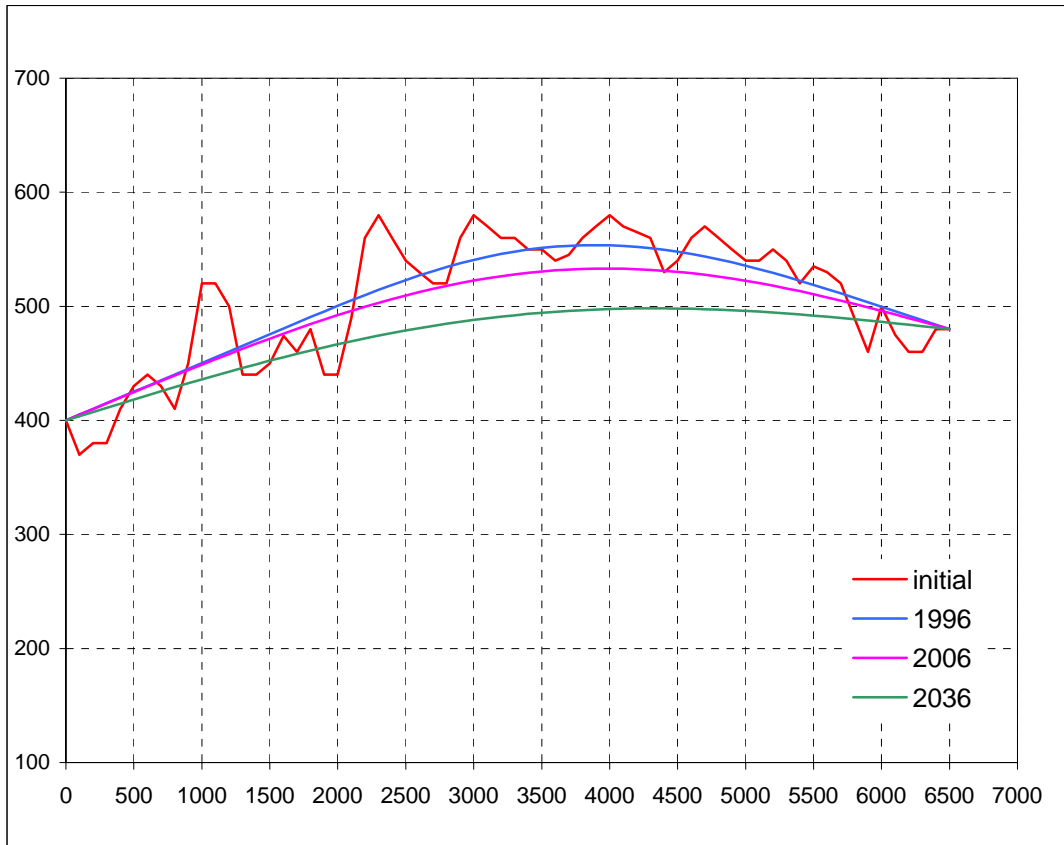
Figure 3.22 Shoreline positions for the years of 1996, 2006 and 2036

CHAPTER 4

4. DISCUSSION OF RESULT

This chapter includes discussion of the results that were obtained from the numerical modeling of shoreline around the Manavgat River mouth. Firstly, a discussion of nearshore wave modeling results is presented. This is followed by a discussion of shoreline change modeling results obtained by means of the model GENESIS.

4.1. REF/DIF 1 and SWAN Results

- The Ref/Dif 1 model is more sensitive to the grid intervals than the SWAN model. For example Ref/Dif 1 did not work at a grid interval of 100 m. with small wave heights while SWAN did. This is due to the fact that Ref/Dif 1 is a phase resolving model. It can not offer physically consistent simulations of fine-scale variations in the nearshore area due to bathymetric and current effects.

- Ref/Dif 1 could not work with small waves over large grid steps including deep conditions for these waves while SWAN could easily do since it is suitable for propagating waves over global distances to shelf regions as all models in the phase averaging realm.

- It was seen from the figures presenting the nearshore wave fields of SWAN and Ref/Dif 1 that the wave height variations in SWAN field are more complex than those of Ref/Dif 1. In SWAN, the affected areas with errors are typically regions with the apex at the corners of the water boundary with wave information, spreading towards shore at an angle of 30^0 to 45^0 for wind sea conditions to either side of the imposed mean wave direction. The difference in the wave field between Ref/Dif 1 and SWAN at the lateral boundaries is clearly seen in the Figures (3.8) and (3.9). This results in greater differences in wave parameters obtained from SWAN at the three location selected over the reference line of GENESIS than those resulted from Ref/Dif 1 runs. However these differences are in acceptable ranges for both models

- Nearshore wave heights obtained from Ref/Dif 1 are generally bigger than those obtained from SWAN. This could be due to the fact that SWAN is a spectral model and that the wave energy dissipation is active during wave generation by wind action, as caused by dissipation by white-capping, dissipation by depth-induced wave breaking, dissipation by bottom friction, and redistribution of wave energy over the spectrum by non-linear wave-wave interactions (both quadruplets and triads).

4.2. GENESIS Results

- GENESIS exhibits very lows sensitivity to changes in the numerical value of k2. However, its sensitivity is much stronger to changes in the k1 values.

- The method used for calibration requires verification since it is based on an empirical formula which may or may not work well for the conditions of the Manavgat case.

- Verification of the model by using the results obtained from digitising the maps prepared by Yuksel Proje could not be carried out for the reasons listed below:
    - Bathymetry in the region was not yet stable (in equilibrium) since the controlling protection structure was not completely finished.
    - The bathymetric maps covered a very small area compared to that considered in the model simulations.
    - The bathymetric measurements were carried out periodically. For calibration and verification of the model, it is necessary that measurements are taken in the same seasons with time intervals more than one year between successive campaigns.

- During the first years of simulation as it is in 1996, a smoothing of shoreline can be clearly seen. And this is logical process in such

sandy coast. The range of this smoothing is varying from very small values to 50 m in few part of the shore.

▪ After the smoothing period, the shoreline movement has more uniform displacements according to the shoreline of 1996. These displacements reach 40-50 m. range in maximum for year of 2036 with average of 1 m./year.

▪ The shoreline changes according to the initial shoreline in the part of shore that located west of the river mouth shows almost the same behaviour for different period of simulation. However it shows the same shape with bigger displacement and this should be a result of the dominant wave direction that affecting the studied area.

▪ From the figures that are presenting the sediment transport rates it can be seen that at 1996 (first years of smoothing the shore) the transport rates' changes along the shore are taking place in a random way with a general trend to change from negative in west to positive in east parts. Later on these changes get regular with linear shape of about 10 thousand m cub/year/100 m.

CHAPTER 5

5.   CONCLUSIONS AND RECOMMENDATIONS

Modelling of shoreline changes is an essential step before the design of any coastal engineering project. The present study attempted to develop a system of numerical models that could carry out this task. The system of models was applied to predict the shoreline changes around the Manavgat River mouth, which is frequently used by small sailing and fishing boats. As the first step, deep water wave characteristics including the annual wave rose affecting Manavgat River mouth were obtained from the database of the NATO TU-WAVES Project. Then Ref/Dif 1 and SWAN nearshore wave models were used to find out nearshore wave conditions. The results obtained from this modelling stage were presented in plots that were prepared by a series of FORTRAN programs that were written for this purpose. The Ref/Dif 1 wave model was used for preparing the time series nearshore reference wave file with three hours time intervals by employing a FORTRAN program (see Appendix C). This reference file was used to run the GENESIS model. The last step of the numerical shoreline change modelling of Manavgat River mouth was the calibration procedure in which the numerical values of the "transport parameters" k1 and k2 were determined as k1=0.516 and k2=0.9.

At the beginning of simulation (few years till 1996), a smoothing of the shoreline is clearly seen as it is shown in Figure 3.12. Than a seaward

displacement is recognised at the middle of studied shoreline and this displacement is in the order of 50 m. from the 1996 shoreline position.

The conclusions that are reached at the end of this study can be listed as follows:

- SWAN and Ref/Dif 1 models both give similar and reasonable predictions of the nearshore fields adjacent to the Manavgat River mouth area. Ref/Dif 1 model is simpler and easier to use than the SWAN model. However, the SWAN model has many well developed features, which give the user many options on how each model run is executed. These features range from purely convenient options that allow several different formats for input and output data, to options that allow control of fundamental physical processes in the model like wave generation, dissipation, and interaction.

- Finer the bathymetric grid, one obtains more accurate results of the nearshore wave fields, especially with Ref/Dif 1. A grid with 25 m cell spacing provided reasonable results for the Manavgat case.

- Care should be given to the lateral boundaries and the regions at the corners of the water boundary when using the SWAN model.

- Satisfactory preparation of wave boundary conditions for GENESIS while giving importance to control whether constant or variable boundary conditions are available, is important in modelling shoreline changes. These control the success of the simulation.

- A displacement of shoreline in the order of 1m/year should be considered when planning or designing of any coastal project in Manavgat River mouth region.

- The present numerical model simulations based on the available data provided reasonable shoreline changes around the Manavgat River mouth. However, in order to get more reliable results, verification is necessary.

There was a significant deficiency in the measured data for the Manavgat River mouth case and this caused major difficulties in the numerical simulation of shoreline changes. To avoid such difficulties it is recommended to:

- Take good measurements of nearshore wave data and make comparison of these data with the results of SWAN and Ref/Dif 1 models to find out the agreement levels. This will allow the verification of these wave propagation models. Than, the results of the better model could be used to prepare the time serious nearshore wave file which would be the input files for the GENESIS model.

- Take good periodic measurements of the shoreline positions for several years in the summer season (especially in July if the same initial shoreline is used in simulation) in order to carry out good calibration and verification of the GENESIS model.

- Obtain good and reliable information about the beach material (especially grain size).

- Get good measurement of all possible physical and technical operations taking place in the special structure region in order to have a good set of data can be used in calibration and verification for river mouth part only as this is possible in GENESIS model.

REFERENCES

Abdalla, S., 1991, "Devolopment of a third generation wind wave model applicable to finite depths", PhD. Thesis, Middle Technical University, Ankara, Turkey.

Abdallah, S. And Özhan, E., 1993, "Third-generation wind-wave model for use on personal computers.", J. Wtrwy., Port, Coast. And Oc. Div., ASCE, 119 (1), 1-14.

Abdallah, S. And Özhan, E., 1994, "METU models for wind-wave prediction", a METU-KLARE Special Report Middle Technical University, Ankara, Turkey.

Abul-Azm, A.G., and Rakha, K.A., 1997, "Environmental concerns for marina planning in the Gulf of Suez", Proceedings of the MEDCOAST 97 conference, pp.783-995.

Battjes, J.A. and J.P.F.M. Janssen, 1978, "Energy loss and set-up due to breaking of random waves", Proc. 16th Int. Conf. Coastal Engineering, ASCE, 569-587.

Berkhoff, J.C.W., 1972, "Computation of combined refraction-diffraction," Proc.13th Int. Conf. Coastal Engrg., ASCE, Vancouver.

Bodge, K. R., Creed C. G., and Raichle, A. W., 1996, "Improving Input Wave Data for Use with Shoreline Change Models", J. Waterway, Port, Coastal and Ocean Eng., ASCE, Vol. 122, No.5;Sept/Oct1996.

Booij, N., 1981, "Gravity Waves on Water with Non-uniform Depth and Current" Doctoral Dissertation, Technical University of Delft, The Netherlands, 131 PP.

Booji N., Ris, R. c., and Holthuijsen, L. H., 1999, "A Third-Generation Wave Prediction Model for coastal regions. 1. Model description and validation", J. Of Geophysical Research, 104 (C4), 7649-7666.

CEM-III, 1998, Coastal Engineering Manual, I, U.S. Army Corps of Engineers, Washington D.C.

Chu, V.C. and C.C. Mei, 1970, "On slowly varying Stokes waves," J. Fluid Mech., 41, 873-887.

Daniel J., 1971, "The Mediterranean Sea; a natural sedimentation laboratory", Stroudsburg, Pa., Dowden, Hutchinson & Ross.

Denny, M.W., 1988, "Biology and the Mechanics of the Wave-Swept Environment.", Princeton University Press, New Jersey.

Djordjevic, V.D. and L.G. Redekopp "On the development of packets of surface gravity waves moving over and uneven bottom," Z. Angew. Math. and phys., 29, 950-962.

Eldeberky, Y. and J.A. Battjes, 1996, "Spectral modelling of wave breaking: Application to Boussinesq equations," J. Geophys. Res., 101, No. C1, 1253-1264.

Hanson, H., 1987, "GENESIS, a Generalized Shoreline Change Model for Engineering Use", Report No. 1007, Department of Water Resources Engineering, University of Lund, Lund, Sweden.

Hanson, H., and Kraus, N.C., 1989, "GENESIS: Generalized Model for Simulating Shoreline Change, Report 1, Technical Reference", Technical Report CERC-89-19, Coastal Engineering Research Center, US Army Engineer Waterways Experiment Station, Vicksburg, MS.

Hasselmann, K., T.P. Barnett, E. Bouws, H. Carlson, D.E. Cartwright, K. Enke, J.A. Ewing, H. Gienapp, D.E. Hasselmann, P. Kruseman, A. Meerburg, P. Müller, D.J. Olbers, K. Richter, W. Sell and H. Walden, 1973, " Measurements of wind-wave growth and swell decay during the Joint North Sea Wave Project (JONSWAP)", Dtsch. Hydrogr. Z. Suppl., 12, A8

Hasselmann, K., D.B. Ross, P. Müller and W. Sell, 1976: A parametric wave prediction model, J. Phys. Oceanogr., 6, 200-228

Hsu, Y.L., Kaihatu, J.M., and MacNaughton, A., 1997, "Validation test report for shallow water wave refraction and diffraction (REFDIF1) model", NRL/FR/7322—97-9669, Naval Research Laboratory, Stennis Space Center, Miss., 1-25.

Güler I., Ergin A., Yalçiner A.C., 2003, "Monitoring Sediment Transport Processes at Manavgat River Mouth, Antalya Turkey", COPEDC, VI, Colombo Sri Lanka.

Güler I., 1996, "Manavgat Irmak Ağzi Düzenlemesi Araştırması" Yüksel proje Uluslararası A.Ş

Kaihatu, J.M., 1997, "Review and verification of numerical wave models for near coastal areas- Part 1: Review of mild-slope equation, relevant approximations, and technical details of numerical wave models", NRL/FR/7322-97-9669, Naval Research Laboratory, Stennis Space Center, Miss., 1-27.

Kamphuis, J.W., 1991, "Alongshore sediment transport rate". J. Waterway, Port, Coastal and Ocean Engineering. Vol. 117(6), pp. 624-640.

Kirby, J.T., 1986, "propagation of weakly-nonlinear surface water waves in regions with varraing depth and current", ONR Tech. Rept. 14, Res. Rept. CE-83-37, Department of Civil Engineering, University of Delaware, Newark, Del.

Kirby, J.T. and Dalrymple, R.A., 1986, "Approximate modeling of nonlinear dispersion in monochromatic wave models." Coastal Engineering, 9, 545-561. Reply to discussion, 11,87-92,1987.

Kirby, J.T. and R.A. Dalrymple, 1993, "REF/DIF1 Version 2.5, documentation and users manual", Centre for Applied Coastal Research, Dept. of Civil Engineering, University of Delaware, Newark, Del.

Komar, P. D., and Inman, D. L., 1970, "Longshore Sand Transport on Beaches", J. of Geophysical Research, Vol 73, No. 30, pp 5914-5927.

Komar, P. D., 1976, 'Beach Prosses and Sedimentation', Prentic-Hall, Inc., Englewood Cliffs, NJ.

Manavgat Su Temini Projesi, Batimetri Rapou, İçme Suyu ve Kanalizasiyon Dairesi, D. S.İ. Genel Müdürlüğü, Ankara

Mei, C.C. and E.O. Truk, 1980, "Forward scattering by thin bodies" SIAM J. Appl. Math., 39, 178-191.

Miles, J. w., 1957, " on the generation of surface waves by shear flows." J. Fluid mechanics, 3, 185-204

Özhan, E., Abdalla, S., 1992, "Wave Climatology of the Turkish Coast: Measurement-Analysis-Modeling, NATO TU-WAVES", Presented to Science for Stability Programme, NATO Scientific Affairs Division, Middle East Technical University, Ankara, Turkey.

Özhan, E., Abdalla, S., 1993, "Wave Climatology of the Turkish Coast: NATO TU-WAVES Project", Proceedings of the 1st International Conference on the Mediterranean Coastal Environment, MEDCOAST 93, E. Özhan (ed.), MEDCOAST Publications, Ankara, Turkey.

Özhan, E., Abdalla, S., Seziş-Papila S., Turhan M., 1995, "Measurements and Modeling of Wind Waves along the Turkish Mediterranean Coasts and the Black Sea", Proceedings of the 2nd International Conference on the Mediterranean Coastal Environment, MEDCOAST 95, E. Özhan (ed.), MEDCOAST Publications, Ankara, Turkey.

Özhan E., Abdalla S., 1997, "Wind waves Climatology of the Black Sea and the Remaining Turkish Coast", The Progress of the NATO-TU WAVES Project., Proceedings of the Second International Conference on the Mediterranean Coastal Environment, MEDCOAST 97, E. Özhan (ed.), MEDCOAST Publications, Ankara, Turkey.

Philips, O.M., 1957, "On the Generation of Waves by Turbulent Wind", Journal of Fluid Mechanics, V. 2, pp. 417-445.

Ris, R.C.; Booji, N.; Holthuijsen, L.H.; Padilla-Hernandez, R. and Haagsma, IJ.G. 1998, SWAN user manual (not the short version), Delft, (The Netherlands), Delft University of Technology.

Ris, R.C.; Holthuijsen, L.H.; Booji, N.; 1999, " A Third-Generation Wave Model for coastal regions. 2. verification", J. Of Geophysical Research, VOL. 104, NO.C4, pp 7667-7681.

SPM, 1984, Shore Protection Manual, I, U.S. Army Corps of Engineers, Washington D.C.

WAMDI Group, Hasselmann S., Hasselmann K., Bauer E., Janssen P.A:E.M., Komen G.J., Bertotti L., Lionello P., Guillaume A., Cardone V.C., Greenwood J.A., Reistad M., Zambresky L., Ewing J.A., 1988, "The WAM Model - A Third Generation Ocean Wave Prediction Model", J. of Phys. Oceanogr., 18, 1775-1810.

whitham, G. B., 1974, "Linear and Nonlinear Waves" New York.

Yue, D.K.P. and C.C. Mie, 1980, "Forward diffraction of stokes waves by a thin wedge," J. Fluid Mech., 99, 33-52.

APPENDIX A

Table A.1 Bathymetric Data during Yuksel Project

Altit.	Long.	27.05. 1996	19.12. 1996	24.04. 1997	21.11. 1998	4.12. 1998	15.12. 1998	03.06. 1999	10.02. 2000
34000	24300	-6.7	-5.98	-6.1	-5.75	-4.85			
34100	24300	-6.7	-5.7	-6.02	-5.53	-4.8			
34200	24300	-6.5	-5.6	-6.05	-5.3	-4.2			
34300	24300	-6.25	-5.5	-6.2	-4.9	-4.23			
34400	24300	-6.2	-5.3	-6.3	-4.44	-4.8			
34500	24300	-6	-5.2	-6.08	-4.18	-4.44			
34600	24300	-5.5	-5.15	-5.6	-3.96	-4.54			
34000	24400	-6.1	-5.13	-5.18	-5.16	-4.3	-5.38	-2.45	-3.76
34100	24400	-5.99	-5.02	-4.87	-4.69	-3.75	-5.65	-3.01	-3.74
34200	24400	-5.8	-4.8	-4.61	-4.29	-3.63	-6.32	-2.17	-2.81
34300	24400	-5.47	-4.5	-4.73	-4.02	-3.57	-6.45	-2.22	-2.58
34400	24400	-5.12	-3.94	-5.03	-2.87	-2.78	-5.22	-3.05	-2.6
34500	24400	-4.75	-3.78	-4.26	-2.5	-2.81	-3.83	-2.26	-2.39
34600	24400	-4.5	-3.5	-2.69	-2.19	-2.81	-1.9	-2.25	-2.35
34000	24500	-5.14	-4.3	-4.39	-4.04	-3.92	-4.35	-2.43	-2.24
34100	24500	-5.15	-3.97	-3.92	-4.3	-2.82	-5.07	-1.6	-2.64
34200	24500	-4.97	-3.56	-3.16	-3.23	-2.92	-6.15	-0.65	-1.5
34300	24500	-4.52	-3.01	-3.29	-2.08	-3.03	-5.11	-1.83	-1.47
34400	24500	-3.88	-2.53	-4.33	-0.83	-2.12	-1.61	-1.71	-1.76
34500	24500	-4.3	-2.25	-2.78	0	0	0	0	0
34600	24500	-3.23	-2.2	-2.35	0	0	0	0	0
34000	24600	-4.05	-3.33	-3.4	-2.73	-2.7	-5.88	-1.68	-0.58
34100	24600	-4.1	-3.06	-2.71	-2.67	-2.25	-5.64	-0.38	-2.5
34200	24600	-3.95	-2.61	-1.06	-1	0	-3.21	-1.92	-0.345
34300	24600	-2.98	-1.91	-2.71	0	0	0	-0.38	0
34400	24600	-1.49	-1.17	-2.44	-2.9	-2.75	-3.15	-0.64	-1.8
34500	24600	0	0	0	0	0	0	0	0
34600	24600	0	0	0	0	0	0	0	0
34000	24700	-2.16	-2.13	-2.07	-2	0	-1.5	-1.55	0
34100	24700	-2.26	-1.88	-1.73	-0.02	0	-5.71	-1.6	-1.44
34200	24700	-1.57	-1.28	-1.84	-2.03	-0.85	-1.23	0	-0.8
34300	24700	-1.1	-1.2	-4.07	-2.85	-1.96	-3.25	-0.75	-2.2
34400	24700	-0.05	-0.04	-0.11	-2.8	-3	-3.15	-0.55	-1.99
34500	24700	0	0	0	0	0	0	0	0
34600	24700	0	0	0	0	0	0	0	0
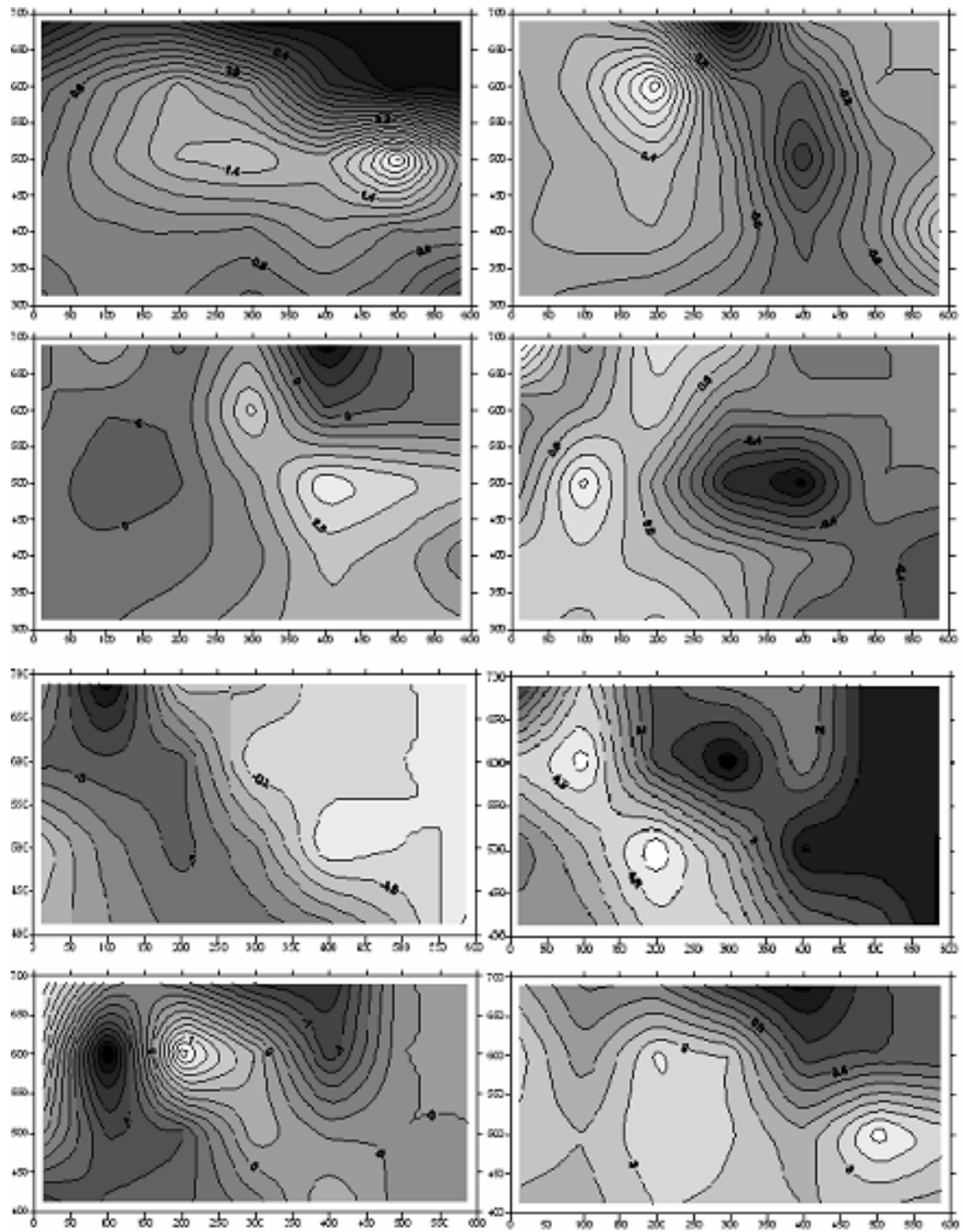
Figure A.2 Bottom Changes during Yuksel Project

Figure A.1 show changes in bottom depth from left to right during the fallowing periods: 19.12.1996-27.05.1996, 21.11.1998-27.04.1997, 27.04.1997-19.12.1996, 0.4.12.1998-21.11.1998, 15.12.1998-04.12.1998, 10.02.2000-03.06.1999, 03.06.1999-15.12.1998, 10.02-2000-27.05.1996.
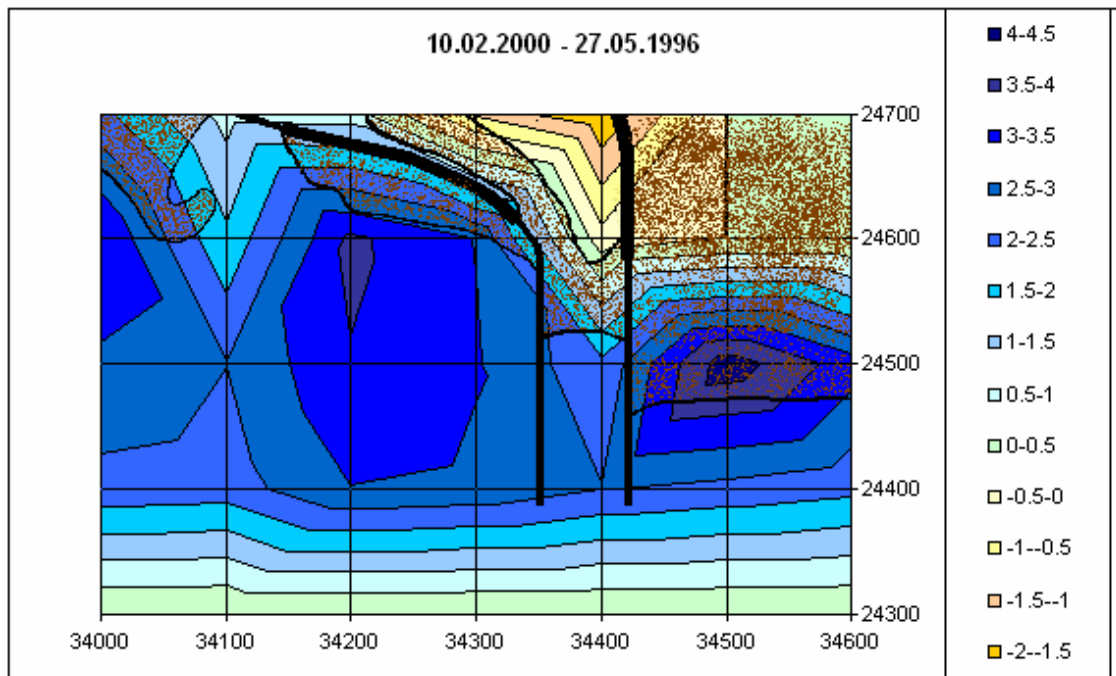
Figure A.2 Bottom Changes during the Period between

10.02.2000 and 27.05.1996.

APPENDIX B

INPUT AND OUTPUT EXAMPLE FILES

1. EXAMPLE INPUT FILES OF REF/DIF 1

- **param.h**

this file includes the parameter of the maximum cell numbers in x and y-axis and the subdividing interval that can be used when needed.

----

parameter(ixr=700,iyr=700,ix=21,iy=1000,ncomp=1)

- **indat.dat (141*255)**

This file is input file of REF/DIF1 on the grid dimension of (141*255) cells and wave of 4.5 m. in high, 10.2 in period and 0.5^0 incoming wave angles.

&FNAMES

FNAME1 = 'refdat.dat',

FNAME2 = 'outdat.dat',

FNAME3 = ' ',

FNAME4 = ' ',

FNAME5 = ' ',

FNAME6 = '',

FNAME7 = ' ',

FNAME8 = 'angle.dat',

FNAME9 = ' ',

FNAME10 = 'refdif1.log',

FNAME11 = 'height.dat',

FNAME12 = ' ',

FNAME13 = ' ',

FNAME14 = ' ',

FNAME15 = 'depth.dat'/

&INGRID

MR =141,

NR = 255,

IU = 1,

NTYPE = 1,

ICUR = 0,

IBC = 1,

DXR = 25.,

DYR = 25.,

DT = 3.,

ISPACE = 0,

ND = 1,

IFF = 0 0 0,

ISP = 0,

IINPUT = 1,

```
   IOUTPUT = 1/
   &WAVES1A
   IWAVE = 1,
   NFREQS = 1/
   &WAVES1B
   FREQS = 10.2,
   TIDE =  0.,
   NWAVS = 1,
   AMP = 2.25,
   DIR = 0.5/
```

----

2.   EXAMPLE INPUT FILES SWAN

▪   **Manavgat1.swn**

```
$************HEADING*******************************
$
PROJ 'manavgat1' '89'
$
$ PURPOSE OF TEST:obtain the nearshore wave caracteristics around
manavgat
$mouth
$
$
$ Hs   = 4.5 m
$ Tm   = 10.2 s
```

$ theta= 89.5

$ --|---|--

$ | This SWAN input file is part of the Ph. D. theses |

$ | Fatima AL SALEH |

$ --|---|--

$

$***********MODEL

INPUT******************************** ***

$

SET 0 113

$

CGRID 0. 0. 0. 6500. 3500. 65 35 SECTOR -25. 205. 36 0.04 1.00 40

$

INPGRID BOTTOM 0. 0. 0. 65 35 100. 100.

READINP BOTTOM 1. '100.dat' 1 0 FREE

$

BOU SHAPE JON 3.3 MEAN DSPR DEGR

BOUN SIDE SW CON PAR 4.5 10.2 89.5 31.5

$

$

OFF QUAD

$

$

$

$*********** OUTPUT REQUESTS ************************

$

$

POINTS 'POINT' FILE   'grid.loc'

SPEC   'POINT' SPEC1D 'manavgat1.spc'

TABLE 'POINT' HEAD   'manavgat1.tbl' HS RTP TM01 TM02 FSPR

TABLE 'POINT' HEAD   'manavgat1.tab'   XP DEP HS RTP TM01

TM02 FSPR DIR SETUP

$

TEST 0,0

POOL

COMPUTE

STOP

----

3. EXAMPLE INPUT FILES GENESIS

- **Shorl**

INITIAL SHORELINE POSITION OF 920724; CELL SPACING (DX=100. m)

THESE DATA WERE OBTAINED FROM THE "Manvgat Su temin projesi,24-july-1992"

STARTING AT ALONGSHORE POSITION X= 0. AND ENDING AT X= 6500.
****
400.0 370.0 380.0 380.0 410.0 430.0 440.0 430.0 410.0 450.0
520.0 520.0 500.0 440.0 440.0 450.0 474.0 460.0 480.0 440.0
440.0 490.0 560.0 580.0 560.0 540.0 530.0 520.0 520.0 560.0
580.0 570.0 560.0 560.0 550.0 550.0 540.0 545.0 560.0 570.0
580.0 570.0 565.0 560.0 530.0 540.0 560.0 570.0 560.0 550.0
540.0 540.0 550.0 540.0 520.0 535.0 530.0 520.0 490.0 460.0
500.0 475.0 460.0 460.0 480.0 480.0

- **Shorm**

INITIAL SHORELINE POSITION OF 920724; CELL SPACING (DX=100. m)

THESE DATA WERE OBTAINED FROM THE "Manvgat Su temin projesi,24-july-1992"

STARTING AT ALONGSHORE POSITION X= 0. AND ENDING AT X= 6500.
****
400.0 370.0 380.0 380.0 410.0 430.0 440.0 430.0 410.0 450.0
520.0 520.0 500.0 440.0 440.0 450.0 474.0 460.0 480.0 440.0

440.0 490.0 560.0 580.0 560.0 540.0 530.0 520.0 520.0 560.0
580.0 570.0 560.0 560.0 550.0 550.0 540.0 545.0 560.0 570.0
580.0 570.0 565.0 560.0 530.0 540.0 560.0 570.0 560.0 550.0
540.0 540.0 550.0 540.0 520.0 535.0 530.0 520.0 490.0 460.0
500.0 475.0 460.0 460.0 480.0 480.0

- **Seawl**

MEASURED SHORELINE POSITION OF 820101; CELL SPACING (DX=100. m)

THESE DATA WERE OBTAINED FROM " "
STARTING AT ALONGSHORE POSITION X= 0. AND ENDING AT X= 6500.
****
-9999 -9999 -9999 -9999 -9999 -9999 -9999 -9999 -9999 -9999
-9999 -9999 -9999 -9999 -9999 -9999 -9999 -9999 -9999 -9999
-9999 -9999 -9999 -9999 -9999 -9999 -9999 -9999 -9999 -9999
-9999 -9999 -9999 -9999 -9999 -9999 -9999 -9999 -9999 -9999
-9999 -9999 -9999 -9999 -9999 -9999 -9999 -9999 -9999 -9999
-9999 -9999 -9999 -9999 -9999 -9999 -9999 -9999 -9999 -9999
-9999 -9999 -9999 -9999 -9999 -9999

----

4. SHORELINE POSITIONS FOR 1996, 2006, AND 2036 (SHOC GENESIS' OUTPUT FILE).

- **Shorc for 1996**

****
FINAL SHORELINE LOCATION. BY COPYING THIS FILE TO SHORL.DAT
AND UP-DATING
START.DAT, THE MODEL MAY BE RUN AGAIN FOR A NEW
CONFIGURATION.
****
400.00 405.02 410.05 415.07 420.09 425.11 430.13 435.16 440.18 445.21

```
450.25  455.29  460.33  465.38  470.43  475.48  480.51  485.52  490.49  495.42
500.28  505.05  509.71  514.24  518.61  522.81  526.81  530.59  534.13  537.41
540.42  543.13  545.54  547.63  549.40  550.85  551.97  552.75  553.21  553.33
553.14  552.63  551.80  550.68  549.27  547.58  545.63  543.42  540.98  538.32
535.45  532.40  529.18  525.82  522.34  518.74  515.06  511.30  507.48  503.62
499.72  495.79  491.85  487.90  483.95  480.00
```

- **Shorc for 2006**

```
***************************************************************
```
 FINAL SHORELINE LOCATION. BY COPYING THIS FILE TO SHORL.DAT AND UP-DATING
 START.DAT, THE MODEL MAY BE RUN AGAIN FOR A NEW CONFIGURATION.
```
***************************************************************
 400.00  404.96  409.92  414.88  419.82  424.75  429.66  434.53  439.36  444.16
 448.90  453.60  458.23  462.79  467.29  471.69  476.01  480.23  484.34  488.34
 492.22  495.96  499.58  503.04  506.35  509.50  512.48  515.28  517.89  520.32
 522.54  524.57  526.39  527.99  529.38  530.55  531.50  532.23  532.74  533.03
 533.09  532.94  532.56  531.98  531.19  530.20  529.01  527.63  526.06  524.32
 522.41  520.34  518.11  515.74  513.24  510.61  507.87  505.03  502.09  499.08
 495.99  492.85  489.66  486.45  483.23  480.00
```

- **Shorc for 2036**

```
***************************************************************
```
 FINAL SHORELINE LOCATION. BY COPYING THIS FILE TO SHORL.DAT AND UP-DATING
 START.DAT, THE MODEL MAY BE RUN AGAIN FOR A NEW CONFIGURATION.
```
***************************************************************
 400.00  403.68  407.36  411.04  414.70  418.34  421.96  425.54  429.08  432.58
 436.03  439.42  442.76  446.03  449.23  452.36  455.42  458.39  461.27  464.07
 466.77  469.38  471.89  474.30  476.60  478.79  480.87  482.83  484.69  486.42
 488.04  489.54  490.92  492.18  493.32  494.33  495.23  496.00  496.65  497.19
 497.62  497.93  498.13  498.22  498.21  498.08  497.85  497.52  497.10  496.59
```

130

495.99 495.31 494.56 493.73 492.83 491.87 490.85 489.78 488.66 487.50
486.30 485.06 483.81 482.54 481.27 480.00
----

5. OUTPUT FILES OF GENESIS FOR 1996

▪ **Shorc**

The example is available in the previous part.

▪ **Setup**

C O A S T A L   E N G I N E E R I N G   R E S E A R C H   C E N T E R
&
L U N D   I N S T I T U T E   O F   T E C H N O L O G Y

```
 *****  ******* ** ** ******* *****  *****  *****
******* ******* ** ** ******* ******* ***** *******
** ** **    *** ** **    ** ** ** ** **
** ** **    *** ** **    ** ** ** ** **
**    **  **** ** **    **    ** **
**    ***** **** ** ***** ******  **   ******
** *** ***** ** **** *****  ****** **   ******
** *** **    ** **** **      ** **    **
** ** **    ** *** **    ** ** ** ** **
** ** **    ** *** **    ** ** ** ** **
******* ******* ** ** ******* ******* ***** *******
 *****  ******* ** ** ******* *****  *****  *****
```

```
        +---------------+
        | VERSION  3.0 |
        +---------------+

        USER No. 521
```

VERSION 3.0, DEC 1995

RUN: manavgat river mouth

METRIC UNITS

GROIN X-COORDINATES
   16
DISTANCE TO GROIN TIPS FROM X-AXIS
 274.00
GROIN PERMEABILITIES
   0.00

DX = 100.0   DT =   3.00   ISSTART = 1   N =   66   NTS = 11680
NWAVES = 1   DCLOS = 9.0   ABH =   1.0   DZ = 12.0   D50 = 1.00
HCNGF = 1.0   ZCNGF = 1.0   ZCNGA = 0.0   K1 =   0.52   K2 =   1.03

 SHORELINE POSITION AFTER 1.YEARS = 2920 TIME STEPS. DATE IS
930724
 400.00 405.09 410.24 415.49 420.86 426.31 431.76 437.13 442.32 447.24
 451.86 456.17 460.22 464.12 468.01 472.04 476.37 481.11 486.33 492.04
 498.17 504.60 511.15 517.66 523.93 529.80 535.14 539.89 543.99 547.45
 550.31 552.62 554.45 555.88 556.97 557.78 558.38 558.78 559.01 559.08
 558.97 558.66 558.14 557.38 556.34 555.00 553.31 551.23 548.74 545.79
 542.38 538.52 534.22 529.55 524.59 519.45 514.25 509.13 504.22 499.63
 495.45 491.71 488.38 485.39 482.63 480.00

 SHORELINE CHANGE AFTER 1.YEARS = 2920 TIME STEPS. DATE IS
930724
   0.00   35.09   30.24   35.49   10.86   -3.69   -8.24   7.13   32.32   -2.76
 -68.14 -63.83 -39.78   24.12   28.01   22.04   2.37   21.11   6.33   52.04
  58.17   14.60 -48.85 -62.34 -36.07 -10.20   5.14   19.89   23.99 -12.55
 -29.69 -17.38   -5.55   -4.12   6.97   7.78   18.38   13.78   -0.99 -10.92
 -21.03 -11.34   -6.86   -2.62   26.34   15.00   -6.69 -18.77 -11.26   -4.21
   2.38   -1.48 -15.78 -10.45   4.59 -15.55 -15.75 -10.87   14.22   39.63
  -4.55   16.71   28.38   25.39   2.63   0.00

 SHORELINE POSITION AFTER 2.YEARS = 5840 TIME STEPS. DATE IS
940724
 400.00 405.18 410.36 415.51 420.63 425.70 430.70 435.65 440.54 445.37
 450.17 454.94 459.72 464.54 469.40 474.34 479.37 484.50 489.73 495.03
 500.38 505.74 511.07 516.30 521.38 526.26 530.86 535.16 539.11 542.69
 545.88 548.68 551.07 553.08 554.72 556.01 556.97 557.60 557.94 557.99
 557.74 557.22 556.40 555.29 553.88 552.16 550.12 547.77 545.09 542.11
 538.85 535.32 531.57 527.63 523.56 519.40 515.20 511.00 506.84 502.76
 498.76 494.87 491.06 487.33 483.65 480.00

132

SHORELINE CHANGE AFTER 2.YEARS = 5840 TIME STEPS. DATE IS 940724

```
  0.00  35.18  30.36  35.51  10.63  -4.30  -9.30   5.65  30.54  -4.63
-69.83 -65.06 -40.28  24.54  29.40  24.34   5.37  24.50   9.73  55.03
 60.38  15.74 -48.93 -63.70 -38.62 -13.74   0.86  15.16  19.11 -17.31
-34.12 -21.32  -8.93  -6.92   4.72   6.01  16.97  12.60  -2.06 -12.01
-22.26 -12.78  -8.60  -4.71  23.88  12.16  -9.88 -22.23 -14.91  -7.89
 -1.15  -4.68 -18.43 -12.37   3.56 -15.60 -14.80  -9.00  16.84  42.76
 -1.24  19.87  31.06  27.33   3.65   0.00
```

SHORELINE POSITION AFTER 3.YEARS = 8760 TIME STEPS. DATE IS 950724

```
400.00 405.06 410.11 415.16 420.19 425.21 430.21 435.20 440.18 445.15
450.12 455.10 460.09 465.10 470.13 475.19 480.27 485.37 490.46 495.55
500.60 505.59 510.49 515.28 519.91 524.35 528.59 532.58 536.30 539.74
542.86 545.66 548.12 550.24 552.02 553.46 554.55 555.30 555.72 555.81
555.58 555.02 554.15 552.98 551.50 549.73 547.69 545.37 542.79 539.96
536.92 533.67 530.26 526.69 522.99 519.21 515.35 511.44 507.50 503.55
499.60 495.65 491.72 487.81 483.90 480.00
```

SHORELINE CHANGE AFTER 3.YEARS = 8760 TIME STEPS. DATE IS 950724

```
  0.00  35.06  30.11  35.16  10.19  -4.79  -9.79   5.20  30.18  -4.85
-69.88 -64.90 -39.91  25.10  30.13  25.19   6.27  25.37  10.46  55.55
 60.60  15.59 -49.51 -64.72 -40.09 -15.65  -1.41  12.58  16.30 -20.26
-37.14 -24.34 -11.88  -9.76   2.02   3.46  14.55  10.30  -4.28 -14.19
-24.42 -14.98 -10.85  -7.02  21.50   9.73 -12.31 -24.63 -17.21 -10.04
 -3.08  -6.33 -19.74 -13.31   2.99 -15.79 -14.65  -8.56  17.50  43.55
 -0.40  20.65  31.72  27.81   3.90   0.00
```

SHORELINE POSITION AFTER 4.YEARS = 11680 TIME STEPS. DATE IS 960723

```
400.00 405.02 410.05 415.07 420.09 425.11 430.13 435.16 440.18 445.21
450.25 455.29 460.33 465.38 470.43 475.48 480.51 485.52 490.49 495.42
500.28 505.05 509.71 514.24 518.61 522.81 526.81 530.59 534.13 537.41
540.42 543.13 545.54 547.63 549.40 550.85 551.97 552.75 553.21 553.33
553.14 552.63 551.80 550.68 549.27 547.58 545.63 543.42 540.98 538.32
535.45 532.40 529.18 525.82 522.34 518.74 515.06 511.30 507.48 503.62
499.72 495.79 491.85 487.90 483.95 480.00
```

SHORELINE CHANGE AFTER 4.YEARS = 11680 TIME STEPS. DATE IS 960723

```
  0.00  35.02  30.05  35.07  10.09  -4.89  -9.87   5.16  30.18  -4.79
-69.75 -64.71 -39.67  25.38  30.43  25.48   6.51  25.52  10.49  55.42
 60.28  15.05 -50.29 -65.76 -41.39 -17.19  -3.19  10.59  14.13 -22.59
-39.58 -26.87 -14.46 -12.37  -0.60   0.85  11.97   7.75  -6.79 -16.67
```

```
-26.86 -17.37 -13.20  -9.32  19.27   7.58 -14.37 -26.58 -19.02 -11.68
 -4.55  -7.60 -20.82 -14.18   2.34 -16.26 -14.94  -8.70  17.48  43.62
 -0.28  20.79  31.85  27.90   3.95   0.00
```

SHORELINE POSITION AFTER 4.YEARS = 11688 TIME STEPS. DATE IS 960724
```
400.00 405.02 410.05 415.07 420.09 425.11 430.13 435.16 440.18 445.21
450.25 455.29 460.33 465.38 470.43 475.48 480.51 485.52 490.49 495.42
500.28 505.05 509.71 514.24 518.61 522.81 526.81 530.59 534.13 537.41
540.42 543.13 545.54 547.63 549.40 550.85 551.97 552.75 553.21 553.33
553.14 552.63 551.80 550.68 549.27 547.58 545.63 543.42 540.98 538.32
535.45 532.40 529.18 525.82 522.34 518.74 515.06 511.30 507.48 503.62
499.72 495.79 491.85 487.90 483.95 480.00
```

SHORELINE CHANGE AFTER 4.YEARS = 11688 TIME STEPS. DATE IS 960724
```
  0.00  35.02  30.05  35.07  10.09  -4.89  -9.87   5.16  30.18  -4.79
-69.75 -64.71 -39.67  25.38  30.43  25.48   6.51  25.52  10.49  55.42
 60.28  15.05 -50.29 -65.76 -41.39 -17.19  -3.19  10.59  14.13 -22.59
-39.58 -26.87 -14.46 -12.37  -0.60   0.85  11.97   7.75  -6.79 -16.67
-26.86 -17.37 -13.20  -9.32  19.27   7.58 -14.37 -26.58 -19.02 -11.68
 -4.55  -7.60 -20.82 -14.18   2.34 -16.26 -14.94  -8.70  17.48  43.62
 -0.28  20.79  31.85  27.90   3.95   0.00
```

OUTPUT LAST TIMESTEP NO. 11688 DATE IS   960724

OFFSHORE WAVE DATA INPUT:
 HZ = 0.100000   T =   1.00000   ZZ = 0.000000

CALIBRATION/VERIFICATION ERROR =   20.5657

CALCULATED VOLUMETRIC CHANGE = -1.17E+05 (M3)

SIGN CONVENTION: EROSION (-), ACCRETION (+)

- **Output1996**

RUN: manavgat river mouth

INITIAL SHORELINE POSITION (M)

400.00	370.00	380.00	380.00	410.00	430.00	440.00	430.00	410.00	450.00
520.00	520.00	500.00	440.00	440.00	450.00	474.00	460.00	480.00	440.00
440.00	490.00	560.00	580.00	560.00	540.00	530.00	520.00	520.00	560.00
580.00	570.00	560.00	560.00	550.00	550.00	540.00	545.00	560.00	570.00
580.00	570.00	565.00	560.00	530.00	540.00	560.00	570.00	560.00	550.00
540.00	540.00	550.00	540.00	520.00	535.00	530.00	520.00	490.00	460.00
500.00	475.00	460.00	460.00	480.00	480.00				

****

GROSS TRANSPORT VOLUME (M3/1000) FROM   920724 TO   930724

307	307	289	290	303	309	316	332	329	326
327	287	304	318	289	272	273	290	303	335
325	352	365	327	331	327	314	303	288	294
286	294	297	292	294	292	295	289	286	285
286	295	295	298	304	287	287	286	299	302
300	293	290	298	300	288	291	299	308	302
289	299	302	295	293	295	295			

NET TRANSPORT VOLUME (M3/1000) FROM   920724 TO   930724

-31	-31	-66	-96	-132	-142	-139	-131	-138	-170
-167	-99	-35	4	-20	-48	-70	-72	-93	-99
-152	-210	-224	-175	-113	-77	-67	-72	-92	-116
-103	-74	-56	-51	-46	-53	-61	-80	-93	-92

```
-81   -60   -49   -42   -40   -66   -81   -74   -55   -44
-40   -42   -41   -25   -15   -19    -4    11    22     8
-31   -26   -43   -71   -97   -99   -99
```

TRANSPORT VOLUME TO THE LEFT (M3/1000) FROM   920724 TO
930724

```
-169  -169  -178  -193  -217  -226  -227  -231  -233  -248
-247  -193  -170  -156  -154  -160  -171  -181  -198  -217
-238  -281  -295  -251  -222  -202  -191  -187  -190  -205
-195  -184  -176  -171  -170  -173  -178  -184  -190  -189
-184  -178  -172  -170  -172  -176  -184  -180  -177  -173
-170  -168  -165  -162  -157  -154  -147  -143  -143  -146
-160  -163  -173  -183  -195  -197  -197
```

TRANSPORT VOLUME TO THE RIGHT (M3/1000) FROM   920724 TO
930724

```
138   138   111    96    85    83    88   100    95    77
 79    94   134   161   134   112   101   108   104   117
 86    70    70    75   108   124   123   115    97    88
 91   110   120   120   123   119   116   104    96    96
102   117   123   127   132   110   103   106   121   129
130   125   124   136   142   134   143   155   165   155
128   136   129   111    98    97    97
```

****

GROSS TRANSPORT VOLUME (M3/1000) FROM   930724 TO   940724

```
300   300   300   300   300   299   299   298   298   297
297   296   296   296   296   297   298   299   300   301
302   303   303   303   303   301   300   298   296   294
292   291   290   289   289   289   290   290   290   291
291   291   292   292   293   293   293   294   294   294
```

294 295 295 295 295 295 295 295 295 295
294 294 294 294 294 294 294

NET TRANSPORT VOLUME (M3/1000) FROM   930724 TO   940724

-105 -105 -105 -105 -105 -105 -104 -103 -101 -100
-98 -96 -95 -94 -95 -96 -98 -101 -105 -108
-111 -113 -115 -115 -113 -111 -107 -103 -98 -93
-88 -84 -80 -77 -74 -71 -70 -68 -67 -66
-65 -64 -62 -61 -58 -56 -53 -50 -46 -43
-39 -35 -32 -30 -28 -27 -27 -28 -29 -32
-35 -38 -42 -44 -46 -47 -47

TRANSPORT VOLUME TO THE LEFT (M3/1000) FROM   930724 TO 940724

-202 -202 -202 -202 -202 -202 -201 -201 -200 -198
-197 -196 -195 -195 -195 -196 -198 -200 -202 -205
-207 -208 -209 -209 -208 -206 -204 -200 -197 -194
-190 -187 -185 -183 -181 -180 -180 -179 -179 -178
-178 -178 -177 -176 -176 -174 -173 -172 -170 -168
-167 -165 -163 -162 -161 -161 -161 -161 -162 -163
-165 -166 -168 -169 -170 -171 -171

TRANSPORT VOLUME TO THE RIGHT (M3/1000) FROM   930724 TO 940724

97 97 97 97 97 97 97 97 98 98
99 100 100 100 100 100 99 98 97 96
95 94 94 94 94 95 96 97 99 100
102 103 105 106 107 108 110 110 111 112
113 113 114 115 117 118 120 121 123 125
127 129 131 132 133 134 134 133 132 131
129 127 126 125 124 123 123

SHORELINE POSITION (M) AFTER 5841 TIME STEPS. DATE IS   940724

400.00 405.18 410.36 415.51 420.63 425.70 430.70 435.65 440.54 445.37

450.17 454.94 459.72 464.54 469.40 474.34 479.37 484.50 489.73 495.03

500.38 505.74 511.07 516.30 521.38 526.26 530.86 535.16 539.11 542.69

545.88 548.68 551.07 553.08 554.72 556.01 556.97 557.60 557.94 557.99

557.74 557.22 556.40 555.29 553.88 552.16 550.12 547.77 545.09 542.11

538.85 535.32 531.57 527.63 523.56 519.40 515.20 511.00 506.84 502.76

498.76 494.87 491.06 487.33 483.65 480.00

****

GROSS TRANSPORT VOLUME (M3/1000) FROM   940724 TO   950724

 299   299   299   299   299   299   298   298   298   298

 298   298   298   298   298   299   299   299   300   300

 300   300   300   300   299   298   297   296   295   294

 293   291   291   290   290   289   290   290   290   291

 291   291   292   292   293   293   293   294   294   294

 294   294   294   294   295   295   295   295   295   295

 295   295   295   295   295   295   295

NET TRANSPORT VOLUME (M3/1000) FROM   940724 TO   950724

 -103 -103 -103 -103 -103 -102 -102 -101 -101 -100

 -100 -100 -100 -101 -101 -102 -103 -104 -105 -105

 -106 -106 -106 -105 -104 -103 -101   -99   -96   -93

  -90   -87   -84   -81   -78   -76   -73   -71   -68   -66

  -64   -62   -60   -57   -55   -53   -50   -48   -45   -43

  -41   -39   -37   -36   -35   -34   -34   -34   -35   -35

  -36   -37   -38   -39   -39   -39   -39

TRANSPORT VOLUME TO THE LEFT (M3/1000) FROM   940724 TO
950724

 -201 -201 -201 -201 -201 -200 -200 -200 -199 -199

```
-199  -199  -199  -199  -200  -200  -201  -202  -202  -203

-203  -203  -203  -202  -202  -201  -199  -197  -196  -194

-191  -189  -187  -186  -184  -182  -181  -180  -179  -178

-178  -177  -176  -175  -174  -173  -172  -171  -170  -168

-167  -167  -166  -165  -165  -164  -164  -164  -165  -165

-165  -166  -166  -167  -167  -167  -167
```

TRANSPORT VOLUME TO THE RIGHT (M3/1000) FROM   940724 TO 950724

```
 97    97    97    97    98    98    98    98    98    98

 98    98    98    98    98    98    98    97    97    97

 97    96    96    97    97    97    98    98    99   100

101   102   103   104   105   106   108   109   111   112

113   114   116   117   118   120   121   122   124   125

126   127   128   129   129   130   130   130   129   129

129   128   128   127   127   127   127
```

****

GROSS TRANSPORT VOLUME (M3/1000) FROM   950724 TO   960723

```
299   299   299   299   299   298   298   298   298   298

298   299   299   299   299   299   299   299   299   299

299   299   298   298   297   297   296   295   294   293

292   291   291   290   290   289   290   290   290   291

291   291   292   292   293   293   293   293   294   294

294   294   294   294   294   294   294   295   295   295

295   295   295   295   295   295   295
```

NET TRANSPORT VOLUME (M3/1000) FROM   950724 TO   960723

```
-102  -102  -102  -102  -102  -102  -102  -102  -102  -102

-102  -102  -102  -102  -103  -103  -103  -103  -104  -104

-104  -103  -103  -102  -101  -100   -98   -96   -94   -92
```

```
-90  -87  -85  -82  -79  -77  -74  -72  -69  -67
-64  -62  -59  -57  -55  -52  -50  -48  -46  -44
-43  -41  -40  -39  -38  -37  -37  -37  -36  -36
-36  -37  -37  -37  -37  -37  -37
```

TRANSPORT VOLUME TO THE LEFT (M3/1000) FROM   950724 TO 960723

```
-200  -200  -200  -200  -200  -200  -200  -200  -200  -200
-200  -200  -200  -201  -201  -201  -201  -201  -201  -201
-201  -201  -201  -200  -199  -198  -197  -196  -194  -193
-191  -189  -188  -186  -185  -183  -182  -181  -180  -179
-178  -176  -175  -174  -174  -173  -172  -171  -170  -169
-168  -168  -167  -167  -166  -166  -166  -166  -165  -165
-166  -166  -166  -166  -166  -166  -166
```

TRANSPORT VOLUME TO THE RIGHT (M3/1000) FROM   950724 TO 960723

```
 98    98    98    98    98    98    98    98    98    98
 98    98    98    98    98    98    97    97    97    97
 97    97    97    98    98    98    98    99   100   100
101   102   103   104   105   106   107   109   110   112
113   114   116   117   119   120   121   122   123   124
125   126   127   127   128   128   128   128   129   129
129   128   128   128   128   128   128
```

****

LAST TIME STEP. DIFFRACTED WAVES ALONGSHORE

BREAKING WAVE HEIGHT

```
0.10  0.10  0.10  0.10  0.10  0.10  0.10  0.10  0.10  0.10
0.10  0.10  0.10  0.10  0.10  0.10  0.10  0.10  0.10  0.10
```

0.10 0.10 0.10 0.10 0.10 0.10 0.10 0.10 0.10 0.10

0.10 0.10 0.10 0.10 0.10 0.10 0.10 0.10 0.10 0.10

0.10 0.10 0.10 0.10 0.10 0.10 0.10 0.10 0.10 0.10

0.10 0.10 0.10 0.10 0.10 0.10 0.10 0.10 0.10 0.10

0.10 0.10 0.10 0.10 0.10 0.10 0.10

BREAKING WAVE ANGLE TO X-AXIS

1.15 1.15 1.15 1.15 1.15 1.15 1.15 1.15 1.15 1.15

1.15 1.15 1.15 1.14 1.14 1.13 1.13 1.12 1.10 1.09

1.07 1.04 1.02 0.99 0.95 0.91 0.87 0.82 0.77 0.71

0.65 0.59 0.53 0.46 0.39 0.32 0.25 0.18 0.11 0.04

-0.03 -0.10 -0.17 -0.23 -0.30 -0.36 -0.41 -0.47 -0.52 -0.57

-0.61 -0.66 -0.69 -0.73 -0.76 -0.78 -0.81 -0.83 -0.84 -0.86

-0.87 -0.88 -0.89 -0.89 -0.89 -0.89 -0.89

****

GROSS TRANSPORT VOLUME (M3) FROM   960723 TO   960724

 0   0   0   0   0   0   0   0   0   0

 0   0   0   0   0   0   0   0   0   0

 0   0   0   0   0   0   0   0   0   0

 0   0   0   0   0   0   0   0   0   0

 0   0   0   0   0   0   0   0   0   0

 0   0   0   0   0   0   0   0   0   0

 0   0   0   0   0   0   0

NET TRANSPORT VOLUME (M3) FROM   960723 TO   960724

 0   0   0   0   0   0   0   0   0   0

 0   0   0   0   0   0   0   0   0   0

 0   0   0   0   0   0   0   0   0   0

 0   0   0   0   0   0   0   0   0   0

 0   0   0   0   0   0   0   0   0   0

```
0    0    0    0    0    0    0    0    0    0

0    0    0    0    0    0    0
```

TRANSPORT VOLUME TO THE LEFT (M3) FROM   960723 TO   960724

```
0    0    0    0    0    0    0    0    0    0

0    0    0    0    0    0    0    0    0    0

0    0    0    0    0    0    0    0    0    0

0    0    0    0    0    0    0    0    0    0

0    0    0    0    0    0    0    0    0    0

0    0    0    0    0    0    0    0    0    0

0    0    0    0    0    0    0
```

TRANSPORT VOLUME TO THE RIGHT (M3) FROM   960723 TO   960724

```
0    0    0    0    0    0    0    0    0    0

0    0    0    0    0    0    0    0    0    0

0    0    0    0    0    0    0    0    0    0

0    0    0    0    0    0    0    0    0    0

0    0    0    0    0    0    0    0    0    0

0    0    0    0    0    0    0    0    0    0

0    0    0    0    0    0    0
```

****

OUTPUT   OF   BREAKING   WAVE   STATISTICS   FOR   SELECTED
LOCATIONS

N.B. WAVE DIFFRACTION IS NOT ACCOUNTED FOR!

GRID CELL NUMBERS

```
 1    1    2    3    5    6    7    9   10   11

13   14   15   17   18   19   21   22   23   25

26   27   29   30   31   33   34   35   36   38

39   40   42   43   44   46   47   48   50   51

52   54   55   56   58   59   60   62   63   64
```

AVERAGE UNDIFFRACTED BREAKING WAVE HEIGHTS (M).

 0.44 0.44 0.44 0.44 0.44 0.44 0.44 0.44 0.44 0.44

 0.44 0.44 0.44 0.44 0.44 0.44 0.44 0.44 0.44 0.44

 0.44 0.44 0.44 0.44 0.44 0.44 0.44 0.44 0.44 0.44

 0.44 0.44 0.44 0.44 0.44 0.44 0.44 0.44 0.44 0.44

 0.44 0.44 0.44 0.44 0.44 0.44 0.44 0.44 0.44 0.44

 AVERAGE UNDIFFRACTED BREAKING WAVE ANGLE TO SHORELINE (DEG)

 -0.59 -0.59 -0.59 -1.50 -2.26 -2.13 -1.88 -1.36 -2.57 -2.97

 -0.65 0.22 -0.94 -1.76 -1.17 -1.81 -1.92 -3.14 -3.51 -1.27

 -0.94 -0.99 -1.24 -1.94 -1.44 -0.38 -0.41 -0.14 -0.27 -0.39

 -0.59 -0.44 0.25 0.33 0.45 0.16 -0.03 0.26 0.99 1.09

  0.96 1.34 1.59 1.01 1.65 2.04 1.90 1.55 1.27 0.81

 AVERAGE LONGSHORE TRANSPORT RATE BASED ON UNDIFFRACTED WAVES *100 (M3/SEC)

 -0.27 -0.27 -0.27 -0.30 -0.35 -0.36 -0.35 -0.35 -0.37 -0.37

 -0.26 -0.23 -0.25 -0.29 -0.30 -0.32 -0.37 -0.42 -0.43 -0.34

 -0.31 -0.29 -0.30 -0.31 -0.29 -0.24 -0.23 -0.22 -0.22 -0.23

 -0.23 -0.23 -0.20 -0.19 -0.18 -0.19 -0.19 -0.18 -0.14 -0.13

 -0.13 -0.11 -0.10 -0.10 -0.07 -0.07 -0.08 -0.11 -0.13 -0.16

LONGSHORE TRANSPORT FOR LAST TIME STEP *100 (M3/SEC)

 0.00 0.00 0.00 0.00 0.00 0.00 0.00 0.00 0.00 0.00

 0.00 0.00 0.00 0.00 0.00 0.00 0.00 0.00 0.00 0.00

 0.00 0.00 0.00 0.00 0.00 0.00 0.00 0.00 0.00 0.00

 0.00 0.00 0.00 0.00 0.00 0.00 0.00 0.00 0.00 0.00

 0.00 0.00 0.00 0.00 0.00 0.00 0.00 0.00 0.00 0.00

 0.00 0.00 0.00 0.00 0.00 0.00 0.00 0.00 0.00 0.00

0.00 0.00 0.00 0.00 0.00 0.00 0.00

CALCULATED FINAL SHORELINE POSITION (M)
400.00 405.02 410.05 415.07 420.09 425.11 430.13 435.16 440.18 445.21
450.25 455.29 460.33 465.38 470.43 475.48 480.51 485.52 490.49 495.42
500.28 505.05 509.71 514.24 518.61 522.81 526.81 530.59 534.13 537.41
540.42 543.13 545.54 547.63 549.40 550.85 551.97 552.75 553.21 553.33
553.14 552.63 551.80 550.68 549.27 547.58 545.63 543.42 540.98 538.32
535.45 532.40 529.18 525.82 522.34 518.74 515.06 511.30 507.48 503.62
499.72 495.79 491.85 487.90 483.95 480.00

CALCULATED SEAWARDMOST SHORELINE POSITION (M)
400.00 405.26 410.52 415.79 421.08 430.00 440.00 438.93 449.34 462.90
520.00 520.00 500.00 469.46 470.43 475.48 480.52 485.56 490.59 495.61
500.69 505.84 560.00 580.00 560.00 544.09 542.78 545.80 548.87 560.00
580.00 570.00 562.77 560.00 557.44 558.05 558.57 558.94 560.00 570.00
580.00 570.53 565.00 560.00 557.41 556.25 560.00 570.00 560.00 551.47
547.74 544.20 550.00 540.00 532.25 535.00 530.00 520.00 507.59 503.68
500.00 495.81 491.85 487.90 483.95 480.00

CALCULATED LANDWARDMOST SHORELINE POSITION (M)
400.00 370.00 379.29 380.00 407.23 417.55 426.86 428.95 410.00 445.15
450.09 454.94 459.62 440.00 440.00 450.00 459.89 460.00 462.24 440.00
440.00 490.00 509.71 514.24 518.61 522.81 526.81 520.00 520.00 537.41
540.42 543.13 545.54 547.63 549.40 548.34 540.00 545.00 553.21 553.33
553.14 552.63 551.80 550.68 530.00 540.00 545.63 543.42 540.98 538.32
535.45 532.40 529.18 525.82 520.00 518.74 513.92 507.18 490.00 460.00
480.20 475.00 460.00 460.00 474.45 480.00

CALCULATED REPRESENTATIVE OFFSHORE CONTOUR POSITION (M)
700.00 705.02 710.05 715.07 720.10 725.12 730.15 735.18 740.21 745.24
750.27 755.29 760.31 765.31 770.30 775.26 780.19 785.08 789.91 794.67

144

799.35 803.92 808.38 812.70 816.86 820.85 824.65 828.24 831.61 834.73

837.59 840.18 842.49 844.50 846.22 847.63 848.73 849.52 850.00 850.17

850.03 849.59 848.86 847.84 846.54 844.97 843.16 841.10 838.82 836.32

833.63 830.76 827.72 824.54 821.23 817.80 814.26 810.64 806.95 803.20

799.40 795.52 791.64 787.76 783.88 780.00

CALIBRATION/VERIFICATION ERROR =   20.5657

CALCULATED VOLUMETRIC CHANGE = -1.17E+05 (M3)
SIGN CONVENTION: EROSION (-), ACCRETION (+)
----

6.   OUTPUT FILE (2006)

RUN: manavgat river mouth

INITIAL SHORELINE POSITION (M)
 400.00 370.00 380.00 380.00 410.00 430.00 440.00 430.00 410.00 450.00

 520.00 520.00 500.00 440.00 440.00 450.00 474.00 460.00 480.00 440.00

 440.00 490.00 560.00 580.00 560.00 540.00 530.00 520.00 520.00 560.00

 580.00 570.00 560.00 560.00 550.00 550.00 540.00 545.00 560.00 570.00

 580.00 570.00 565.00 560.00 530.00 540.00 560.00 570.00 560.00 550.00

 540.00 540.00 550.00 540.00 520.00 535.00 530.00 520.00 490.00 460.00

 500.00 475.00 460.00 460.00 480.00 480.00

****

GROSS TRANSPORT VOLUME (M3/1000) FROM   820724 TO   830724

```
307  307  289  290  303  309  316  332  329  326
327  287  304  318  289  272  273  290  303  335
325  352  365  327  331  327  314  303  288  294
286  294  297  292  294  292  295  289  286  285
286  295  295  298  304  287  287  286  299  302
300  293  290  298  300  288  291  299  308  302
289  299  302  295  293  295  295
```

NET TRANSPORT VOLUME (M3/1000) FROM   820724 TO   830724

```
 -31   -31   -66   -96  -132  -142  -139  -131  -138  -170
-167   -99   -35     4   -20   -48   -70   -72   -93   -99
-152  -210  -224  -175  -113   -77   -67   -72   -92  -116
-103   -74   -56   -51   -46   -53   -61   -80   -93   -92
 -81   -60   -49   -42   -40   -66   -81   -74   -55   -44
 -40   -42   -41   -25   -15   -19    -4    11    22     8
 -31   -26   -43   -71   -97   -99   -99
```

TRANSPORT VOLUME TO THE LEFT (M3/1000) FROM   820724 TO 830724

```
-169  -169  -178  -193  -217  -226  -227  -231  -233  -248
-247  -193  -170  -156  -154  -160  -171  -181  -198  -217
-238  -281  -295  -251  -222  -202  -191  -187  -190  -205
-195  -184  -176  -171  -170  -173  -178  -184  -190  -189
-184  -178  -172  -170  -172  -176  -184  -180  -177  -173
-170  -168  -165  -162  -157  -154  -147  -143  -143  -146
-160  -163  -173  -183  -195  -197  -197
```

TRANSPORT VOLUME TO THE RIGHT (M3/1000) FROM   820724 TO 830724

```
138  138  111   96   85   83   88  100   95   77
 79   94  134  161  134  112  101  108  104  117
```

```
 86    70    70    75   108   124   123   115    97    88

 91   110   120   120   123   119   116   104    96    96

102   117   123   127   132   110   103   106   121   129

130   125   124   136   142   134   143   155   165   155

128   136   129   111    98    97    97
```

****

GROSS TRANSPORT VOLUME (M3/1000) FROM   830724 TO   840723

```
300   300   300   300   300   299   299   298   298   297

297   296   296   296   296   297   298   299   300   301

302   303   303   303   303   301   300   298   296   294

292   291   290   289   289   289   290   290   290   291

291   291   292   292   293   293   293   294   294   294

294   295   295   295   295   295   295   295   295   295

294   294   294   294   294   294   294
```

NET TRANSPORT VOLUME (M3/1000) FROM   830724 TO   840723

```
-105  -105  -105  -105  -105  -105  -104  -103  -101  -100

 -98   -96   -95   -94   -95   -96   -98  -101  -105  -108

-111  -113  -115  -115  -113  -111  -107  -103   -98   -93

 -88   -84   -80   -77   -74   -71   -70   -68   -67   -66

 -65   -64   -62   -61   -58   -56   -53   -50   -46   -43

 -39   -35   -32   -30   -28   -27   -27   -28   -29   -32

 -35   -38   -42   -44   -46   -47   -47
```

 TRANSPORT VOLUME TO THE LEFT (M3/1000) FROM   830724 TO
840723

```
-202  -202  -202  -202  -202  -202  -201  -201  -200  -198

-197  -196  -195  -195  -195  -196  -198  -200  -202  -205

-207  -208  -209  -209  -208  -206  -204  -200  -197  -194

-190  -187  -185  -183  -181  -180  -180  -179  -179  -178
```

```
-178  -178  -177  -176  -176  -174  -173  -172  -170  -168
-167  -165  -163  -162  -161  -161  -161  -161  -162  -163
-165  -166  -168  -169  -170  -171  -171
```

TRANSPORT VOLUME TO THE RIGHT (M3/1000) FROM   830724 TO
840723

```
 97   97   97   97   97   97   97   97   98   98
 99  100  100  100  100  100   99   98   97   96
 95   94   94   94   94   95   96   97   99  100
102  103  105  106  107  108  110  110  111  112
113  113  114  115  117  118  120  121  123  125
127  129  131  132  133  134  134  133  132  131
129  127  126  125  124  123  123
```

****

GROSS TRANSPORT VOLUME (M3/1000) FROM   840723 TO   850723

```
299  299  299  299  299  299  298  298  298  298
298  298  298  298  298  299  299  299  300  300
300  300  300  300  299  298  297  296  295  294
293  291  291  290  290  289  290  290  290  291
291  291  292  292  293  293  293  294  294  294
294  294  294  294  295  295  295  295  295  295
295  295  295  295  295  295  295
```

NET TRANSPORT VOLUME (M3/1000) FROM   840723 TO   850723

```
-103  -103  -103  -103  -103  -102  -102  -101  -101  -100
-100  -100  -100  -101  -101  -102  -103  -104  -105  -105
-106  -106  -106  -105  -104  -103  -101   -99   -96   -93
 -90   -87   -84   -81   -78   -76   -73   -71   -68   -66
 -64   -62   -60   -57   -55   -53   -50   -48   -45   -43
 -41   -39   -37   -36   -35   -34   -34   -34   -35   -35
```

-36   -37   -38   -39   -39   -39   -39

TRANSPORT VOLUME TO THE LEFT (M3/1000) FROM   840723 TO 850723

-201 -201 -201 -201 -201 -200 -200 -200 -199 -199

-199 -199 -199 -199 -200 -200 -201 -202 -202 -203

-203 -203 -203 -202 -202 -201 -199 -197 -196 -194

-191 -189 -187 -186 -184 -182 -181 -180 -179 -178

-178 -177 -176 -175 -174 -173 -172 -171 -170 -168

-167 -167 -166 -165 -165 -164 -164 -164 -165 -165

-165 -166 -166 -167 -167 -167 -167

TRANSPORT VOLUME TO THE RIGHT (M3/1000) FROM   840723 TO 850723

97   97   97   97   98   98   98   98   98   98

98   98   98   98   98   98   98   97   97   97

97   96   96   97   97   97   98   98   99   100

101   102   103   104   105   106   108   109   111   112

113   114   116   117   118   120   121   122   124   125

126   127   128   129   129   130   130   130   129   129

129   128   128   127   127   127   127

****

GROSS TRANSPORT VOLUME (M3/1000) FROM   850723 TO   860723

299   299   299   299   299   298   298   298   298   298

298   299   299   299   299   299   299   299   299   299

299   299   298   298   297   297   296   295   294   293

292   291   291   290   290   289   290   290   290   291

291   291   292   292   293   293   293   293   294   294

294   294   294   294   294   294   294   295   295   295

295   295   295   295   295   295   295

NET TRANSPORT VOLUME (M3/1000) FROM   850723 TO   860723

```
-102  -102  -102  -102  -102  -102  -102  -102  -102  -102
-102  -102  -102  -102  -103  -103  -103  -103  -104  -104
-104  -103  -103  -102  -101  -100   -98   -96   -94   -92
 -90   -87   -85   -82   -79   -77   -74   -72   -69   -67
 -64   -62   -59   -57   -55   -52   -50   -48   -46   -44
 -43   -41   -40   -39   -38   -37   -37   -37   -36   -36
 -36   -37   -37   -37   -37   -37   -37
```

TRANSPORT VOLUME TO THE LEFT (M3/1000) FROM   850723 TO 860723

```
-200  -200  -200  -200  -200  -200  -200  -200  -200  -200
-200  -200  -200  -201  -201  -201  -201  -201  -201  -201
-201  -201  -201  -200  -199  -198  -197  -196  -194  -193
-191  -189  -188  -186  -185  -183  -182  -181  -180  -179
-178  -176  -175  -174  -174  -173  -172  -171  -170  -169
-168  -168  -167  -167  -166  -166  -166  -166  -165  -165
-166  -166  -166  -166  -166  -166  -166
```

TRANSPORT VOLUME TO THE RIGHT (M3/1000) FROM   850723 TO 860723

```
  98    98    98    98    98    98    98    98    98    98
  98    98    98    98    98    98    97    97    97    97
  97    97    97    98    98    98    98    99   100   100
 101   102   103   104   105   106   107   109   110   112
 113   114   116   117   119   120   121   122   123   124
 125   126   127   127   128   128   128   128   129   129
 129   128   128   128   128   128   128
```

****

150

GROSS TRANSPORT VOLUME (M3/1000) FROM   860723 TO   870723

299   299   299   299   299   299   299   299   299   299

299   299   299   299   299   299   299   299   299   299

298   298   298   297   296   296   295   294   294   293

292   291   291   290   290   289   290   290   290   291

291   291   292   292   292   293   293   293   293   294

294   294   294   294   294   294   294   294   294   295

295   295   295   295   295   295   295

NET TRANSPORT VOLUME (M3/1000) FROM   860723 TO   870723

-102 -102 -102 -102 -102 -102 -102 -102 -102 -102

-102 -102 -103 -103 -103 -103 -103 -103 -103 -102

-102 -101 -101 -100   -99   -98   -96   -94   -93   -91

 -89   -86   -84   -82   -79   -77   -74   -72   -69   -67

 -64   -62   -60   -57   -55   -53   -51   -49   -47   -46

 -44   -43   -42   -40   -40   -39   -38   -38   -37   -37

 -37   -37   -37   -36   -36   -36   -36

 TRANSPORT VOLUME TO THE LEFT (M3/1000) FROM   860723 TO 870723

-200 -200 -200 -200 -200 -200 -200 -200 -200 -200

-201 -201 -201 -201 -201 -201 -201 -201 -201 -200

-200 -200 -199 -198 -198 -197 -196 -194 -193 -192

-190 -189 -187 -186 -185 -183 -182 -181 -180 -179

-178 -177 -176 -175 -174 -173 -172 -171 -170 -170

-169 -168 -168 -167 -167 -167 -166 -166 -166 -166

-166 -166 -166 -165 -165 -165 -165

 TRANSPORT VOLUME TO THE RIGHT (M3/1000) FROM   860723 TO 870723

 98   98   98   98   98   98   98   98   98   98

 98   98   98   98   98   98   97   97   97   98

```
  98    98    98    98    98    99    99    99   100   101

 101   102   103   104   105   106   107   109   110   111

 113   114   116   117   118   119   121   122   123   124

 124   125   126   126   127   127   128   128   128   128

 128   128   128   129   129   129   129
```

****

GROSS TRANSPORT VOLUME (M3/1000) FROM   870723 TO   880722

```
 299   299   299   299   299   299   299   299   299   299

 299   299   299   299   299   299   299   298   298   298

 298   297   297   296   296   295   295   294   293   292

 291   291   291   290   290   289   289   290   290   291

 291   291   292   292   292   293   293   293   293   294

 294   294   294   294   294   294   294   294   294   294

 294   294   294   294   294   295   295
```

NET TRANSPORT VOLUME (M3/1000) FROM   870723 TO   880722

```
-102  -102  -102  -102  -102  -102  -102  -102  -102  -102

-103  -103  -103  -103  -103  -103  -102  -102  -102  -101

-101  -100   -99   -98   -97   -96   -95   -93   -91   -90

 -88   -86   -84   -81   -79   -77   -74   -72   -70   -67

 -65   -62   -60   -58   -56   -54   -52   -50   -48   -47

 -45   -44   -43   -42   -41   -40   -39   -39   -38   -38

 -37   -37   -37   -37   -37   -36   -36
```

 TRANSPORT VOLUME TO THE LEFT (M3/1000) FROM   870723 TO
880722

```
-200  -200  -200  -200  -200  -200  -200  -200  -201  -201

-201  -201  -201  -201  -201  -201  -201  -200  -200  -200

-199  -199  -198  -197  -196  -196  -195  -193  -192  -191

-190  -188  -187  -186  -184  -183  -182  -181  -180  -179
```

```
-178  -177  -176  -175  -174  -173  -172  -172  -171  -170
-169  -169  -168  -168  -167  -167  -167  -166  -166  -166
-166  -166  -166  -166  -166  -165  -165
```

TRANSPORT VOLUME TO THE RIGHT (M3/1000) FROM   870723 TO
880722

```
 98    98    98    98    98    98    98    98    98    98
 98    98    98    98    98    98    98    98    98    98
 98    98    98    98    99    99    99   100   100   101
101   102   103   104   105   106   107   108   110   111
113   114   115   116   118   119   120   121   122   123
124   124   125   126   126   127   127   127   128   128
128   128   128   128   128   129   129
```

****
GROSS TRANSPORT VOLUME (M3/1000) FROM   880722 TO   890722

```
299   299   299   299   299   299   299   299   299   299
299   299   299   299   299   298   298   298   298   298
297   297   296   296   295   295   294   293   293   292
291   291   290   290   290   289   290   290   290   291
291   291   291   292   292   292   293   293   293   293
294   294   294   294   294   294   294   294   294   294
294   294   294   294   294   294   294
```

NET TRANSPORT VOLUME (M3/1000) FROM   880722 TO   890722

```
-102  -102  -102  -102  -102  -102  -102  -102  -102  -102
-103  -103  -102  -102  -102  -102  -102  -101  -101  -101
-100   -99   -98   -97   -96   -95   -94   -92   -90   -89
 -87   -85   -83   -81   -79   -76   -74   -72   -70   -67
 -65   -63   -61   -59   -57   -55   -53   -51   -49   -48
 -46   -45   -44   -43   -42   -41   -40   -39   -39   -38
```

```
-38   -37   -37   -37   -37   -37   -37
```

TRANSPORT VOLUME TO THE LEFT (M3/1000) FROM   880722 TO
890722

```
-200  -200  -200  -200  -200  -200  -201  -201  -201  -201
-201  -201  -201  -201  -200  -200  -200  -200  -199  -199
-199  -198  -197  -196  -196  -195  -194  -193  -192  -190
-189  -188  -187  -185  -184  -183  -182  -181  -180  -179
-178  -177  -176  -175  -174  -174  -173  -172  -171  -171
-170  -169  -169  -168  -168  -167  -167  -167  -167  -166
-166  -166  -166  -166  -166  -166  -166
```

TRANSPORT VOLUME TO THE RIGHT (M3/1000) FROM   880722 TO
890722

```
 98    98    98    98    98    98    98    98    98    98
 98    98    98    98    98    98    98    98    98    98
 98    98    98    99    99    99   100   100   101   101
102   102   103   104   105   106   107   108   110   111
112   114   115   116   117   118   120   121   121   122
123   124   125   125   126   126   127   127   127   128
128   128   128   128   128   128   128
```

```
********************
```
GROSS TRANSPORT VOLUME (M3/1000) FROM   890722 TO   900722
```
299   299   299   299   299   299   299   299   299   299
299   299   299   298   298   298   298   298   297   297
297   296   296   295   295   294   294   293   292   291
291   291   290   290   290   289   289   290   290   291
291   291   291   292   292   292   293   293   293   293
293   294   294   294   294   294   294   294   294   294
294   294   294   294   294   294   294
```

NET TRANSPORT VOLUME (M3/1000) FROM   890722 TO   900722

```
-102  -102  -102  -102  -102  -102  -102  -102  -102  -102
-102  -102  -102  -102  -102  -102  -101  -101  -100  -100
 -99   -98   -97   -96   -95   -94   -93   -91   -90   -88
 -86   -84   -82   -80   -78   -76   -74   -72   -70   -67
 -65   -63   -61   -59   -57   -55   -54   -52   -50   -49
 -47   -46   -45   -43   -42   -42   -41   -40   -39   -39
 -38   -38   -38   -37   -37   -37   -37
```

TRANSPORT VOLUME TO THE LEFT (M3/1000) FROM   890722 TO 900722

```
-201  -201  -201  -201  -201  -201  -201  -201  -201  -201
-201  -200  -200  -200  -200  -200  -200  -199  -199  -198
-198  -197  -196  -196  -195  -194  -193  -192  -191  -190
-189  -187  -186  -185  -184  -183  -182  -181  -180  -179
-178  -177  -176  -175  -175  -174  -173  -172  -172  -171
-170  -170  -169  -169  -168  -168  -167  -167  -167  -167
-166  -166  -166  -166  -166  -166  -166
```

TRANSPORT VOLUME TO THE RIGHT (M3/1000) FROM   890722 TO 900722

```
 98    98    98    98    98    98    98    98    98    98
 98    98    98    98    98    98    98    98    98    98
 98    98    99    99    99   100   100   100   101   101
102   103   104   104   105   106   107   109   110   111
112   113   115   116   117   118   119   120   121   122
123   123   124   125   125   126   126   127   127   127
128   128   128   128   128   128   128
```

****

GROSS TRANSPORT VOLUME (M3/1000) FROM   900722 TO   910722

299   299   299   299   299   299   299   299   299   299

299   298   298   298   298   298   298   297   297   297

296   296   295   295   294   294   293   293   292   291

291   291   290   290   289   289   289   290   290   291

291   291   291   292   292   292   293   293   293   293

293   294   294   294   294   294   294   294   294   294

294   294   294   294   294   294   294

NET TRANSPORT VOLUME (M3/1000) FROM   900722 TO   910722

-102   -102   -102   -102   -102   -102   -102   -102   -102   -102

-102   -102   -102   -102   -101   -101   -101   -100   -100   -99

-98   -97   -96   -95   -94   -93   -92   -90   -89   -87

-85   -84   -82   -80   -78   -76   -74   -72   -70   -68

-66   -64   -62   -60   -58   -56   -54   -53   -51   -49

-48   -47   -45   -44   -43   -42   -41   -41   -40   -39

-39   -39   -38   -38   -38   -38   -38

TRANSPORT VOLUME TO THE LEFT (M3/1000) FROM   900722 TO 910722

-201   -201   -201   -201   -201   -201   -201   -201   -201   -200

-200   -200   -200   -200   -200   -199   -199   -199   -198   -198

-197   -197   -196   -195   -194   -193   -192   -191   -190   -189

-188   -187   -186   -185   -184   -183   -182   -181   -180   -179

-178   -177   -176   -176   -175   -174   -173   -173   -172   -171

-171   -170   -170   -169   -169   -168   -168   -167   -167   -167

-167   -166   -166   -166   -166   -166   -166

TRANSPORT VOLUME TO THE RIGHT (M3/1000) FROM   900722 TO 910722

98   98   98   98   98   98   98   98   98   98

98   98   98   98   98   98   98   98   98   98

```
99    99    99    99   100   100   100   101   101   102
102   103   104   105   105   106   107   109   110   111
112   113   114   116   117   118   119   120   121   121
122   123   124   124   125   125   126   126   127   127
127   127   128   128   128   128   128
```

****

GROSS TRANSPORT VOLUME (M3/1000) FROM   910722 TO   920721

```
299   299   299   299   299   299   299   299   299   298
298   298   298   298   298   298   297   297   297   296
296   295   295   294   294   293   293   292   292   291
291   290   290   290   289   289   290   290   290   291
291   291   291   292   292   292   292   293   293   293
293   293   294   294   294   294   294   294   294   294
294   294   294   294   294   294   294
```

NET TRANSPORT VOLUME (M3/1000) FROM   910722 TO   920721

```
-103  -103  -103  -102  -102  -102  -102  -102  -102  -102
-102  -102  -102  -101  -101  -101  -100  -100   -99   -98
 -97   -97   -96   -95   -93   -92   -91   -90   -88   -86
 -85   -83   -81   -79   -78   -76   -74   -72   -70   -68
 -66   -64   -62   -60   -58   -57   -55   -53   -52   -50
 -49   -47   -46   -45   -44   -43   -42   -41   -41   -40
 -40   -39   -39   -39   -38   -38   -38
```

TRANSPORT VOLUME TO THE LEFT (M3/1000) FROM   910722 TO
920721

```
-201  -201  -201  -201  -201  -201  -201  -200  -200  -200
-200  -200  -200  -200  -199  -199  -199  -198  -198  -197
-197  -196  -195  -195  -194  -193  -192  -191  -190  -189
-188  -187  -186  -185  -183  -182  -182  -181  -180  -179
```

157

-178 -177 -177 -176 -175 -174 -174 -173 -172 -172

-171 -170 -170 -169 -169 -168 -168 -168 -167 -167

-167 -167 -166 -166 -166 -166 -166

TRANSPORT VOLUME TO THE RIGHT (M3/1000) FROM   910722 TO 920721

  98   98   98   98   98   98   98   98   98   98

  98   98   98   98   98   98   98   98   98   99

  99   99   99   99 100 100 100 101 101 102

102 103 104 105 105 106 107 109 110 111

112 113 114 115 116 117 118 119 120 121

122 123 123 124 124 125 125 126 126 127

127 127 127 127 127 127 127

****

GROSS TRANSPORT VOLUME (M3/1000) FROM   920721 TO   930721

299 299 299 299 299 299 299 299 298 298

298 298 298 298 298 297 297 297 296 296

295 295 295 294 294 293 293 292 291 291

291 290 290 290 289 289 290 290 290 291

291 291 291 291 292 292 292 293 293 293

293 293 294 294 294 294 294 294 294 294

294 294 294 294 294 294 294

NET TRANSPORT VOLUME (M3/1000) FROM   920721 TO   930721

-103 -103 -103 -102 -102 -102 -102 -102 -102 -102

-102 -101 -101 -101 -100 -100 -100 -99 -98 -98

 -97 -96 -95 -94 -93 -92 -90 -89 -87 -86

 -84 -83 -81 -79 -77 -75 -74 -72 -70 -68

 -66 -64 -62 -60 -59 -57 -55 -54 -52 -51

 -49 -48 -47 -46 -45 -44 -43 -42 -41 -41

-40   -40   -39   -39   -39   -39   -39

TRANSPORT VOLUME TO THE LEFT (M3/1000) FROM   920721 TO 930721

-201 -201 -201 -201 -201 -201 -200 -200 -200 -200

-200 -200 -200 -199 -199 -199 -198 -198 -197 -197

-196 -195 -195 -194 -193 -192 -191 -190 -189 -188

-187 -186 -185 -184 -183 -182 -182 -181 -180 -179

-178 -178 -177 -176 -175 -175 -174 -173 -173 -172

-171 -171 -170 -170 -169 -169 -168 -168 -168 -167

-167 -167 -167 -167 -167 -167 -167

TRANSPORT VOLUME TO THE RIGHT (M3/1000) FROM   920721 TO 930721

98   98   98   98   98   98   98   98   98   98

98   98   98   98   98   98   98   98   99   99

99   99   99   100   100   100   101   101   101   102

103   103   104   105   106   106   108   109   110   111

112   113   114   115   116   117   118   119   120   121

121   122   123   123   124   125   125   125   126   126

126   127   127   127   127   127   127

****

GROSS TRANSPORT VOLUME (M3/1000) FROM   930721 TO   940721

299   299   299   299   299   299   299   298   298   298

298   298   298   298   297   297   297   296   296   296

295   295   294   294   293   293   292   292   291   291

291   290   290   290   289   289   290   290   290   291

291   291   291   291   292   292   292   293   293   293

293   293   293   294   294   294   294   294   294   294

294   294   294   294   294   294   294

159

NET TRANSPORT VOLUME (M3/1000) FROM 930721 TO 940721

```
 -102  -102  -102  -102  -102  -102  -102  -102  -102  -102
 -101  -101  -101  -100  -100  -100   -99   -98   -98   -97
  -96   -95   -94   -93   -92   -91   -90   -88   -87   -85
  -84   -82   -80   -79   -77   -75   -73   -72   -70   -68
  -66   -64   -63   -61   -59   -57   -56   -54   -53   -51
  -50   -49   -47   -46   -45   -44   -43   -43   -42   -41
  -41   -40   -40   -40   -40   -40   -40
```

TRANSPORT VOLUME TO THE LEFT (M3/1000) FROM 930721 TO 940721

```
 -201  -201  -201  -201  -201  -200  -200  -200  -200  -200
 -200  -200  -199  -199  -199  -198  -198  -197  -197  -196
 -196  -195  -194  -194  -193  -192  -191  -190  -189  -188
 -187  -186  -185  -184  -183  -182  -181  -181  -180  -179
 -178  -178  -177  -176  -175  -175  -174  -173  -173  -172
 -172  -171  -170  -170  -169  -169  -169  -168  -168  -168
 -167  -167  -167  -167  -167  -167  -167
```

TRANSPORT VOLUME TO THE RIGHT (M3/1000) FROM 930721 TO 940721

```
   98    98    98    98    98    98    98    98    98    98
   98    98    98    98    98    98    98    99    99    99
   99    99   100   100   100   100   101   101   102   102
  103   104   104   105   106   107   108   109   110   111
  112   113   114   115   116   117   118   119   120   120
  121   122   123   123   124   124   125   125   126   126
  126   126   127   127   127   127   127
```

SHORELINE POSITION (M) AFTER 35065 TIME STEPS. DATE IS 940724
```
 400.00  405.01  410.03  415.04  420.04  425.02  429.99  434.93  439.84  444.71
```

449.54 454.33 459.06 463.73 468.33 472.86 477.30 481.65 485.90 490.03

494.05 497.93 501.69 505.29 508.74 512.02 515.13 518.06 520.79 523.32

525.65 527.76 529.65 531.33 532.77 533.98 534.96 535.70 536.21 536.48

536.51 536.32 535.89 535.24 534.37 533.28 531.99 530.50 528.82 526.95

524.90 522.68 520.30 517.78 515.12 512.33 509.43 506.42 503.31 500.13

496.87 493.55 490.19 486.80 483.40 480.00

****

GROSS TRANSPORT VOLUME (M3/1000) FROM   940721 TO   950721

  299   299   299   299   299   299   298   298   298   298

  298   298   298   297   297   297   297   296   296   295

  295   295   294   294   293   293   292   291   291   291

  290   290   290   290   289   289   290   290   290   290

  291   291   291   291   292   292   292   292   293   293

  293   293   293   293   294   294   294   294   294   294

  294   294   294   294   294   294   294

NET TRANSPORT VOLUME (M3/1000) FROM   940721 TO   950721

 -102   -102   -102   -102   -102   -102   -102   -102   -102   -101

 -101   -101   -101   -100   -100   -99   -99   -98   -97   -96

  -96   -95   -94   -93   -92   -90   -89   -88   -86   -85

  -83   -82   -80   -78   -77   -75   -73   -72   -70   -68

  -66   -64   -63   -61   -59   -58   -56   -55   -53   -52

  -51   -49   -48   -47   -46   -45   -44   -43   -43   -42

  -41   -41   -41   -40   -40   -40   -40

TRANSPORT VOLUME TO THE LEFT (M3/1000) FROM   940721 TO
950721

 -201   -201   -201   -200   -200   -200   -200   -200   -200   -200

 -200   -199   -199   -199   -198   -198   -198   -197   -196   -196

```
-195  -195  -194  -193  -192  -191  -191  -190  -189  -188
-187  -186  -185  -184  -183  -182  -181  -181  -180  -179
-178  -178  -177  -176  -176  -175  -174  -174  -173  -172
-172  -171  -171  -170  -170  -169  -169  -169  -168  -168
-168  -168  -167  -167  -167  -167  -167
```

TRANSPORT VOLUME TO THE RIGHT (M3/1000) FROM   940721 TO 950721

```
 98    98    98    98    98    98    98    98    98    98
 98    98    98    98    98    98    98    99    99    99
 99    99   100   100   100   101   101   101   102   102
103   104   104   105   106   107   108   109   110   111
112   113   114   115   116   117   117   118   119   120
121   121   122   123   123   124   124   125   125   125
126   126   126   126   126   126   126
```

****

GROSS TRANSPORT VOLUME (M3/1000) FROM   950721 TO   960720

```
299   299   299   298   298   298   298   298   298   298
298   298   297   297   297   297   296   296   295   295
295   294   294   293   293   292   292   291   291   291
290   290   290   289   289   289   290   290   290   290
291   291   291   291   292   292   292   292   293   293
293   293   293   293   294   294   294   294   294   294
294   294   294   294   294   294   294
```

NET TRANSPORT VOLUME (M3/1000) FROM   950721 TO   960720

```
-102  -102  -102  -102  -102  -102  -102  -102  -101  -101
-101  -101  -100  -100   -99   -99   -98   -97   -97   -96
 -95   -94   -93   -92   -91   -90   -89   -87   -86   -84
 -83   -81   -80   -78   -77   -75   -73   -71   -70   -68
```

```
-66  -65  -63  -61  -60  -58  -57  -55  -54  -52
-51  -50  -49  -48  -47  -46  -45  -44  -43  -43
-42  -42  -41  -41  -41  -41  -41
```

TRANSPORT VOLUME TO THE LEFT (M3/1000) FROM   950721 TO
960720
```
-200  -200  -200  -200  -200  -200  -200  -200  -200  -200
-199  -199  -199  -198  -198  -198  -197  -197  -196  -195
-195  -194  -193  -193  -192  -191  -190  -189  -188  -188
-187  -186  -185  -184  -183  -182  -181  -181  -180  -179
-179  -178  -177  -176  -176  -175  -174  -174  -173  -173
-172  -171  -171  -170  -170  -170  -169  -169  -169  -168
-168  -168  -168  -168  -167  -167  -167
```

TRANSPORT VOLUME TO THE RIGHT (M3/1000) FROM   950721 TO
960720
```
 98   98   98   98   98   98   98   98   98   98
 98   98   98   98   98   98   99   99   99   99
 99  100  100  100  100  101  101  101  102  103
103  104  105  105  106  107  108  109  110  111
112  113  114  115  115  116  117  118  119  120
120  121  122  122  123  124  124  124  125  125
125  126  126  126  126  126  126
```

****

LAST TIME STEP. DIFFRACTED WAVES ALONGSHORE

BREAKING WAVE HEIGHT
```
0.10  0.10  0.10  0.10  0.10  0.10  0.10  0.10  0.10  0.10
0.10  0.10  0.10  0.10  0.10  0.10  0.10  0.10  0.10  0.10
0.10  0.10  0.10  0.10  0.10  0.10  0.10  0.10  0.10  0.10
```

0.10 0.10 0.10 0.10 0.10 0.10 0.10 0.10 0.10 0.10
0.10 0.10 0.10 0.10 0.10 0.10 0.10 0.10 0.10 0.10
0.10 0.10 0.10 0.10 0.10 0.10 0.10 0.10 0.10 0.10
0.10 0.10 0.10 0.10 0.10 0.10 0.10

BREAKING WAVE ANGLE TO X-AXIS
1.12 1.12 1.12 1.12 1.12 1.12 1.11 1.10 1.09 1.08
1.07 1.06 1.04 1.03 1.01 0.99 0.97 0.95 0.92 0.90
0.87 0.84 0.81 0.77 0.74 0.70 0.66 0.62 0.58 0.54
0.50 0.45 0.41 0.36 0.31 0.26 0.21 0.17 0.12 0.07
0.02 -0.03 -0.08 -0.12 -0.17 -0.21 -0.26 -0.30 -0.34 -0.38
-0.42 -0.45 -0.49 -0.52 -0.55 -0.58 -0.60 -0.63 -0.65 -0.66
-0.68 -0.70 -0.70 -0.70 -0.70 -0.70 -0.70

****
GROSS TRANSPORT VOLUME (M3) FROM   960720 TO   960724
2   2   2   2   2   2   2   2   2   2
2   2   2   2   2   2   2   1   1   1
1   1   1   1   1   1   1   1   1   1
1   0   0   0   0   0   0   0   0   0
0   0   0   0   0   0   0   0   0   0
0   0   1   1   1   1   1   1   1   1
1   1   1   1   1   1   1

NET TRANSPORT VOLUME (M3) FROM   960720 TO   960724
-2   -2   -2   -2   -2   -2   -2   -2   -2   -2
-2   -2   -2   -2   -2   -2   -2   -1   -1   -1
-1   -1   -1   -1   -1   -1   -1   -1   -1   -1
-1   0   0   0   0   0   0   0   0   0
0   0   0   0   0   0   0   0   0   0
0   0   1   1   1   1   1   1   1   1

164

```
1   1   1   1   1   1   1
```

TRANSPORT VOLUME TO THE LEFT (M3) FROM   960720 TO   960724

```
-2  -2  -2  -2  -2  -2  -2  -2  -2  -2
-2  -2  -2  -2  -2  -2  -2  -1  -1  -1
-1  -1  -1  -1  -1  -1  -1  -1  -1  -1
-1   0   0   0   0   0   0   0   0   0
 0   0   0   0   0   0   0   0   0   0
 0   0   0   0   0   0   0   0   0   0
 0   0   0   0   0   0   0
```

TRANSPORT VOLUME TO THE RIGHT (M3) FROM   960720 TO   960724

```
 0   0   0   0   0   0   0   0   0   0
 0   0   0   0   0   0   0   0   0   0
 0   0   0   0   0   0   0   0   0   0
 0   0   0   0   0   0   0   0   0   0
 0   0   0   0   0   0   0   0   0   0
 0   0   1   1   1   1   1   1   1   1
 1   1   1   1   1   1   1
```

****

OUTPUT   OF   BREAKING   WAVE   STATISTICS   FOR   SELECTED
LOCATIONS

N.B. WAVE DIFFRACTION IS NOT ACCOUNTED FOR!

GRID CELL NUMBERS

```
 1   1   2   3   5   6   7   9  10  11
13  14  15  17  18  19  21  22  23  25
26  27  29  30  31  33  34  35  36  38
39  40  42  43  44  46  47  48  50  51
52  54  55  56  58  59  60  62  63  64
```

AVERAGE UNDIFFRACTED BREAKING WAVE HEIGHTS (M).

0.44 0.44 0.44 0.44 0.44 0.44 0.44 0.44 0.44 0.44

0.44 0.44 0.44 0.44 0.44 0.44 0.44 0.44 0.44 0.44

0.44 0.44 0.44 0.44 0.44 0.44 0.44 0.44 0.44 0.44

0.44 0.44 0.44 0.44 0.44 0.44 0.44 0.44 0.44 0.44

0.44 0.44 0.44 0.44 0.44 0.44 0.44 0.44 0.44 0.44

AVERAGE UNDIFFRACTED BREAKING WAVE ANGLE TO SHORELINE (DEG)

-1.32 -1.32 -1.32 -1.58 -1.80 -1.76 -1.69 -1.53 -1.87 -1.98

-1.31 -1.05 -1.37 -1.58 -1.40 -1.56 -1.55 -1.87 -1.95 -1.24

-1.11 -1.08 -1.06 -1.21 -1.02 -0.60 -0.55 -0.42 -0.41 -0.33

-0.33 -0.22   0.09   0.16   0.26   0.28   0.27   0.41   0.71   0.78

 0.78   0.96   1.06   0.93   1.16   1.29   1.26   1.19   1.12   1.00

AVERAGE LONGSHORE TRANSPORT RATE BASED ON UNDIFFRACTED WAVES *100 (M3/SEC)

-0.31 -0.31 -0.31 -0.31 -0.33 -0.33 -0.33 -0.33 -0.34 -0.33

-0.30 -0.29 -0.30 -0.31 -0.31 -0.31 -0.33 -0.34 -0.34 -0.31

-0.30 -0.29 -0.28 -0.28 -0.27 -0.25 -0.24 -0.24 -0.23 -0.23

-0.22 -0.22 -0.20 -0.19 -0.19 -0.18 -0.18 -0.17 -0.16 -0.15

-0.15 -0.13 -0.13 -0.13 -0.12 -0.11 -0.12 -0.12 -0.13 -0.13

LONGSHORE TRANSPORT FOR LAST TIME STEP *100 (M3/SEC)

0.00 0.00 0.00 0.00 0.00 0.00 0.00 0.00 0.00 0.00

0.00 0.00 0.00 0.00 0.00 0.00 0.00 0.00 0.00 0.00

0.00 0.00 0.00 0.00 0.00 0.00 0.00 0.00 0.00 0.00

0.00 0.00 0.00 0.00 0.00 0.00 0.00 0.00 0.00 0.00

0.00 0.00 0.00 0.00 0.00 0.00 0.00 0.00 0.00 0.00

0.00 0.00 0.00 0.00 0.00 0.00 0.00 0.00 0.00 0.00

0.00 0.00 0.00 0.00 0.00 0.00 0.00

CALCULATED FINAL SHORELINE POSITION (M)

400.00 404.96 409.92 414.88 419.82 424.75 429.66 434.53 439.36 444.16

448.90 453.60 458.23 462.79 467.29 471.69 476.01 480.23 484.34 488.34

492.22 495.96 499.58 503.04 506.35 509.50 512.48 515.28 517.89 520.32

522.54 524.57 526.39 527.99 529.38 530.55 531.50 532.23 532.74 533.03

533.09 532.94 532.56 531.98 531.19 530.20 529.01 527.63 526.06 524.32

522.41 520.34 518.11 515.74 513.24 510.61 507.87 505.03 502.09 499.08

495.99 492.85 489.66 486.45 483.23 480.00

CALCULATED SEAWARDMOST SHORELINE POSITION (M)

400.00 405.26 410.52 415.79 421.08 430.00 440.00 438.93 449.34 462.90

520.00 520.00 500.00 469.46 470.53 475.56 480.56 485.56 490.59 495.61

500.69 505.84 560.00 580.00 560.00 544.09 542.78 545.80 548.87 560.00

580.00 570.00 562.77 560.00 557.44 558.05 558.57 558.94 560.00 570.00

580.00 570.53 565.00 560.00 557.41 556.25 560.00 570.00 560.00 551.47

547.74 544.20 550.00 540.00 532.25 535.00 530.00 520.00 507.59 503.68

500.00 495.81 491.85 487.90 483.95 480.00

CALCULATED LANDWARDMOST SHORELINE POSITION (M)

400.00 370.00 379.29 380.00 407.23 417.55 426.86 428.95 410.00 444.16

448.90 453.60 458.23 440.00 440.00 450.00 459.89 460.00 462.24 440.00

440.00 490.00 499.58 503.04 506.35 509.50 512.48 515.28 517.89 520.32

522.54 524.57 526.39 527.99 529.38 530.55 531.50 532.23 532.74 533.03

533.09 532.94 532.56 531.98 530.00 530.20 529.01 527.63 526.06 524.32

522.41 520.34 518.11 515.74 513.24 510.61 507.87 505.03 490.00 460.00

480.20 475.00 460.00 460.00 474.45 480.00

CALCULATED REPRESENTATIVE OFFSHORE CONTOUR POSITION (M)

700.00 704.90 709.80 714.70 719.60 724.49 729.34 734.15 738.93 743.67

748.35 752.98 757.54 762.04 766.45 770.79 775.03 779.17 783.20 787.12

790.92 794.59 798.12 801.51 804.74 807.81 810.72 813.45 816.00 818.37

820.54 822.52 824.29 825.86 827.23 828.38 829.32 830.04 830.55 830.85
830.93 830.81 830.47 829.93 829.19 828.25 827.12 825.81 824.31 822.65
820.82 818.83 816.69 814.42 812.01 809.49 806.85 804.11 801.28 798.38
795.41 792.33 789.25 786.17 783.08 780.00

CALIBRATION/VERIFICATION ERROR =   25.9258

CALCULATED VOLUMETRIC CHANGE = -7.55E+05 (M3)
SIGN CONVENTION: EROSION (-), ACCRETION (+)

APPENDIX C

FORTRAN PROGRAM USED TO GENERATE WAVES.DAT, WAVE INPUT FILE OF GENESIS.

```
    ---------------------------------------------------------------------------------
      Program wavegen
c ******************************************************************
c    This program creates a wave data file
c    for Genesis.
c    From a set of values of H, T, theta, and Prob.
c       By Karim Rakha Sept. 2004
c ******************************************************************
c  X direction is the alongshore direction.
c
c  X  <------------------------
c (genesis)                    |
c                              |
c                              |
c        |\                    |
c        | \                   |
c        |  \                  |
c           + alpha            |
c                   \/ Y (genesis)
c
c ******************************************************************
c    H1(i)         Wave heights
c    A1(i)         Wave angles with axis used for Genesis
c    T1(i)         Wave period
c    Prop (i)      is the probability of occurence of
c                  the wave H1(i) with direction A1(i)
c    calm          Probability of calm periods
c    n1            number of lines in input file
c ******************************************************************
```

```fortran
      real        H1(300),A1(300),T1(300)
      real        Prop(300),calm,dum
      character*70  junk
c ****************************************************
c  Open input and output files:
      open (unit=8,file='wavein.txt')
      open (unit=9,file='waves.dat')
c ****************************************************
c  Data for a specific site:
      dt    = 3          ! dt in hours
      anglim = 79          ! limiting angle
c ****************************************************
c  Read in data:
      read(8,*) n1
         read (8,50) junk

      do i = 1,n1
        read(8,*) H1(i),T1(i),A1(i),Prop(i)
      end do
      read(8,*) calm


c ****************************************************
c  Create a wave height file:
      write                                        (9,150)
'***********************************************'
      write (9,140) ' Wave Condition file for Mnanavgat case '
      numdt = 365.25*24/dt
      ntest = 0
      write (9,160) ' Time step is ',dt,' hr'
      write                                        (9,150)
'***********************************************'

c Loop on wave conditions
      do i = 1,n1
         H   = H1(i)
         ang = A1(i)
            T  = T1(i)
         if (abs(ang).ge.anglim) then
            H = 0.1
            T = 1.0
            ang= 0.0
         end if
         nrepeat = int( Prop(i)*numdt/100.0 + 0.51)
```

170

```fortran
          if (nrepeat.ge.1) then
             do k = 1,nrepeat
                ntest = ntest + 1
                write (9,60) T,H,ang
             end do
          end if
       end do
c  Calm data
       nrepeat = int(calm * numdt / 100.0 + 0.5)
       do k = 1,nrepeat
          ntest = ntest + 1
          H   = 0.1
          ang = 0.0
          T   = 1.0
          write (9,60) T,H,ang
       end do


       nyear = 24*365.25/dt
       print *, ' Total number of records =',ntest
       print *, ' Total number should be =',nyear

       if (ntest.lt.nyear) then
         do i = ntest,nyear
           H   = 0.1
           ang = 0.0
           T   = 1.0
           write (9,60) T,H,ang
         end do
       end if


c ***************************************************
 50    format(a70)
 60    format(3f10.2)
 140   format (A40)
 150   format (A50)
 160   format (A25,f5.2,A5)
c ***************************************************
        stop
       end
 ---------------------------------------------------------------------------------
```

VITA

Fatima AL SALEH was born in Aleppo, Syria on July 10, 1968. She received her B.Sc. in Civil engineering from Aleppo University in 1991. She has been a graduate assistant in the Department of communication and transportation at Aleppo University. She has received her master degree in 1996 from Çukurova University in Turkey. She is talking Arabic Turkish English and French.